THE UNIVERSITY OF MANITOBA

The Investigation of Effect of Stratified Liquid Storage on The Performance of Thermosyphon Solar Domestic Hot Water Systems

by

© Manit Sujumnong

A Thesis

Submitted to the Faculty of Graduate Studies
in partial Fulfillment of the requirements for the
Master of Science Degree in Mechanical Engineering

Winnipeg, Manitoba

1988

ISBN 0-315-47932-9

THE INVESTIGATION OF EFFECT OF STRATIFIED LIQUID STORAGE ON THE PERFORMANCE OF THERMOSYPHON SOLAR DOMESTIC HOT WATER SYSTEMS

BY

MANIT SUJUMNONG

A thesis submitted to the Faculty of Graduate Studies of the University of Manitoba in partial fulfillment of the requirements of the degree of

MASTER OF SCIENCE

ABSTRACT

The improvement of the performance of the Solar Domestic Hot Water (SDHW) systems by the use of stratified liquid storage is well established. In addition, the advantage of using a thermosyphon SDHW system in remote areas is obvious in that there is no need of power supplies.

The purpose of this thesis was aimed at improving the degree of stratification in the liquid storage of a SDHW system applying thermosyphon principles.

A number of perforated baffles were mounted, horizontally, inside the liquid storage tank. The performance characteristics, e.g., thermosyphon mass flow rate, mean storage temperature, vertical storage tank temperature profile changes, collector inlet/outlet temperatures, degree of stratification, and collector efficiency were investigated and compared to these characteristics of a conventional SDHW storage system without baffles. The experimental results from both SDHW systems were compared to simulated results and good agreement was obtained.

However, the results showed that the horizontal perforated baffles mounted inside the liquid storage tank did not improve the degree of stratification. Because the perforated baffles themselves promoted mixing conditions in the storage tank.

Finally, the use of different shapes and arrangements of the baffle should be investigated to determine their effects on stratification.

ACKNOWLEDGEMENTS

The author acknowledges his debt to Prof. R.E. Chant whose continuing interest and guidance have contributed to make this investigation possible. Special thanks are due to Dr. J.S. Townsend and Prof. D.C. Card for their helpful suggestions and corrections.

The author wishes to thank Mr. J. Finken, Mr. M. Kapitoler, and Mr. K. Majury for their indispensable technical assistance.

The auther acknowledges Dr. M.C. Chaturvadi, Khon Kaen University, and Canadian International Development Agency for their financial supports.

I am especially grateful to my parents, brother, and sister for their valuable source of inspiration.

TABLE OF CONTENTS

LIST OF FIGURES

NOMENCLATURE

A	Cross-sectional Area (m^2)
A_c	Collector Absorption Area (m^2)
C_1 , C_2	Constance Values
C_b	Bond Thermal Conductance ($W/m^2 \cdot K$)
C	Thermal Capacitance (J/K)
c_p	Specific Heat ($J/kg \cdot K$)
D	Outside Diameter of The Tubes on Collector (m)
d	Piping Tube Diamater (m)
f	Friction Factor (dimensionless)
F	Fin Efficiency (dimensionless)
F_R	Collector Heat Removal Factor (dimensionless)
F	Collector Efficiency Factor (dimensionless)
F	Collector Flow Factor (dimensionless)
g	Gravitational Acceleration (m/s^2)
G	Instantaneous Solar Intensity (W/m^2)
h	Height (m)
ΔH	Total Hydrostatic Pressure (Pa)
I	Hourly Solar Intensity ($W/m^2 \cdot hr$)
k	Thermal Conductance ($W/m \cdot K$)
K	Resistance Coefficient (dimensionless)
l	Distance between points along collector surface used in Equation 4.9 (m)
L	Length of Collector (m)
m	Mass (kg)
m	Mass Flow Rate (kg/s)
n	Number of Tubes in Collector
N_{Re}	Reynold's Number (dimensionless)

Q	Heat Delivery (J)
R	Ratio of Solar Intensity on tilted surface to on horizontal surface (dimensionless)
S	Solar Energy Absorption on Collector Surface (J)
t	Time (s)
T	Temperature ($^{\circ}C$, K)
U	Overall Heat Loss Coefficient ($W/m^2 \cdot K$)
v	Velocity (m/s)
W	Distance between Tubes on Collector Surface (m)
x	Distance on Collector Surface in Crossectional Direction (m)
Δx , Δy	Unit Length in X , Y Direction (m)
y	Distance along Collector Surface (m)
Z	Distance along Collector Surface used in Equation 4.8 (m)

Greek Symbols

α	Thermal Absorptivity
β	Tilted Angle (degree)
ρ	Reflectance
τ	Transmittance
η	Efficiency
δ	Fin Thickness (m)
ψ	Modified Temperature
γ	Bond everage Thickness
Σ	Summation Sign
ρ	Density (kg/m^3)

Subscripts

b	beam
c	collector
d	diffuse
f	fluid
g	ground
L	loss
m	mean value
n	new value
o	at outlet position
p	on collector plate
T	total value
u	useful value
1,2,3,...	at point 1,2,3,...

Chapter 1
Introduction

Computer simulations have shown that thermal stratification in liquid storage tanks greatly increases the calculated efficiency of Solar Domestic Hot Water (SDHW) systems [1]. In particular at low flow rates, Wuestling et al. [2] found that with a perfectly stratified storage (no mixing takes place) the collected energy was increased 37% relative to a fully mixed storage.

The perfectly stratified liquid storage model assumes the tank to consist of a number of uniform temperature layers of liquid. The interfaces of these isothermal regions move up and down in the tank as cold water or hot water are introduced into the tank. In the perfectly stratified case it is also assumed that the incoming water will automatically, without mixing, find its way into the correct location in the tank to keep the temperature uniform. Therefore, in the perfectly stratified model it is assumed that there is no mixing due to buoyancy or turbulence.

In a real liquid storage tank, however, mixing will occur. Hollands et al. [3] have reviewed some of the mechanisms which tend to cause mixing in the tank and the departure from the perfectly stratified condition. Pluming was identified as an important effect. The pluming occurs when the liquid entering the tank near the top is cooler than the liquid at the top of the tank. The higher density causes a downward-flow and a plume forms, entraining the surrounding water and hence introducing mixing into the tank.

Therefore, there have been several investigations to establish perfectly stratified conditions in liquid storage by introducing different techniques, for instance, using, a floating inlet, or a vertical porous inlet manifold. The purposes of these techniques were to avoid mixing conditions caused by the pluming effect, and momentum effects occuring at inlet ports. Warmer water resulting from the use of improved solar collector

designs, such as a vacuum flat-plate collector or a semi-concentrator collector also reduces pluming effects.

The buoyancy force is due to the combined effect of the fluid density gradient and gravitational body forces. Free convection fluid motion is due to the buoyancy force within the fluid, whereas in forced convection it is created by an imposed external force. A buoyancy force occurs when the temperature of liquid in lower layers is higher than the temperature of the liquid in the upper layers. The dense liquid (in the upper layer) moves down due to the gravitational force and replaces the warmer liquid causing convective currents. Therefore, the storage becomes unstable and fluid mixing occurs.

The purpose of this investigation was aimed at reducing the mixing by using horizontal baffles mounted inside a storage tank in order to reduce the mixing effects of the buoyancy force and pluming. Also, in this investigation the effect of temperature distribution in the storage tank at the starting time on the system performance was studied.

The results from the present investigation show that by using horizontal baffles mounted inside a liquid storage tank there is a decrease in the system performance, because the baffles themselves promote turbulent flow conditions inside the tank causing mixing. In addition, this investigation demonstrates that by using a stratified temperature distribution condition in the liquid storage tank at the starting time better system performance is obtained compared to a uniform temperature distribution condition at the start.

Chapter 2

Literature Review

2.1 Thermosyphon (Natural Circulation) System.

Circulation in a solar water heating system such as that shown in Fig.2.1 occurs when the collector fluid is heated sufficiently to establish a density difference between the fluid in the collector and the fluid in the storage tank. As the sun heats the collector, the hot fluid inside the flow passage rises by natural convection and the colder water in the storage tank flows down to the collector by gravity. The circulation automatically stops during insufficient insolation when the upward buoyancy force in the collector is unable to overcome the fluid friction losses in the system.

The density difference, that causes the buoyancy force, is a function of the temperature difference. The thermosyphon flow rate is then a function of the useful heat gain of the collector which produces that temperature difference. Under these circumstances, the system is self-adjusting, with an increasing heat gain leading to increasing flow rate through the system [4].

No pumps or controllers are required for thermosyphon system operation. The storage tank must be above the collector so that the cold fluid in the down comer causes the fluid warmed by the collector to rise. If the storage tank was below the collector no flow would occur during the day and the collector would chill the fluid at night causing a reversal of flow [5,6].

There are several advantages in using a thermosyphon solar water heating system. First, the main advantage is that the system is totally autonomous requiring no electricity to run pumps or controllers. This may lead to a widespread use of this system in remote locations. Second, the system is inexpensive. Third, the system is not complicated as it is easy to install and maintain.

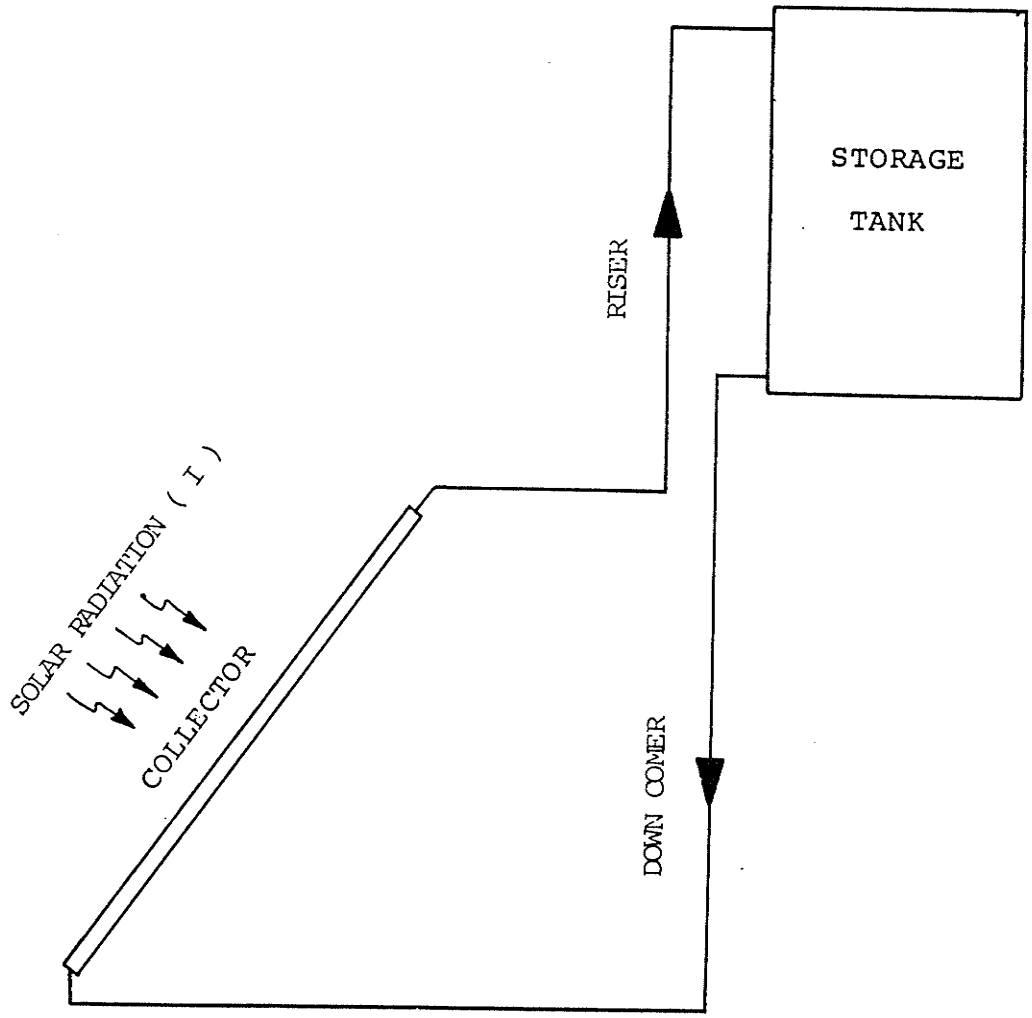

Fig.2.1 Solar water heating system with natural circulation (thermosyphon system).

The system has some disadvantages, for instance, the unsteady flow rate leads to uncertainty in the amount of energy collected. Other factors that make it difficult to predict performance are the variable of solar intensity and surrounding conditions, etc.

To overcome some of the disadvantages, there have been many investigations of thermosyphon systems in order to gain understanding of the system's dynamic behavior. The studies were aimed at improving the system performance by using different techniques. For instance, it has been found that the use of stratified solar water storage is one of the most effective means of improving system efficiency.

The objective of this chapter is to review studies that other investigators have done on solar thermosyphon systems and review the effects of stratified storage on the performance enhancement of solar water heating systems. Section 2.2 covers the works that deal with thermosyphon systems and section 2.3 explains SDHW system performance enhancement by stratification.

2.2 Studies on Thermosyphon SDHW Systems.

Accurate predictions of system behavior and of performance characteristics for thermosyphon SDHW systems are important. The ability, given environmental resources data for a special location and system configuration parameters, to predict the behavior and performance will aid users in selecting the most cost effective SDHW system for their locations and hot water use cycles. The development of predictive models can aid in optimizing system designs. The following paragraphs review papers that relate to the studies of thermosyphon SDHW systems.

Close [7] was the first investigator of thermosyphon SDHW systems who analysed the circulation rate. He compared computed and experimental results of inlet and outlet collector temperatures. The results confirmed the suggestion that a temperature rise across the collector of approximately 10°C was representative of these systems.

DeSa [8] considered the entire water heating system by equating the incident energy received to the sum of heat losses from the system and the heat gained by the water. He predicted temperature variation throughout the day. The results did not show good agreement with measurments made during diffuse radiation and scattered cloud reflection periods. But he recommened that it was possible to predict the temperature rise of water in the system under unsteady operating conditions.

Gupta and Garg [9] created a computer model for predicting the thermal performance of SDHW employing natural circulation. The ideal condition of no drain-off during the day was assumed. Clear and/or cloudy sky conditions were handled by the program. Results were as follows:

- flow rate was dependant on the distance between the tank bottom and the collector top, but this difference did not effect the mean storage temperature,
- for clear sky conditions, the temperature rise through the collector was constant,
- decreasing the distance between the tank bottom and the tank outlet led to higher mean storage temperature,
- mean storage temperature was not dependant on the piping diameter,
- thermosyphon flow rate depended on piping diameter,
- there was a slight increase in the mean storage temperature with an increasing value of length-to-width ratio of the collector,
- for a fixed tank capacity, a slight increase in the mean storage temperature was noticed with an increasing height-to-diameter ratio of the storage tank.

Ong [10] presented a mathematical model that followed closely the analyses of Close, and Gupta and Garg. He assumed that the mean temperatures in each component (collector, storage tank, and connecting piping) were equal. His work was significantly differenct from the others in his solution procedure. He used a finite-difference solution to evaluate the theoretical performance of a thermosyphon system. The results were as follows:

- the mean fluid temperatures in the collector, the storage tank, and the connecting piping were not equal,
- the thermosyphon flow rate varied with solar intensity.

Two years later, Ong [11] improved his previous work [10] by assuming that the mean storage temperatures of each component were not equal. The thermosyphon performance was evaluated from the temperature distribution of the whole system. The work showed good correlation between predicted and measured results. He also showed that the temperature profile in the storage tank was not linear.

Klein et al. [12] created a general simulation program, namely, TRNSYS, in order to simulate the water heating system operating with natural circulation (see Fig.2.2). The simulation of the water heating system was developed by interconnecting mathematical models of each of the system components, such as, the collector, the heat exchanger, and the storage tank.

The TRNSYS simulation program served two distinct purposes. First, the program provided the means of analyzing the dynamic performance of the system (on a short-time scale). Analyses of this type were useful, for example, to investigate the effects of various control strategies and to gain an understanding of the dynamic behavior of the system. Other simulations were used (on a long-time scale) directly as a design tool.

Even the smallest flow restriction placed in the flow lines to measure flow, could drastically reduce the flow rate and change the hydrodynamic behavior of the system.

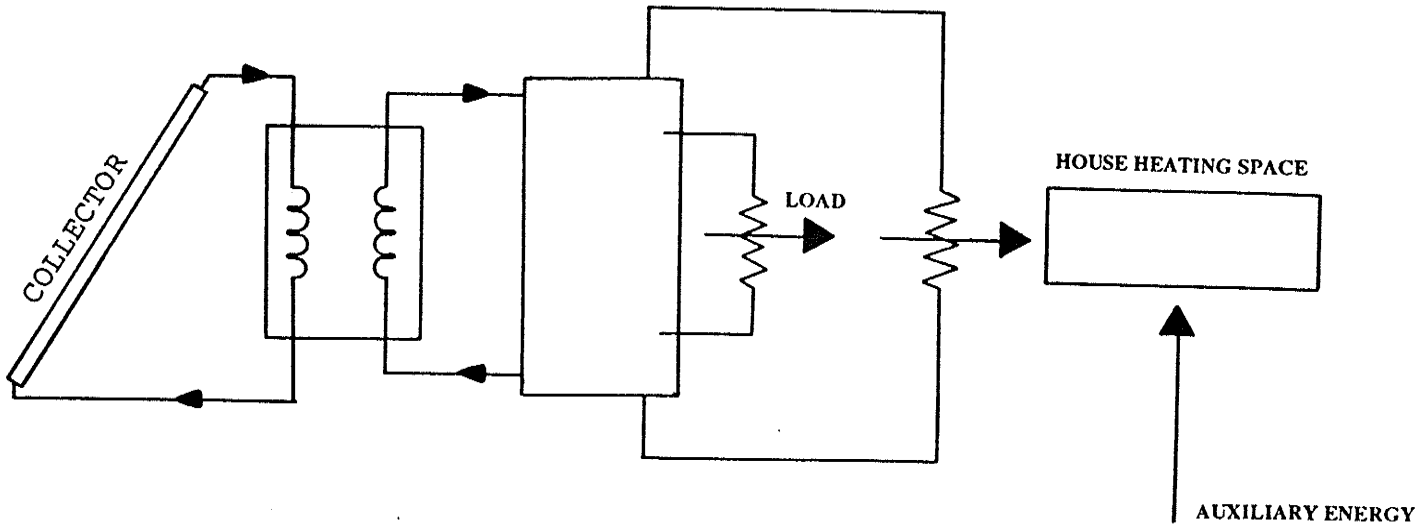

Fig.2.2 The thermosyphon SHW system: as modelled by **TRNSYS program.**

Therefore, some investigators try to measure thermosyphon flow rate by using indirect methods without interfering with the flow.

Morrison and Ranatunga [13] predicted thermosyphon flow rate in solar collectors and compared the results with experimental measuremants obtain using a laser doppler anemometer. The results showed substantial differences between predicted and measured values due to inadequate analysis of thermosyphon flow. However, it was felt that the results were useful since the predicted and measured values behaved similarly showing that it was possible to use an indirect method to determine thermosyphon flow rate.

Another interesting study on thermosyphon systems was reported by Young and Bergquam [14]. They studied the effect of system characteristics on performance, i.e., collector inlet and outlet temperatures, thermosyphon flow rate, and storage temperature profile changes. The practical configuration and sizes of components simulated real conditions. The system characteristics were similar to systems of other investigators but in Young and Bergquam's work an indirect experimental method, using the system temperature distribution, was introduced to evaluate the thermosyphon flow rate. The results of the indirect experimental method were verified by comparison to measurements taken with a turbine flow meter. The two methods showed very good agreement.

2.3 SDHW System Performance Enhancement versus Stratification.

Recently studies have shown that thermal stratification in the solar energy storage tank of a liquid-based system can produce a significant increase in system efficiency for two reasons. First, the collector is supplied with the cooler fluid at the base of the storage tank and thus the collector efficiency is increased. Second, the warmer water supplied to the load is drawn from the warmer fluid at the top of the storage tank, which decreases the auxiliary power requirements.

There have been several investigators who have studied the behavior of SDHW systems with stratified storage in order to optimize the use of stratification. This section is devoted to the studies which show how the thermal stratification develops.

Cabelli [15] studied, numerically, a two-dimensional model of fluid motion in a stratified storage tank. Results from the two-dimensional model were compared with other results from a simple one-dimensional model in the vertical direction. The discrepancy between the two models was small. He suggested that because of the buoyancy effect the fluid was thermally stratified and temperature could be predicted with reasonable accuracy using a simple vertical one-dimensional solution.

Sharp and Loehrke [16] studied theoretically the potential benefits of thermal stratification by comparing the predicted performance of a system using stratified storage with that of the same system using well-mixed storage. They suggested that improved performance would result if stratification could be achieved in the storage tank. The magnitude of the improvement depended strongly on certain design parameters, the most important of which were collector efficiency, mass flow rate, and tank capacity. Results showed that (1) increasing the mass flow rate promoted mixing in the storage, (2)increasing the tank height-to-diameter ratio for a fixed tank capacity would improve the stratification due to the reduction of the effects of wall conduction in the vertical direction.

Loehrke et al. [17] used the technique to introduce a fluid into a storage tank containing a stratified fluid in a manner to enhance the thermal stratification. The technique used a vertical, porous inlet manifold that was designed to remove the momentum of incoming fluid and thus inhibit mixing. Furthermore, a flexible, porous manifold was recommened instead of a rigid porous manifold which showed significant improvement.

Young and Baughn [18] investigated, numerically and experimentally, the thermal behavior of stratification in a horizontal storage tank. Results showed that axial temperature gradients were negligible compared to vertical temperature gradients. Consequently, a one-dimensional treatment was an adequate approximation.

Considerable mixing in the storage tank (at the top and the bottom) were noted when inlet and outlet diffusers were not used.

Veltkamp [19] studied stratified storage behavior using a one-dimensional model, i.e., the temperature was depended on only one direction, i.e., elevation. Results showed that (1) by using a floating inlet, a high degree of stratification could be achieved, and (2) a system with a vacuum collector performed up to 20 percent better than a conventional collector because of less heat loss from collector to surroundings.

Jaluria and Gupta [20] studied experimentally the directional dependence in a thermally stratified water body. Results indicated that the temperature distribution was largely one dimensional, with variation in the vertical direction only. Like other investigators, he pointed out that it was possible to consider only simple one-dimensional temperature profiles without loss in accuracy.

Phillips and Dave [21] studied the effects of stratification on the performance of liquid-based solar water heating systems. Results were represented in terms of a stratification coefficient which was defined as the ratio of the actual useful energy to the energy gain that would be achieved in a full-mixed storage. The results showed that (1) for practical solar water heating systems, with insulation equivalent to 3 cm or more of glass-wool, the stratification is independant to tank insulation, and (2) well designed systems, with inlet diffusers, gave more accurate predicted results.

Jesch and Braun [22] improved water heater performance by using the solar intensity to control the flow rate with stratified storage. Using low and variable flow rates and variable volume storage significantly improved system performance. Results showed that the delivered energy was as much as 25 percent more than for fixed volume flows and full-mixed storage systems. Results also showed that the system, when operated with thermosyphon flows, had greater relative improvement compared to the low-flow rate.

Briggs and Ferguson [23] studied the effectiveness of control strategies to improve system efficiency. They confirmed that reducing the inlet flow rate improved system performance.

Kenneth Rush [24] studied stratified storage tanks for SDHW systems. No load conditions were assumed. He found that with sufficient sunshine, the top 3/4 of the storage tank reached a uniform high temperature and then tank mixing ensued with gradually increased uniform temperature as shown in Fig.2.3.

Den Braven [25] derived the temperature distribution for the liquid storage in a SDHW system using an analytical method. A one-dimensional model was assumed in the vertical direction. The results showed that; (1) to achieve a well stratified storage, a thin wall should be used to reduce the thermal capacity of the tank body, (2) the water inlet to the collector should be taken from the bottom of the storage tank, and (3) the vertical mixing due to buoyancy forces destroyed the temperature gradient.

Shyu and Hsieh [26] studied unsteady natural convection in enclosures with a stratified medium in three different tank configurations, i.e., without insulation, insulation placed over the interior of the tank wall, and insulation placed over the exterior of the tank wall. Results showed that the tank with the interior insulation was the best system to maintain the stratification.

The thermosyphon systems studied in section 2.2 can be summarized as follows:

(1) the fluid temperature rise from inlet to outlet through the collector is constant,

(2) the thermosyphon flow rate varies with insolation,

(3) the thermosyphon flow rate varies with the distance between tank bottom and collector top,

(4) the flow rate depends on piping diameter,

(5) the mean storage temperature does not vary with the distance between the tank bottom and collector top,

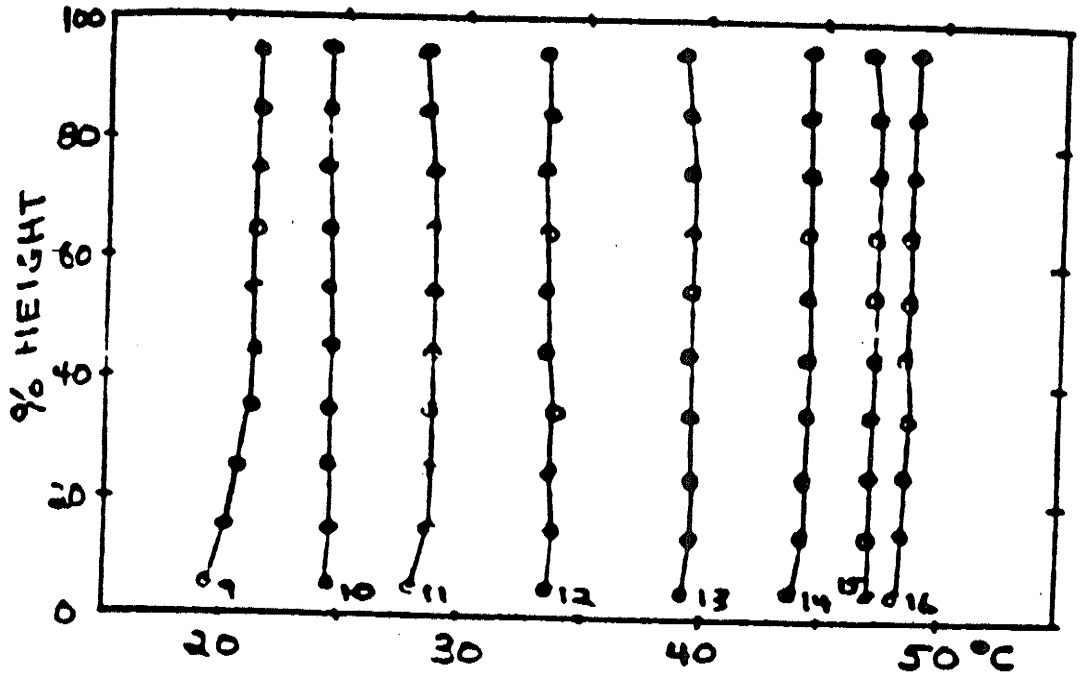

Fig.2.3 Hourly temperature profile changes of a typical thermosyphon SDHW system on a sunny day. From Rush.

(6) the mean storage temperature varies with increase in the distance between the tank bottom and the tank outlet port,

(7) the mean storage temperaure does not vary with piping diameter,

(8) there is a slight increase in mean storage temperature with increasing length-width ratio of the collector,

(9) there is a slight increase in mean storage temperature with increasing height-diameter ratio of the storage tank,

(10) the mean temperatures of the collector, the connecting piping, and the storage tank are not equal, and

(11) the temperature profile in the storage tank is not linear.

In section 2.3, the studies also indicate that stratification enhancement has the following characteristics:

(1) a simple one-dimensional model can be used to predict, with reasonable accuracy, the temperature profile in the storage unit of a SDHW system,

(2) an increasing mass flow rate disturbs the stratification,

(3) an increasing height-diameter ratio of the fixed storage tank capacity can improve stratification,

(4) an improved stratification is acheived by using a vertical, porous inlet manifold,

(5) a high degree of stratification is obtained by using

a floating inlet,

(6) an improved system performance of up to 20 percent occured by using a vacuum collector,

(7) for conventional hot water storage tank the stratification is independent of exterior insulation,

(8) using a low and variable flow rate improves stratification and performance,

(9) the use of thin wall tanks improves stratification,

(10) taking the water from the bottom of the tank improves stratification, and

(11) better stratification is obtained by using interior insulation in the storage tank rather than using exterior insulation.

The subject of stratification, as a means of improving system performance, has been reviewed in section 2.3 Most investigators studied the effects of stratification on active SDHW systems whereas only a few investigators studied the effects on thermosyphon SDHW systems. Therefore, the objective of this thesis is to investigate experimentally the effects of stratified liquid storage on the performance of thermosyphon SDHW systems.

Chapter 3

Flat-Plate Collectors and Solar Domestic Hot Water Systems.

In solar domestic hot water (SDHW) systems, the two most important components are a solar energy absorbing unit and a heat storage unit, generally a flat-plate solar collector, and a hot water tank. The objective of this chapter is to provide the theoretical design on performance details of flat-plate solar energy collectors and SDHW storage systems which are important for a basic understanding of the behavior of a system and for calculating the energy collected. Sections 3.1 and 3.2 are devoted to flat-plate solar energy collector design details and SDHW systems, respectively.

3.1 Flat-Plate Solar Collectors.

A solar energy collector is a special type of heat exchanger. The absorber plate transforms the solar radiation energy into heat. A solar energy collector differs in several respects from a more conventional heat exchanger. The latter only accomplishes a fluid-to-fluid heat exchange with high heat transfer rates. In the solar energy collector, the energy is collected and transferred to a fluid by a heat exchange surface. Without optical concentration, the flux of incident radiation is not greater than 1100 W/m^2 and is variable [4]. Thus, the design of a flat-plate solar energy collector presents unique problems of transforming low and variable energy input fluxes into heat and transferring it into a fluid.

Generally, a commercial flat-plate solar energy collector can be designed for applications requiring energy delivery at moderate temperatures, up to perhaps 100 $^{\circ}C$ [4]. Flat-plate solar collectors use both beam and diffuse solar radiation, tracking of the sun is not necessary and they require little maintenance. Flat- plate collectors are mechanically simpler than concentrating collectors. The major applications of these collectors currently

are for DHW and space heating, but the potential uses include building cooling and industial process heat.

The objective of this section is to deal primarily with the theory of flat-plate solar collectors and the basic design concepts. These will develop an understanding of the component functions and expressions for collector performance.

3.1.1 General Description of Flat-Plate Collectors.

The important parts of a typical flat-plate solar collector as shown in Fig.3.1 are: the "black" solar energy absorbing surface with a means for transferring the absorbed energy to a fluid, the cover which is transparent to solar radiation and opaque to infrared thermal radiation and covers the black surface in order to reduce convection and reradiation losses to the atmosphere, and the back insulation which reduces conduction losses to the surroundings.

3.1.2 Transmittance-Absorptance Product.

For the analysis of a flat-plate solar energy collector, it is necessary to evaluate the transmitance- absorptance product ($\tau\alpha$). Some of the radiation passing through the cover system and striking the absorbing plate is reflected back to the cover system. However, all of this reflected radiation is not lost since most is reflected back to the absorbing plate again.

The situation is illustrated in Fig.3.2, where τ is the transmitance of the cover system and α is the absorptance of the absorber plate. A $\tau\alpha$ portion of the incident energy is absorbed by the absorber plate and a $(1-\alpha)\tau$ portion is reflected back to the cover system. The reflection from the absorber plate is assumed to be diffuse (and unpolarized) so that the fraction $(1-\alpha)\tau$ that strikes the cover plate is diffuse radiation and $(1-\alpha)\tau\rho_d$ portion is reflected back to the absorber plate. The symbol ρ_d refers to reflectance of the cover system for diffuse radiation incident on the bottom side. The multiple reflections of diffuse radiation continue so that the energy ultimately absorbed is

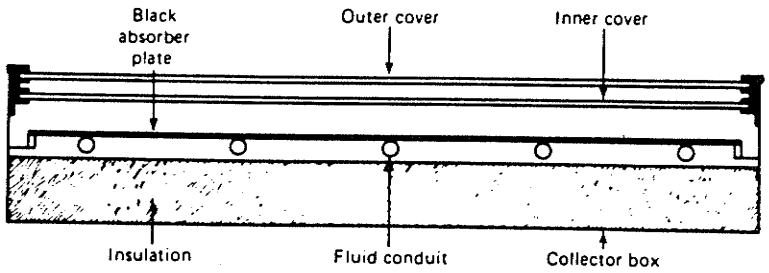

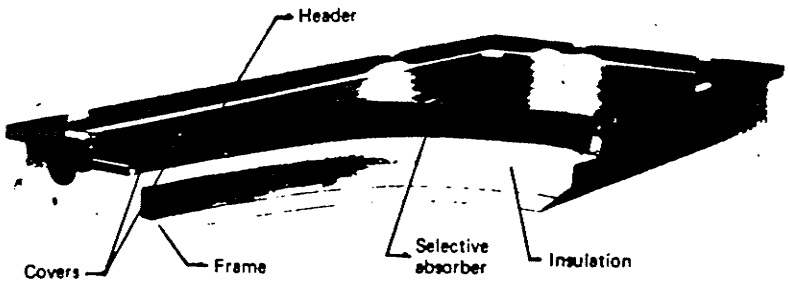

Fig.3.1 (a) Cross section of basic flat-plate collector.

(b) Construction details of a commercial flat-plate liquid heater.

From Duffie, J.A. and Beckman, W.A.

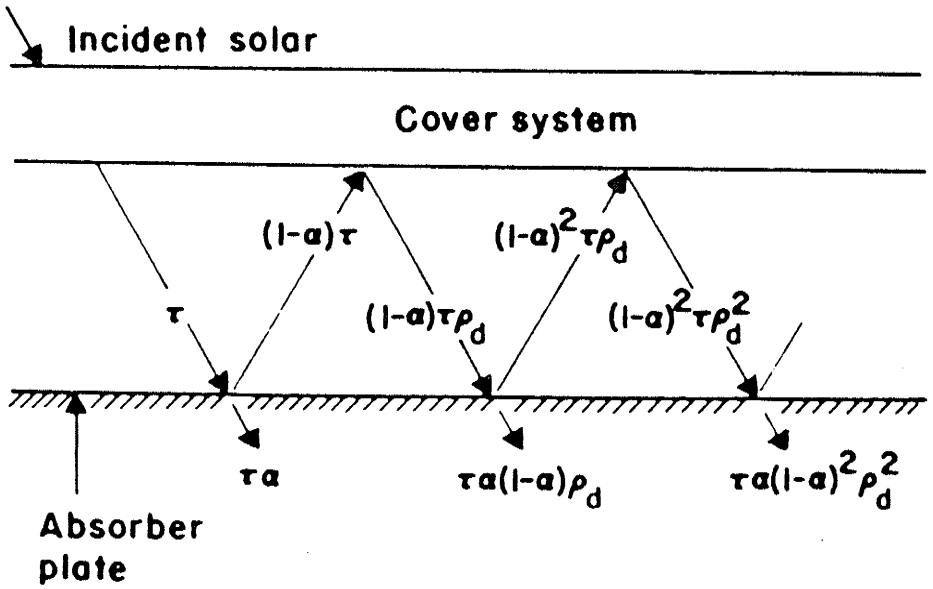

Fig.3.2 Absorption of solar radiation at absorber plate.

From Duffie, J.A. and Beckman, W.A.

$$(\tau\alpha)_{used} = \tau\alpha \sum_{n=o}^{\alpha} \left[(1-\alpha)\,\rho_d\right]^n = \frac{\tau\alpha}{1-(1-\alpha)\rho_d}\,. \qquad (3.1)$$

It is reasonable to use an approximate value of the transmittance-absorptance product. Equation 3.2 can be used as a close approximation to Equation 3.1 [4].

$$(\tau\alpha)_{approx.} = 1.01\ (\tau\alpha). \qquad (3.2)$$

3.1.3 Solar Energy Absorption.

The prediction of collector performance requires information on the solar energy absorbed by the collector absorber plate. When solar radiation is incident on a tilted collector, the radiation has three different spatial distributions, namely, beam radiation, diffuse sky radiation, and diffuse ground-reflected radiation. Each must be treated separately. On an hourly basis the absorbed radiation (S) is,

$$S = I_b R_b\,(\tau\alpha)_b + I_d\,(\tau\alpha)_d\,\frac{(1+\cos\beta)}{2} + \rho_g\,(I_b + I_d)\,(\tau\alpha)_g\,\frac{(1-\cos\beta)}{2}\,, \qquad (3.3)$$

where

S = solar energy absorbed by the absorbing plate,

I = hourly solar radiation intensity,

R_b = ratio of the beam radiation on the tilted surface to that on the horizontal surface,

$\tau\alpha$ = transmittance-absorptance product,

ρ = reflectance,

β = tilt angle of collector to the horizontal.

The quantities $(1+\cos\beta)/2$ and $(1-\cos\beta)/2$ are view (confriguration) factors from collector to sky and from collector to ground, respectively.

Sometimes it is convenient to define an average transmittance-absorptance product as the ratio of the absorbed solar radiation (S) to the total incident solar radiation (I_T) as in Equation 3.4.

$$S = (\tau\alpha)_{ave} \cdot I_T . \qquad (3.4)$$

This is especially convenient when direct measurements are available for total solar radiation. This approximation is often made in estimating S from existing data which is measured on a horizontal surface (I_b and I_T) as in the general calculation procedure for solar collector performance. The method works best when the beam radiation is high. The contribution of the diffuse sky and ground reflected radiation will then be relatively low so that $(\tau\alpha)_d$ and $(\tau\alpha)_g$ can be approximated by $(\tau\alpha)_b$ with little error [4].

3.1.4 Collector Overall Heat Loss Coefficient.

It is useful to develop the concept of an overall heat loss coefficient for a solar energy collector. To simplify the mathematics the electrical analogy of the thermal network as shown for the one-cover system shown in Fig.3.3 may be used. At a typical location on the plate where the temperature is T_p, S is the absorbed solar radiation on the absorber plate shown in section 3.1.3. This absorbed energy S is distributed to thermal losses via the top and the bottom, and to the useful energy gained (Q_u) by the working fluid. The purpose of this section is to convert the thermal network of Fig.3.3 to the equivalent thermal network in Fig.3.4. In Fig.3.3 and 3.4,

$h_{r,p-c}$ = the heat transfer coefficient for
radiation between the plate and the cover,

$h_{c,p-c}$ = the heat transfer coefficient for
convection between the plate and the
cover,

$h_{r,c-a}$ = the heat transfer coefficient for

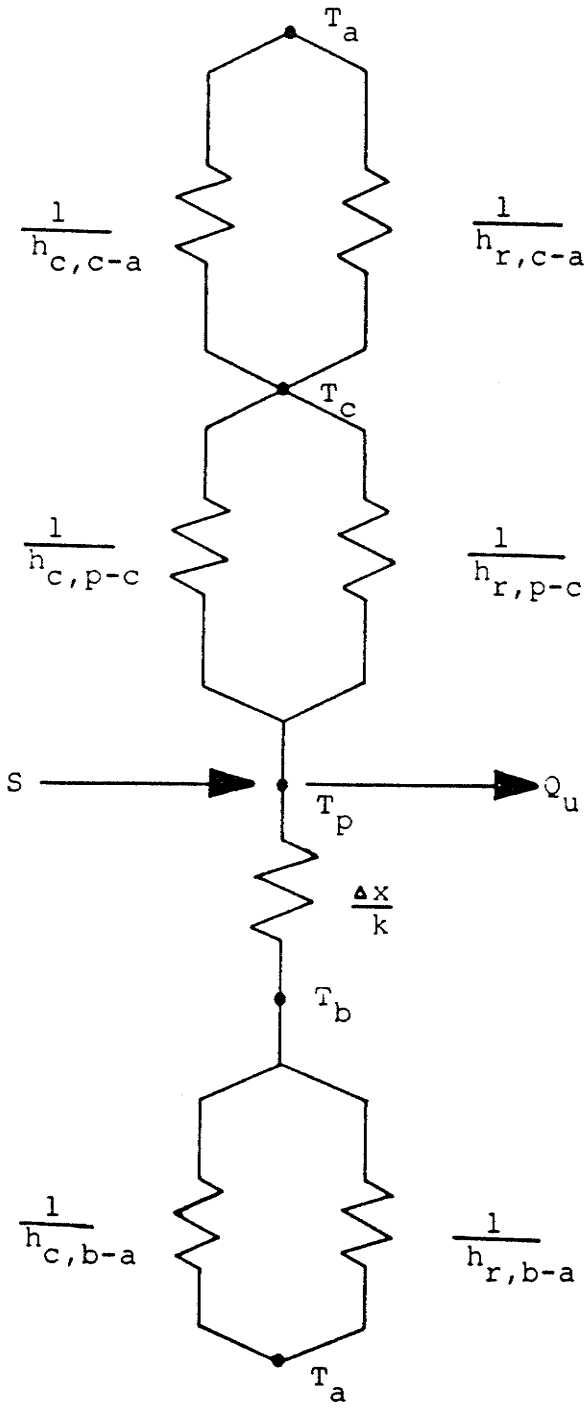

Fig.3.3 Thermal network of a one-cover flat-plate collector.
(a) In terms of conduction, convection, and radiation.

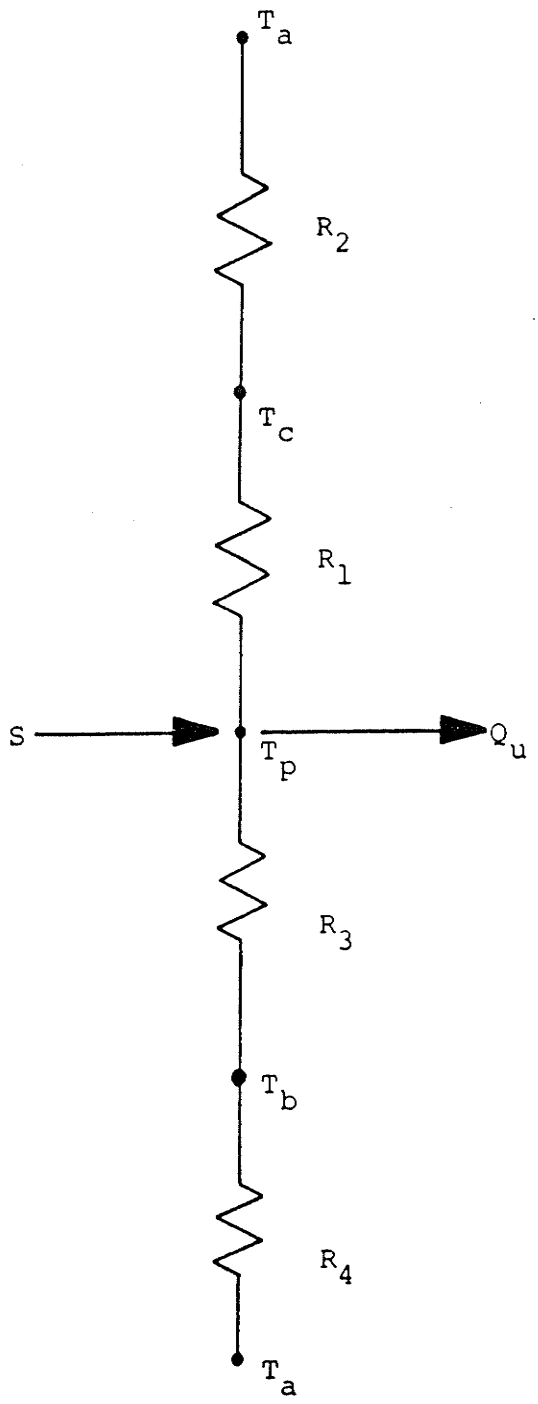

(b)

Fig.3.3 Thermal network of a one-cover flat-plate collector.
(b) In terms of resistances between plates.

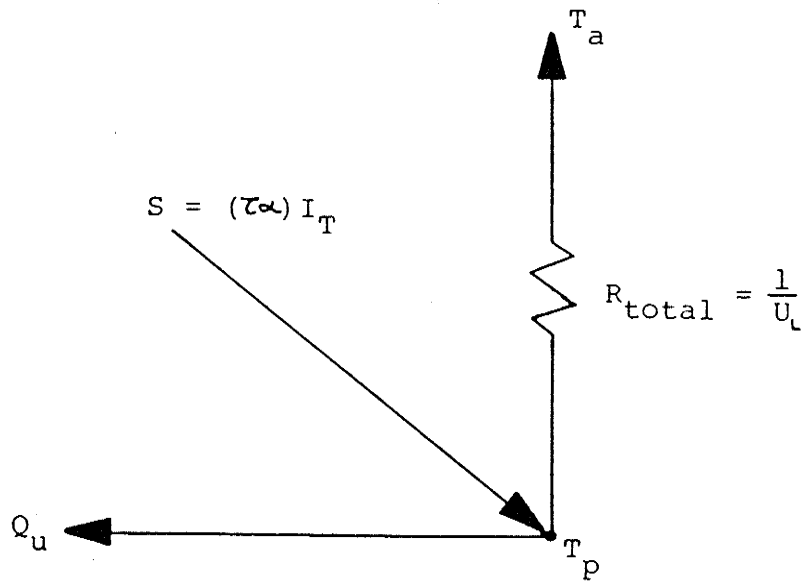

Fig.3.4 Equivalent thermal network for solar energy collector.

radiation between the cover and the ambient air,

$h_{c,c-a}$ = the heat transfer coefficient for convection between the cover and the ambient air,

$\Delta x/k$ = the conductive resistance of the insulation between the plate and the back of the collector,

$h_{r,b-a}$ = the heat transfer coefficient for radiation between the back and the ambient air,

$h_{c,b-a}$ = the heat transfer coefficient for convection between the back and the ambient air,

$R_1 = 1/(h_r + h_c)_{p-c}$,

$R_2 = 1/(h_r + h_c)_{c-a}$,

$R_3 = \Delta x/k$,

$R_4 = 1/(h_r + h_c)_{b-a}$,

T_a = the ambient air temperature,

T_c = temperature of the cover system,

T_p = temperature of the absorber plate.

To evaluaete U , Fig.3.3(b) was modified as shown in Fig.3.5. Thus, the total thermal resistance (R) between the absorber plate and the ambient surroundings is as follows where $U_L = 1/R_T$:

$$U_L = \frac{1}{R_T} = \frac{1}{R_1 + R_2} + \frac{1}{R_3 + R_4} . \qquad (3.5)$$

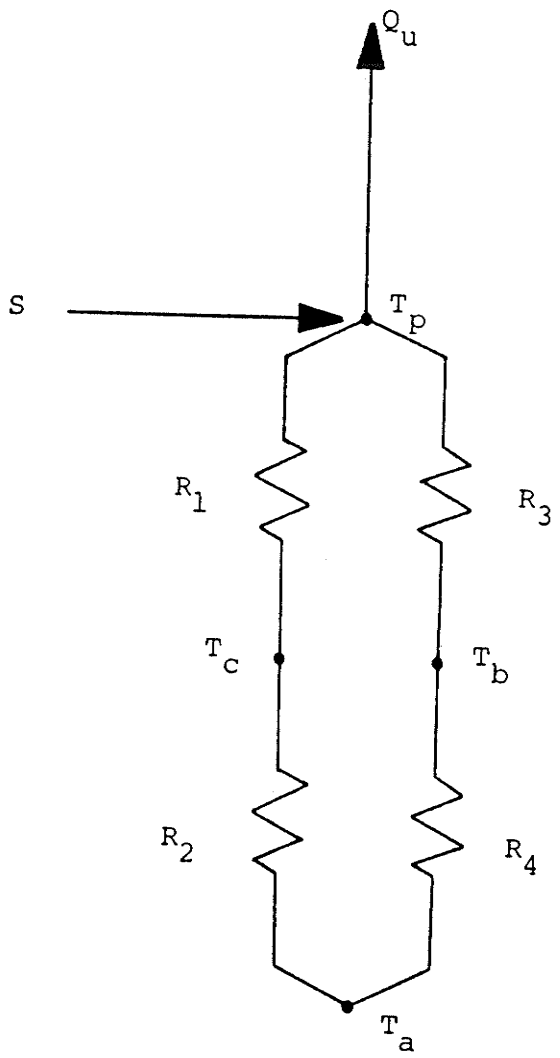

Fig.3.5 Modified equivalent thermal network of Fig.1.3 (b).

The total heat loss from the absorber plate to the ambient surroundings via the top and the bottom (neglecting the side) of the plate is

$$\underset{\text{Loss}}{Q} = A_C U_L (T_p - T_a). \tag{3.6}$$

3.1.5 The Basic Flat-Plate Energy Balance Equation.

At steady state the performance of a solar energy collector can be determined by an energy balance, whereby the incident solar energy is devided into useful energy gain, optical loss, and thermal loss. The solar radiation absorbed by the collector (S) is equal to the difference between the incident solar radiation and the optical loss and is defined by Equation 3.3 and 3.4 . The thermal energy lost per unit area of collector surface from the collector to surroundings by conduction, convection, and radiation can be represented by the overall heat loss coefficient (U_L) times the difference between the mean absorber plate temperature ($T_{p,m}$) and the ambient temperature (T_a). At steady state the useful energy output of a collector is then the difference between the absorbed solar radiation and the thermal losses. Mathematically, the useful energy is given by,

$$Q_U = A_C [S - U_L (T_{p,m} - T_a)]. \tag{3.7}$$

The problem with this equation is that the mean absorber plate temperature cannot be calculated directly since it is a function of collector design, the incident solar radiation, and the entering fluid conditions. It is useful to reformulate Equation 3.7 so that the useful energy can be expressed in terms of the fluid inlet temperature of the fluid and a parameter called the collector heat removal factor (F_R) which can be evaluated from basic principles or measured experimentally.

A measure of collector performance is the collector efficiency (η) defined as the ratio of the useful energy gain, over some specified period, to the incident solar energy over the same time period.

$$\eta = \frac{\int Q_U dt}{A_C \int G_T dt} \tag{3.8}$$

where G_T is an instantaneous solar intensity.

3.1.6 Temperature Distribution Between Tubes and The Collector Efficientcy Factor

The temperature distribution between two tubes can be derived if it can be temporarily assumed that the temperature gradient in the flow direction is negligible [4]. Consider the sheet-tube configuration shown in Fig.3.6. The distance between the tubes is W, the tube diameter is D, and the sheet is thin with a thickness γ. Because the sheet material is a good conductor, the temperature gradient through the sheet is negligible. It will be assumed that the sheet above the bond is at some local base temperature, T_b. The region between the centerline separating the tube and the tube base can then be considered as a classical fin problem.

The fin, shown in Fig.3.7(a), is of length (W - D)/2. An elemental region of width Δx and unit length in flow direction is shown in Fig.3.7(b). An energy balance on this element yields

$$S\Delta x + U_L \Delta x\,(Ta - T) + \left(-K\delta \frac{dT}{dx}\right)_x - \left(-K\delta \frac{dT}{dx}\right)_{x+\Delta x} = O \tag{3.9}$$

where S is the absorbed solar energy defined by Equation 3.4. Dividing through by Δx and finding the limit as Δx approaces zero yields

$$\frac{d^2T}{dx^2} = \frac{U_L}{k\delta}\left[T - T_a - \frac{S}{U_L}\right]. \tag{3.10}$$

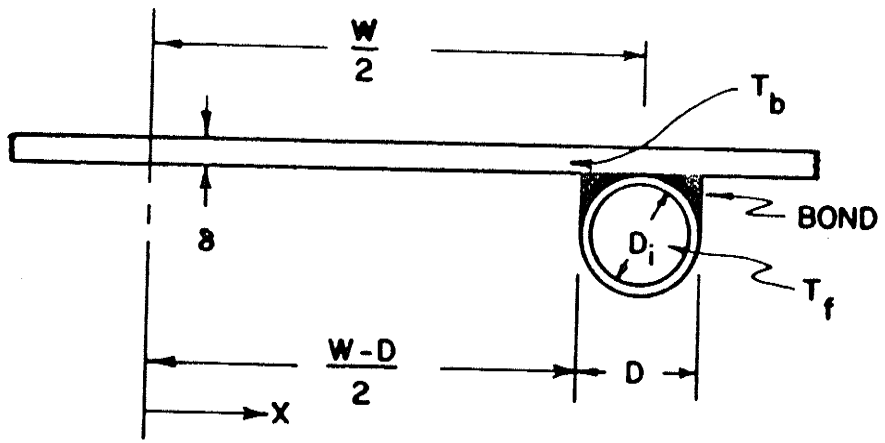

Fig.3.6 Sheet and Tube Dimensions

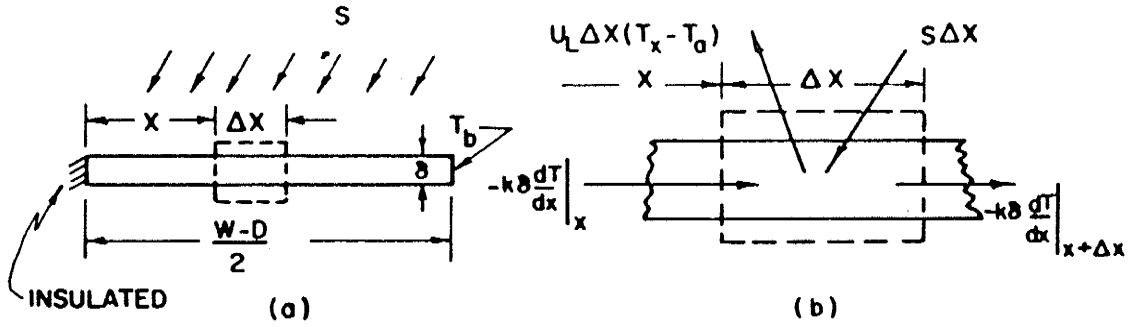

Fig.3.7 Energy Balance on Fin Element

The two boundary conditions necessary to solve this second-order differential equation are symmetry at the centerline and known root temperature;

$$\frac{dT}{dx}\Big|_{x=O} = O \qquad T\Big|_{x=(W-d)/2} = T_b \ . \tag{3.11}$$

Let $m^2 = U_L/k\delta$ and $\psi = T - T_a - S/U_L$, Equation 3.10 becomes

$$\frac{d^2\psi}{dx^2} - m^2\psi = O \tag{3.12}$$

which has the boundary conditions

$$\frac{d\psi}{dx}\Big|_{x=o} = O \ , \qquad \psi\Big|_{x=(W-d)/2} = T_b - T_a - \frac{S}{U_L} . \tag{3.13}$$

The general solution is then

$$\psi = C_1 \sinh mx + C_2 \cosh mx. \tag{3.14}$$

The constant C_1 and C_2 can be found by substituting the boundary conditions, Equation 3.13, into the general solution. The result is

$$\frac{T - T_a - \frac{S}{U_L}}{T_b - T_a - \frac{S}{U_L}} = \frac{\cosh mx}{\cosh m\,(W-D)/2} \ . \tag{3.15}$$

The energy conducted to the region of the tube per unit of length in the flow direction can now be found by evaluating Fourier's law at the fin base

$$q'_{fin} = -k\delta \frac{dT}{dx}\Big|_{x=(W-D)/2}$$

$$= \frac{k\delta m}{U_L}[S - U_L (T_b - T_a)] \tanh m\,(W-D)/2 \tag{3.16}$$

but $k\delta m/U_L$ is 1/m. Equation 3.16 accounts for the energy collected on only one side of the tube; for both sides, the energy collection is

$$q'_{fin} = (W-D)\ [S-U_L\ (T_b-T_a)]\frac{\tanh m\ (W-D)/2}{m\ (W-D)/2} \tag{3.17}$$

It is convenient to use the concept of a fin efficiency to rewrite Equation 3.17 as

$$q'_{fin} = (W-D)\ F\ [S-U_L\ (T_b-T_a)] \tag{3.18}$$

when

$$F = \frac{[\tanh m\ (W-D)/2]}{m\ (W-D)/2} \tag{3.19}$$

The function F is the standard fin efficiency for straight fins with rectangular profile. The useful gain of the collector also includes the energy collected above the tube region. The energy gain for this region is

$$q'_{tube} = D\ [S-U_L\ (T_b-T_a)] \tag{3.20}$$

and the useful gain for the collector of unit length in the flow direction is the sum of Equations 3.18 and 3.20.

$$q'_U = [(W-D)\ F + D]\ [S-U_L\ (T_b-T_a)]. \tag{3.21}$$

Ultimately, the useful gain from Equation3.21 must be transferred to the fluid. The resistance to heat flow to the fluid results from the bond and the fluid to tube resistance. The useful gain can be expressed in terms of these two resistances as

$$q'_u = \frac{Tb - Tf}{\frac{1}{(h_{f,i}\pi D_i)} + \frac{1}{C_b}} \tag{3.22}$$

where D_i is the inside tube diameter and $h_{f,i}$ is the heat transfer coefficient between the fluid and the tube wall. The bond conductance, C_b, can be estimated from knowledge of

the bond conductivity, k, the bond average thickness, γ, and the bond width, b. On a per unit length basis,

$$C_b = \frac{k_b.b}{\gamma} . \tag{3.23}$$

To eliminate T_b solve Equation 3.22 for T_b and substitute it into Equation 3.21, resulting in the useful gain,

$$q'_u = WF [S - U_L (T_f - T_a)] \tag{3.24}$$

where F', the collector efficiency factor, is

$$F' = \frac{UL}{W \left[\frac{1}{U_L[D+(W-D)F]} + \frac{1}{C_b} + \frac{1}{\pi D_i h_{f,i}} \right]} . \tag{3.25}$$

A physical interpretation for F' results from examining Equation 3.24. At a particular location, F' represents the ratio of the actual useful energy gain to the useful energy gain that would result if the collector absorbing surface had been at the local fluid temperature. Another interpretation for the parameter F' becomes clear when it is recognized that the denominator of Equation 3.25 is the heat transfer resistance from the fluid to the ambient air. This resistance will be given the symbol $1/U_O$. The numerator is the heat transfer resistance from the absorber plate to the ambient air. F' is thus the ratio of these two heat transfer coefficients

$$F' = \frac{U_o}{U_L} . \tag{3.26}$$

3.1.7 Temperature Distribution in Flow Direction.

The useful gain per unit of flow length as calculated from Equation 3.24 is ultimately the heat transfer to the fluid. The fluid enters the collector at temperature T_i and increases

in temperature until at the exit it is T_o. Referring to Fig.3.8, we can express an energy balance on the fluid flowing through a single tube of length Δy as

$$\left(\frac{\dot{m}}{n}\right) C_p T \Big|_{y} - \left(\frac{\dot{m}}{n}\right) C_p T \Big|_{y+\Delta y} + (\Delta y) q_u' = 0 \qquad (3.27)$$

where $\dot{m}$ is the total collector mass flow rate and n is the number of parallel tubes. Dividing through by Δy, finding the limit as Δy approaches zero, and substituting Equation 3.24 for q_u', we obtain

$$\dot{m} C_p \frac{dT}{dy} - nWF\,[S - U_L (T-T_a)] = 0 \qquad (3.28)$$

then the solution for the temperature at any position y is

$$\frac{T - T_a - \frac{S}{U_L}}{T - T_a - \frac{S}{U_L}} = e^{-[U_L n W F' y/\dot{m} C_p]} \qquad (3.29)$$

If the collector has length L in the flow direction, then the outlet fluid temperature, T_o, is found by substituting L for y in Equation 3.29. The quantity nWL is the collector area so that

$$\frac{T_o - T_a - \frac{S}{U_L}}{T_i - T_a - \frac{S}{U_L}} = e^{-[A_C U_L F'/\dot{m} C_p]} \qquad (3.30)$$

3.1.8 Collector Heat Removal Factor and Flow Factor.

It is convenient to define a quantity that relates the actual useful energy gain of a collector to the useful gain if the whole collector surface were at the fluid inlet temperature. This quantity is called the collector heat removal factor, F_R, and mathematically is given by

$$F_R = \frac{\dot{m} c_p (T_o - T_i)}{A_c [S - U_L (T_i - T_a)]} \qquad (3.31)$$

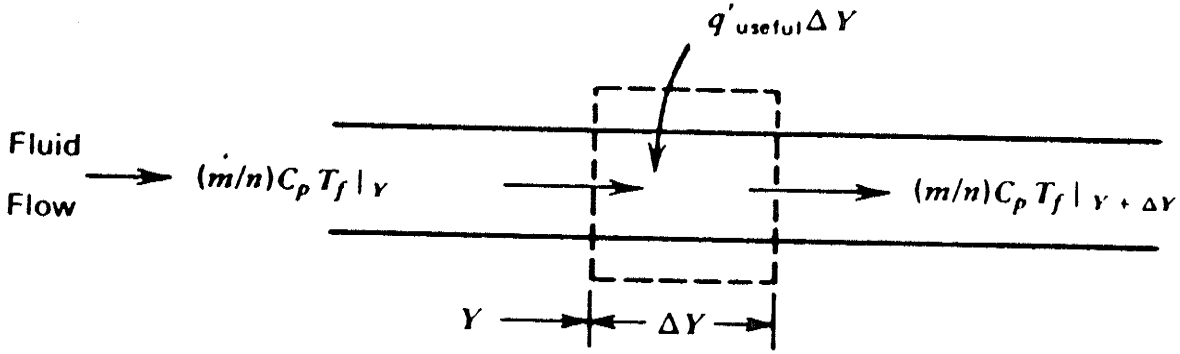

Fig.3.8 Energy Balance on Fluid Element

The collector heat removal factor can be expressed as

$$F_R = \frac{\dot{m}c_p}{A_cU_L}\left[\frac{T_o - T_i}{\frac{S}{U_L} - (T_i - T_a)}\right]$$

$$= \frac{\dot{m}c_p}{A_cU_L}\left[\frac{(T_o - T_a - \frac{S}{U_L})(T_i - T_a - \frac{S}{U_L})}{\frac{S}{U_L} - (T_i - T_a)}\right] \quad (3.32)$$

$$\text{or} \quad F_R = \frac{\dot{m}c_p}{A_cU_L}\left[1 - \frac{\frac{S}{U_L} - (T_o - T_a)}{\frac{S}{U_L} - (T_i - T_a)}\right] \quad (3.33)$$

which, from Equation 3.30 can be expressed as

$$F_R = \frac{\dot{m}c_p}{A_cU_L}\left[1 - e^{-(A_cU_LF'/\dot{m}c_p)}\right]. \quad (3.34)$$

The heat removal factor, F_R , is made up of two components which are the collector efficiency factor, F', and collector flow factor , F''. This factor is of common occurrence in heat exchanger calculations and is given by

$$F'' = \frac{\dot{m}c_p}{A_cU_LF'}\left[1 - e^{-(A_cU_LF'/\dot{m}c_p)}\right]. \quad (3.35)$$

$$\text{or} \quad F_R = F' \cdot F''. \quad (3.36)$$

The quantity F_R is equivalent to a conventional heat exchanger effectiveness, which is defined as the ratio of the actual heat transfer to the maximum possible heat transfer. The maximum useful energy gain (heat transfer) in a solar collector occurs when the whole collector is at the inlet fluid temperature; heat losses to the surroundings are then at a minimum. The collector heat removal factor times this maximum possible useful energy gain is equal to the actual useful energy gain, Q_u.

$$Q_u = A_cF_R[S - U_L(T_i - T_a)]. \quad (3.37)$$

Equation 3.37 is the most important equation for calculation of energy output from a solar flat plate collector.

3.1.9 Collector Efficiency and Performance Tests.

By combining Equation 3.4 and 3.37 the actual useful energy gain from a flat-plate solar energy collector becomes

$$Q_u = A_c F_R [(\tau\alpha)_{ave}^{\bullet} I_T - U_L (T_i - T_a)]. \quad (3.38)$$

Equation 3.38 may be rewritten as efficiency of solar collection, that is, useful energy gain divided by the total absorbed radiation that is incident on the collector surface ($A_C I_T$) and is given numerically by

$$\eta = \frac{Q_u}{A_c I_T}$$

or

$$\eta = F_R (\tau\alpha)_{ave} - F_R U_L \frac{(T_i - T_a)}{I_T}. \quad (3.39)$$

For a specific collector operating at a constant fluid circulation rate, the values of F_R and U_L can be assumed constant with little error regardless of the solar intensity and the temperature. Equation 3.39 then becomes a straight line on a graph of efficiency versus $(T_i-T_a)/I_T$(see Fig.3.9). The mathematical characteristics of this line are: the Y-intercept is $F_R(\tau\alpha)$ and the slope is $(-F_R U_L)$. If experimental data, including the heat collected (Q_u) at various temperatures and solar conditions are plotted on the graph, with the efficiency as the vertical axis and $(T_i-T_a)/I_T$ as the horizontal axis, the best straight line through the data points correlates collector performance with solar and operating conditions. The Y-intercept of the performance line corresponds to the point where the inlet fluid temperature is equal to the ambient temperature, that is, $T_i = T_a$, and the collector efficiency is a maximum. At the intersection of the line with the horizontal axis collector efficiency is zero. This condition represents such a low radiation level or such a high temperature for the fluid supply to the collector that the heat losses are equal to the

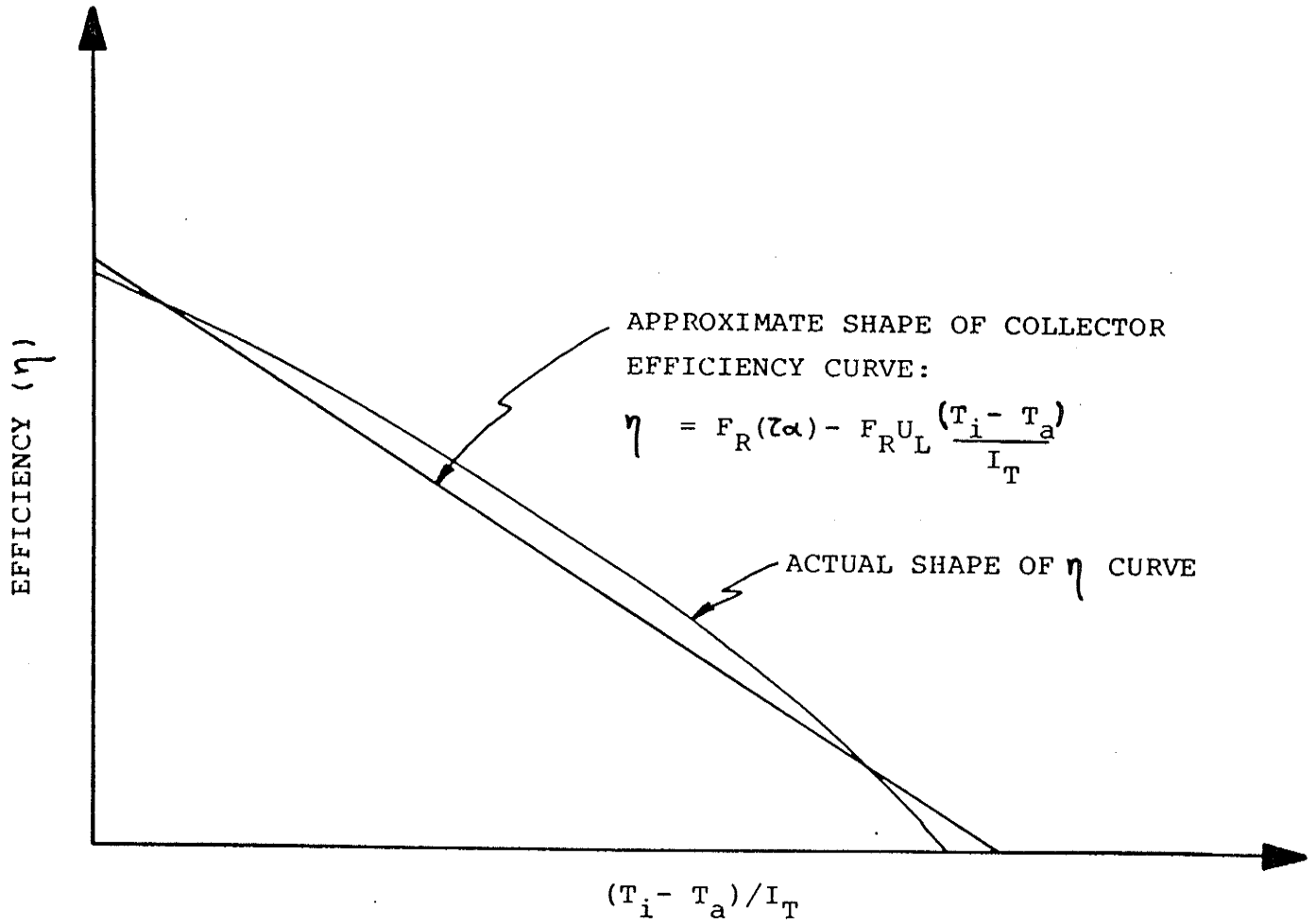

Fig.3.9 **Solar flat-plate performance curves.**

solar absorption, and no useful heat is delivered from the collector. That is $\eta = 0$ and $I_T F_R \tau\alpha = U_L F_R (T_i = T_a)$.

The linearity of Equation 3.12 depends on the assumption that the values of $F_R \tau\alpha$ and $F_R U_L$ are constant and independent of T_i, T_a, and I_T. Although the influence is small, F_R and U_L both depend on collector temperature and the fluid inlet temperature. Since radiation loss is a function of the fourth power of the inlet and ambient temperatures, and the convection loss is dependent of the first power of temperature, the heat loss coefficient increases with a rise in collector temperature and with temperature difference. Therefore the actual efficiency versus $(T_i-T_a)/I_T$ must curve slightly downward as the ratio of the temperature difference to solar radiation increases. But the magnitude of this effect is small and in the usual operating range its effect is seldom encountered. Therefore, the linear assumption is adequate for pratical operating and/or design purposes [5].

3.2 Water Storage

For many solar energy systems water is an ideal storage fluid. It is readily available at a low cost and energy may be readily added and removed from the system and the fluid media may be used to transport the heat from the collector directly, thus eliminating the temperature drop between the transport fluid and the storage medium which is required by a heat exchanger. Such a water storage system is represented in Fig.3.10.

Forced circulation is shown in Fig.3.10, but the system could be a thermosyphon (natural circulation) type. The energy storage capacity of a water (or liquid) storage unit at uniform temperature operating over a finite temperature difference is given by,

$$Q_S = (mc_p)_S - (\Delta T_S). \qquad (3.40)$$

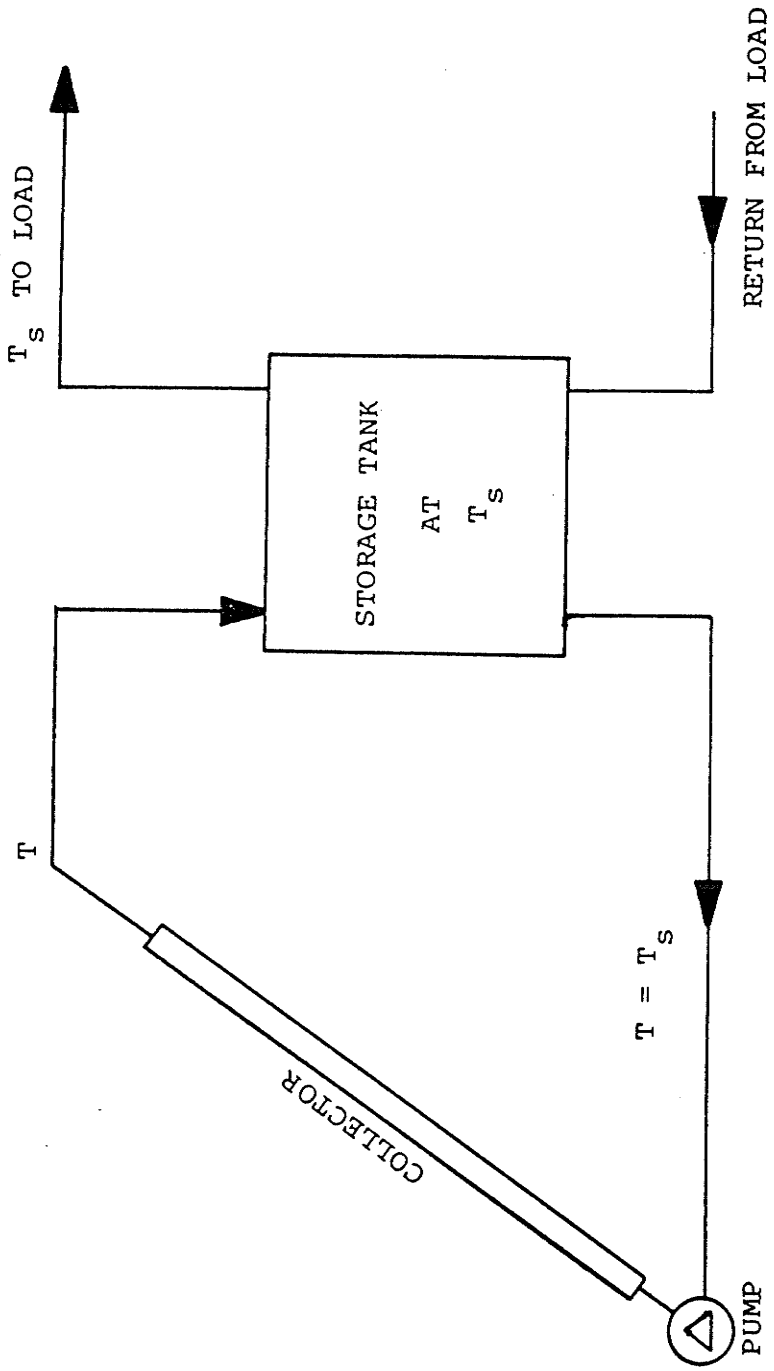

Fig.3.10 **A typical system using water storage.**

Q_S is the total heat capacity for a cycle operating through the temperature range ΔT_S with a storage mass, m. The temperature range over which such a system can operate is limited by the process and the collector heat loss.

For a nonstratified storage unit, as shown in Fig.3.11, an energy balance on the storage unit yields,

$$(mc_p)_S \frac{dT_S}{dt} = Q_U - L - (UA)_S (Ts - Ta). \quad (3.41)$$

The last term represents the heat loss from the storage system and L represents the load on the system.

The water storage unit may be operated with a significant degree of stratification, that is, with the top of the storage tank considerably hotter than the bottom. In this case, the storage can be modeled by dividing it into N nodes (sections), with an energy balance performed on each section of the tank. The result is a set of N differential equations that can be solved for the temperature of the N nodes as function of time.

To formulate these equations, it is necessary to make assumptions about how the water entering the tank is distributed to the various nodes. For example, for the five-node tank shown in Fig.3.12, water from the collector enters at a temperature T_O which is between $T_{S,2}$ and $T_{S,3}$. Or it can be assumed that all the water from the inlet finds its way down inside the tank to node 3, where the density nearly matches that of the water in the tank at node 3. Alternatively, it can be assumed that the inlet water distributes itself in some way to nodes 1,2, and 3. Unfortunately it is not now possible to state with certainty which is the best model, as the actual flow will depend on the design of a particular tank, the size, the elevation, and design of inlet and outlet, and the condition of the flow of the entering and leaving fluid streams.

Stratification is a phenomenon that is difficult to evaluate without considering the end use. If the load can use the energy at the same efficiency without regard to its temperature, then, maximum stratification would be provided by the lowest possible

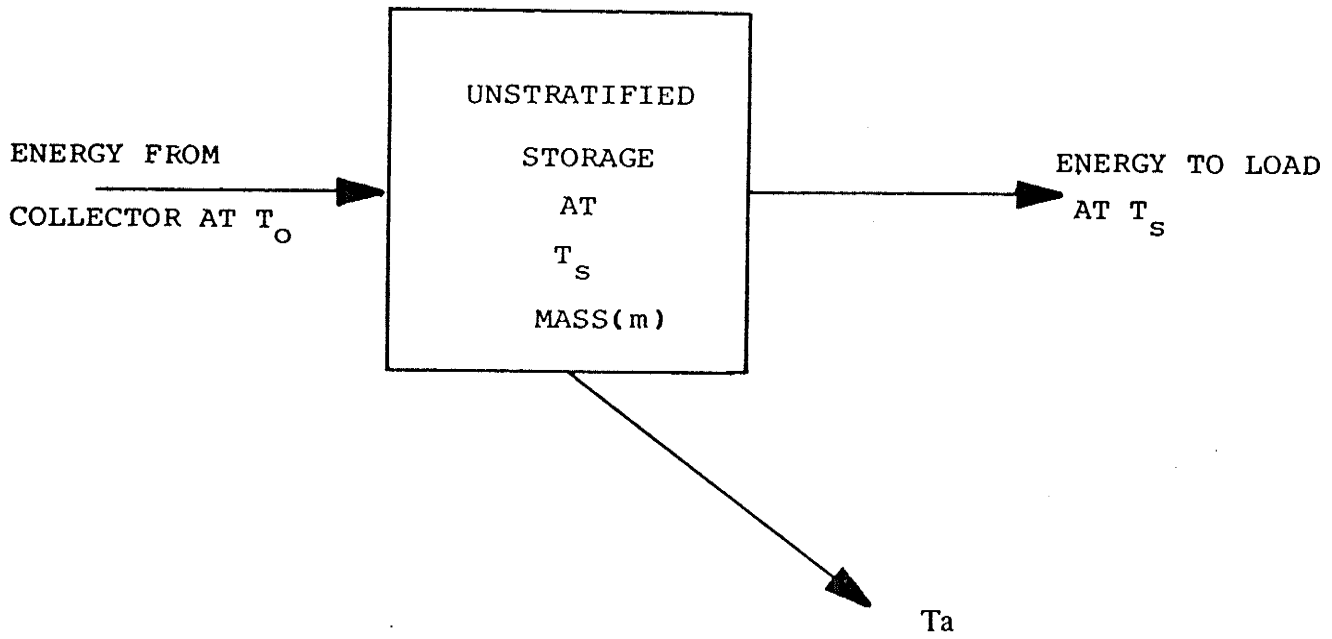

Fig.3.11 **Unstratified storage of mass operating with time-dependent temperature (T_S) in ambient temperature T_a.**

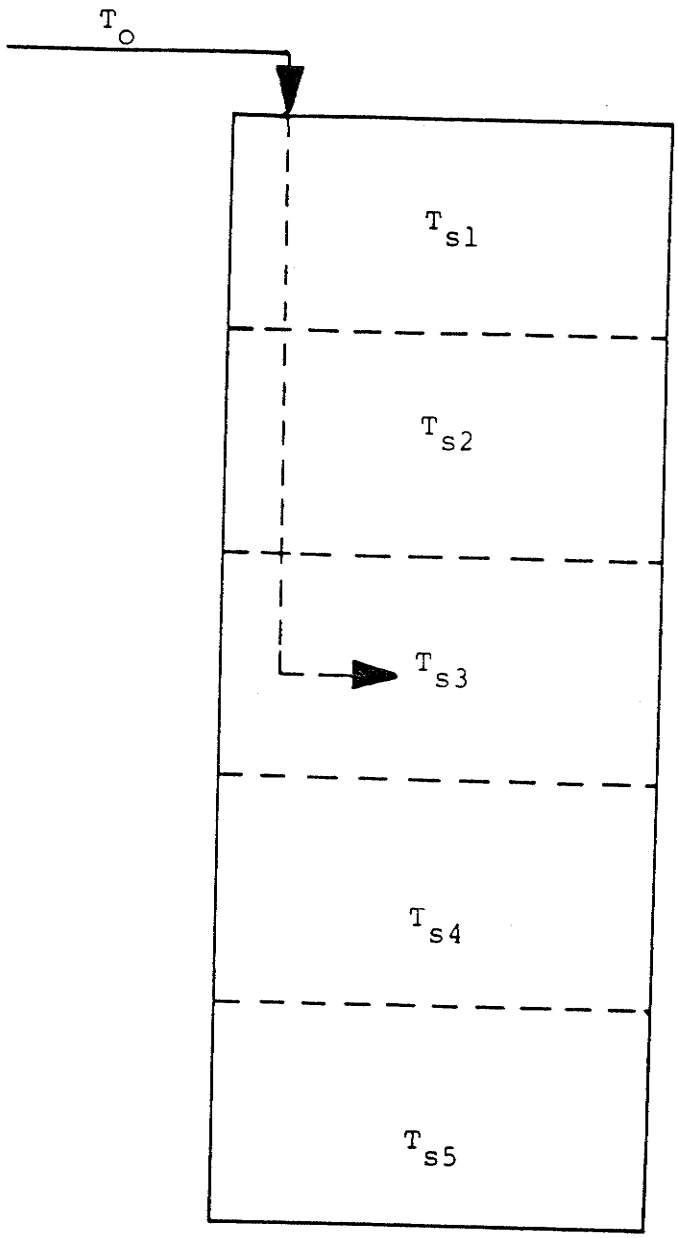

Fig.3.12 **A hypothetical five-node storage tank $T_{s,2} > T_o > T_{s,3}$. Water can be considered to enter at node 3, or to be distributed among nodes 1, 2, and 3.**

temperature near the bottom of the storage and which would maximize the efficiency of the collector. If the temperature of the energy is important to the load, then, the stratification may have to be reduced.

There are two factors that can significantly reduce stratification. First, a stratified storage tank will have a tendency to destratify over time due to diffusion and wall conduction effects. These effects have been studied experimentally by Lavan and Thompson [28]. The second factor is the case where there is an auxiliary heat supply in the tank, the stratification may then be reduced by a natural convection depending on the location of the heat source.

3.2.1 Component Model.

In previous sections performance of the solar energy collector and the storage unit were mathematically modeled. For a flat-plate solar energy colletor, Equation 3.37 is applicable, and can be written as

$$Q_U = A_c F_R [S - U_L (T_i - T_a)]^+ \quad (3.42)$$

The "+" sign implies that only positive values should be used. For example, the operation of a forced circulation collector would not occur when Q_U was less than zero. In a real situation, this is accomplished by comparing the temperature of the fluid leaving the collector (i.e., in the top header) with the temperature of the fluid leaving the storage tank and operating the pump only when the difference in temperatures is positive. The useful energy is also given by

$$Q_U = (\dot{m} c_p)_C (T_o - T_i) \quad (3.43)$$

where $\dot{m}$ is mass flow rate of the circulating fluid through the collector.

If the storage is a fully-mixed sensible heat storage unit, its performance is given by Equation 3.41. Here again

$$Q_U - L - (UA)_S (T_s - T_a) = (\dot{m} c_p)_S \frac{dT_S}{dt} .$$

In some experiments that are run at a no load condition, Equation 3.41 becomes

$$Q_U - (UA)_S (T_s - T_a) = (\dot{m} c_p)_S \frac{dT_S}{dt} . \quad (3.44)$$

The performance models discussed so far have been based on the fundamental equation describing the behavior of the equipment. Models can also be expressed as empirical or stochastic representations of operating data from particular items of equipment. These empirical relations may be in form of equations, graphs, or tabular data.

There is another factor that can affect the performance of a system, that is, heat loss from the ducting or piping to the ambient surroundings, if the ducting or piping are not well insulated. This loss can be accounted for by simple modifications to Equation 3.42, as described in the next section.

3.2.2 Duct and Pipe Loss.

The energy loss from ducts and pipes leading to and and returning from the collector in a solar energy system can be significant. Beckman [5] has shown that the combination of ducts or pipes plus the solar collector is equivalent in thermal performance to a solar collector with different values of U_L and ($\tau\alpha$).

A presentation of the temperature change in the system fluid is shown in Fig.3.13. The fluid temperature is lowered by an amount ΔT_i before it enters the solar collector due to losses to the ambient air at temperature T_a. The fluid passes through the collector and it is heated to collector output temperature. This temperature is then reduced to T_o as the fluid loses heat to the ambient surroundings while passing through the outlet ducts.

Thus, the energy heat gain can be related to the energy gain of the collector minus duct losses by the following rate equation.

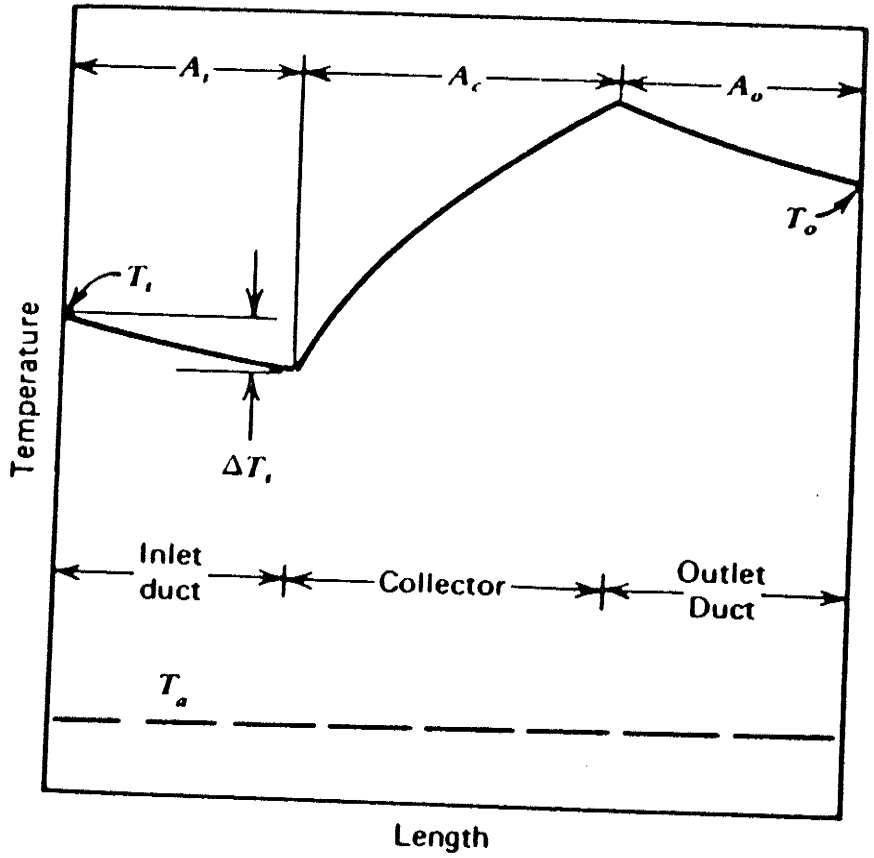

Fig.3.13 **Temperature changes through a duct-collector system. From Beckman, W.A.**

$$Q_U = A_C F_R [I_T (\tau\alpha) - U_L (T_i - \Delta T_i - T_a)] - \text{Loss}. \quad (3.45)$$

The duct losses are equal to the integrated losses over the inlet and outlet ducts and are given mathematically by

$$\text{Loss} = U_d \int (T - Ta)\, dA \quad (3.46)$$

where U_d is the loss coefficient of the ducts. It is possible to integrate Equation 3.46, but in well-designed systems the losses from the ducts will be small. The integral can be approximated to an adequate degree of accuracy in terms of inlet and outlet temperatures by,

$$\text{Loss} = U_d A_i (Ti - Ta) + U_d A_o (T_o - T_a) \quad (3.47)$$

where A_i and A_O are the area of the inlet and the outlet ducts from which the heat losses occur.

3.2.3 Solar Domestic Hot Water Systems.

The basic elements in SDHW systems can be arranged in several configurations. The most common of these are shown in Fig.3.14. Auxiliary energy is added in two different ways. However, they are interchangeable.

A passive water heater, that is, a thermosyphon system, is shown in Fig.3.14(a). The storage tank is located above the collector and water circulates by natural convection. Whenever the solar collector adds energy to the water it establishes a density difference causing the natural convection. Fig.3.14(b) shows an example of a forced circulation system. A pump is required, which is usually controlled by a differential thermostat turning on the pump when the temperature at the top header is higher than the temperature of the water in the bottom of the tank by a sufficient margin to assure control

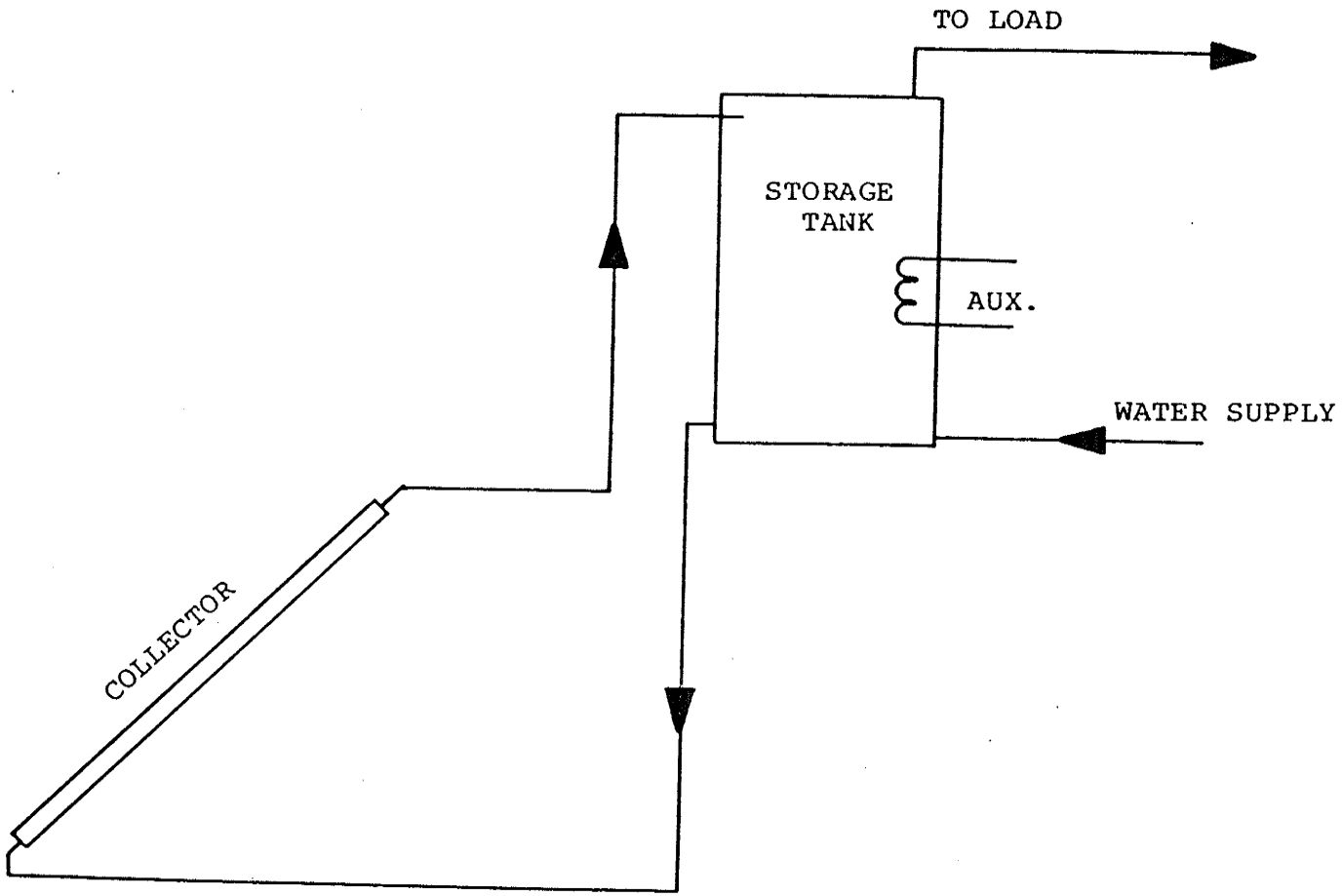

Fig.3.14 **Schematics of common configurations of water heater. (a) A thermosyphon SHW system.**

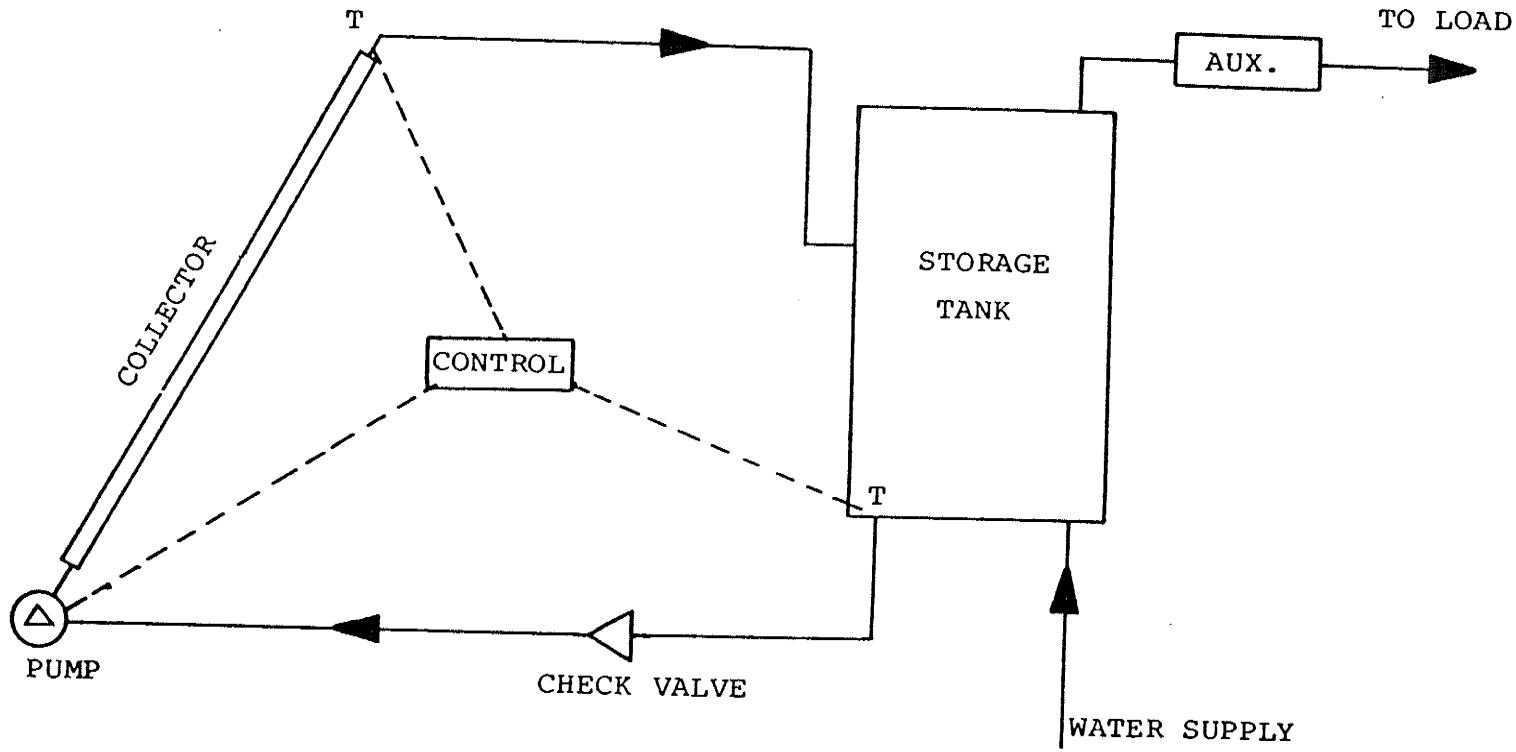

(b)

Fig.3.14 **Schematics of common configurations of water heater.**

(b) A one-tank forced circulation system.

stability. A check valve is needed to prevent reverse circulation and the resultant night time thermal losses from the collector. Auxiliary energy is shown added to the water in the pipe leaving the tank to the load by an in-line heater having no storage capacity.

Some details of flat-plate energy collectors and domestic hot water storage systems have been described in this section. More specific details in thermosyphon SDHW systems were described in Chapter 2. Also, in Chapter 2, studies of thermosyphon SDHW systems and investigations of the effects of stratifications on SDHW systems were reviewed (sections 2.2 and 2.3, respectively).

Chapter 4

Experimental Programs

In chapter three the theory and design of a flat-plate collector and liquid-based storage systems were described. Chapter 2 reviewed investigations on thermosyphon systems and the effects of stratification on SDWH system performance. In this chapter the details of the experimental programs, the equipment and instrumentation, the data collection system, mathematical analysis, and the cumputer program for the mathematical anlyses are described. Finally, the experimental results are shown in terms of system performance characteristics.

4.1 Description of Equipment.

In this investigation, for comparison purposes two operationally different configurations for liquid storage were used in a SDWH system. These configurations are designated Type A and Type B. Type A refers to a thermosyphon SDWH system with a conventional storage tank. Type B refers to the SDWH system as in Type A but connected with another storage unit on the top with horizontal baffles inside. Four 25 mm diameter holds were dilled in each baffle to permit the liquid pass through the baffles. The configurations of type A and Type B are illustrated in Fig. 4.1 and 4.2, respectively.

In both types of tank configurations energy was added to the system at the highest elevation. All connecting piping was 19 mm ID hose insulated by commercial insulation. The collector was 2.13X1.63 m with absorption area of 2.35 m^2. The collector performance, in terms of efficiency, was provided by manufacturer as follow:

$$\eta = 0.736 - 4.98 \frac{(T_i - T_a)}{I_T} .$$

The construction details of the two storage tanks are described in Appendix A.

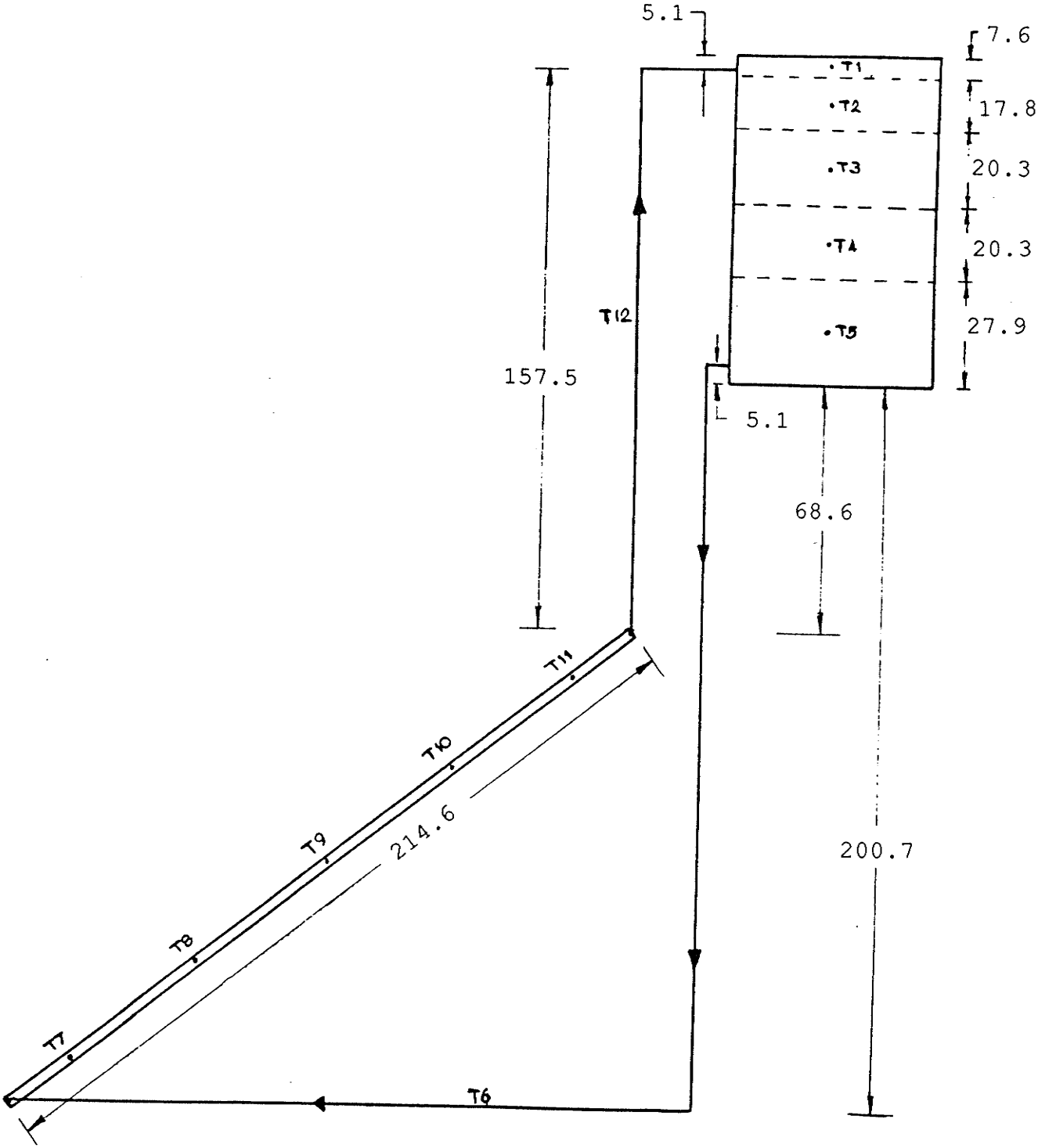

Fig.4.1 A Conventional Thermosyphon SDHW System, Type-A.

note : all dimensions are in cm

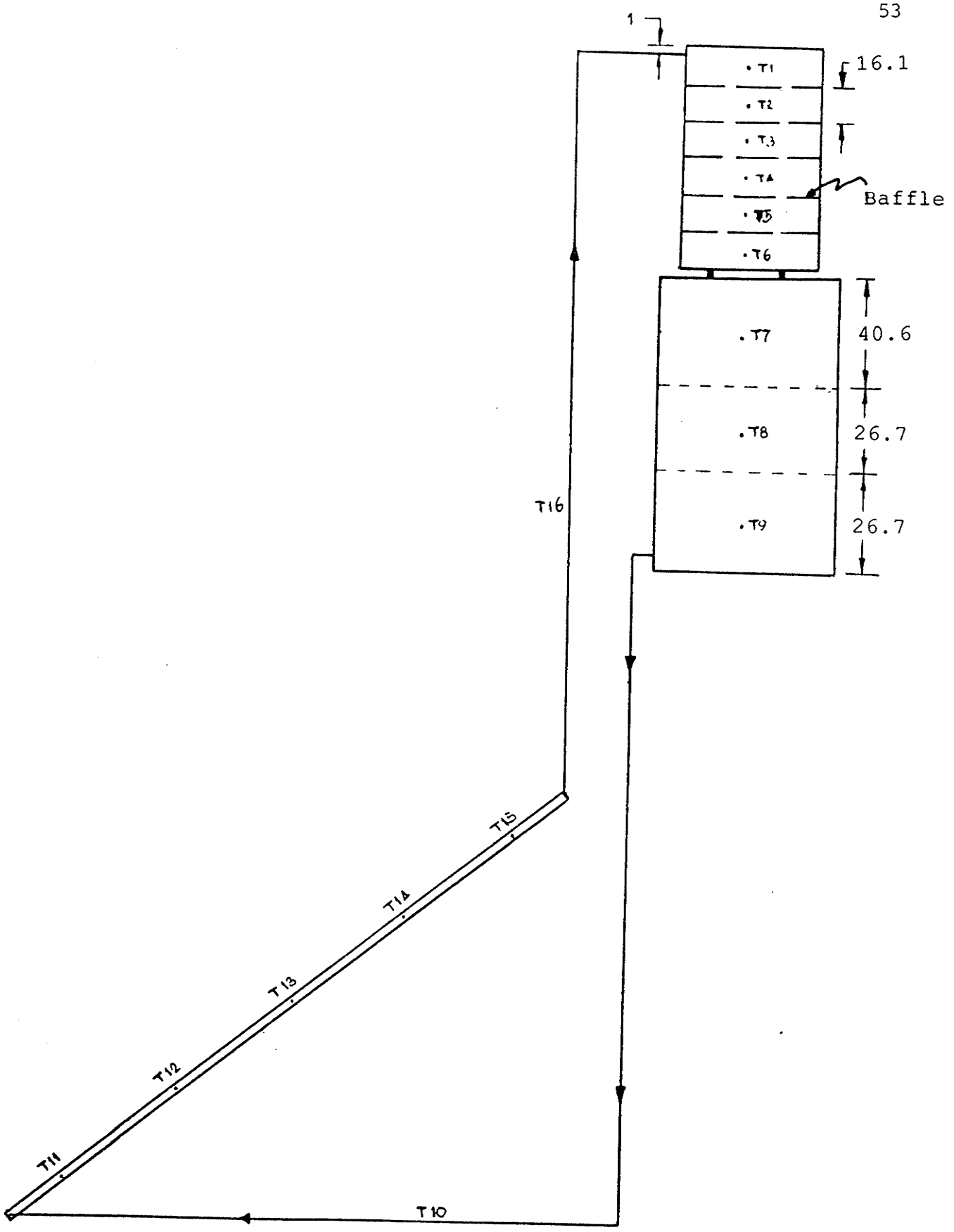

Fig.4.2 A Thermosyphon SDHW System with Baffles, Type-B.

note : all dimensions are in cm

4.2 Instrumentation and Data Collection.

Total radiation (I_T) incident on the collector surface was measured by a pyranometer mounted in the same plane as the collector (tilt angle 39 degrees). The orientation of the collector was changed hourly so that it was normal to the direct radiation. The collector system and the pyranometer were located free from shadows. The output from the pyranometer was fed directly to a strip chart recorder. The acquisition of data was accomplished by using a 20 channel programmable data logger (Hewlett Packard model #3421a) equipped with a computer for data processing.

Temperatures were measured throughout the system by using type-T (copper-constantan) thermocouples. The tank vertical temperature profile was measured by thermocouples inserted into the tank at evenly spaced intervals. Two of the thermocouples were mounted at the outlet and the inlet ports of the collector. A thermocouple was placed in a shaded area near the test equipment in order to measure the outside ambient temperature. The output signals from the thermocouples were fed directly into the data logger. These signals were read at one hour intervals in order to coincide with the changing of the colector's orientation. The arrangement of instrumentation is illustrated in Fig.4.3.

4.3 Mathematical Analyses.

In this section mathematical processes used in experiments are described. The method of computing the mean storage temperature and the evaluation of the mean storage temperature from experimental data are described in section 4.3.1. The indirect method for evaluating thermosyphon mass flow rate is described in section 4.3.2.

4.3.1 Mean Storage Temperatures [7].

Examining the storage and the solar collector separately, instantaneous heat balance equations were obtained as follows:

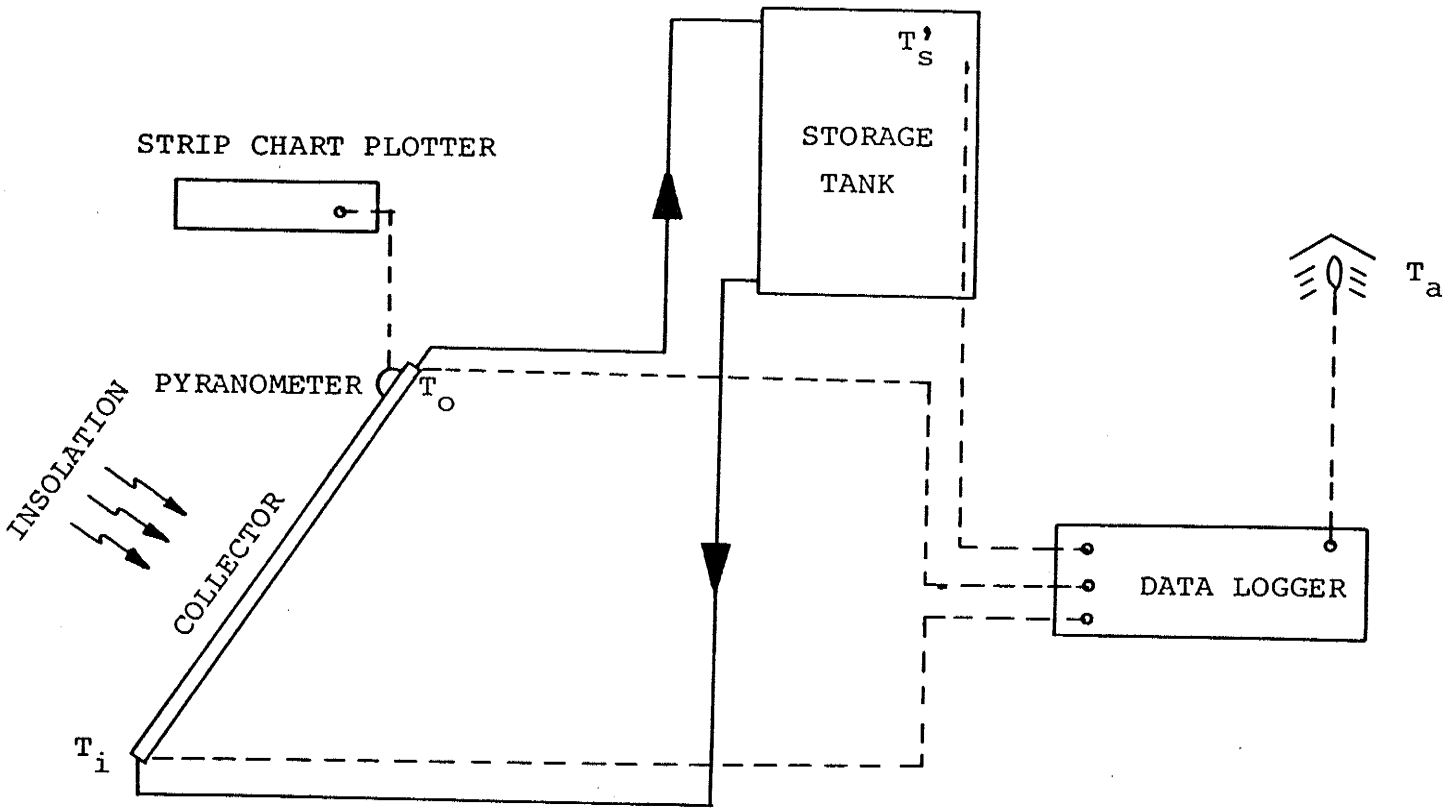

Fig.4.3 The Arrangement of Instrumentation.

For the collector

$$\eta = F_R(\tau\alpha) - F_R U_L \frac{(T_i - T_a)}{I_T} .$$

The collector efficiency is defined by

$$\eta = \frac{Q_u}{A_C I_T} . \tag{4.1}$$

For the storage unit, assuming that no heat loss occured in the connecting piping,

$$Q_U = Q_{LT} + C\frac{dT_m}{dt} \tag{4.2}$$

where Q_{LT} is the thermal loss from the storage tank to ambient surroundings. C is the thermal capacity of the storage including the thermal capacity of the tank body, $m_w c_{pw} + m_T c_{pT}$.

Combining Equations 4.1 and 4.2 and rearranging, the energy balance equation for the storage becomes

$$\eta A_c I_T = Q_{LT} + C\frac{dT_m}{dt} . \tag{4.3}$$

Where the loss from the storage (Q_{LT}) is expressed by

$$Q_{LT} = U_T A_T (T_m - T_a) . \tag{4.4}$$

Again, combining equations 4.3 and 4.4, using finite-difference methods and rearranging, the new mean storage temperature can be obtained by:

$$T_{m,n} = \frac{[\eta A_c I_T + U_T A T_a + C(T_m/\Delta t)]}{[U_T A_T + (C/\Delta t)]} . \tag{4.5}$$

U_T is an average overall heat loss coefficient between the storage tank and the surroundings. A_T is the area of the storage tank from which the heat loss (Q_{LT}) occurs. The numerical value of collector efficiency (η) in Equation 4.5 can be obtained from Equation 3.39.

Equation 4.5 is used to determine the computed value of mean storage temperature. The mean storage temperature can also be evaluated from experimental data by using the following relationship [10,11].

$$T_m = \frac{[\Sigma C_i T_i]}{\Sigma C_i}, \qquad (4.6)$$

where C_i is the thermal capacity for each layer of water and T_i is the temperature for the layer. Fig.4.5 shows the computer flow chart which is used to determine the mean storage temperatures.

4.3.2 Thermosyphon Mass Flow Rate [14].

Mass flow rate in a thermosyphon SDWH system is not constant but depends on the buoyancy force caused by the temperature differences throughout the system. These temperature differences are in turn dependant to a large extent upon the solar radiation incident on the collector surface. In this section an indirect method is used to evaluate the flow by equating the hydrostatic pressure caused by the density difference to the total friction losses in the system.

The total hydrostatic pressure (ΔH) throughout the system can be expressed by

$$\Delta H = \int_{tank} \rho g dy + \int_{down-comer} \rho g dy - \int_{collector} \rho g dy - \int_{riser} \rho g dy \qquad (4.7)$$

where ρ is the fluid density, g is the acceleration due to gravity, and y is the thickness of each fluid layer in vertical direction.

The collector hydrostatic pressure is computed by assuming the collector temperature varies linearly from inlet to outlet and is expressed by

$$T_c = T_i + (T_o - T_i)\frac{Z}{L}. \tag{4.8}$$

Where Z/L is the fraction of the distance through the collector and the temperature of the fluid at the point Z is T_c. The assumption (Equation 4.8) was supported by references [5,9].

The hydrostatic pressures in the riser and the down-comer are computed by assuming the temperatures along these sections are constant. The storage tank hydrostatic pressure is computed by using the vertical temperature profile as measured in the experiments.

Then, the thermosyphon mass flow rate was computed by balancing the total hydrostatic pressure against to the total friction losses in the system as:

$$\Delta H = \Sigma f.\frac{(l)}{d}.\frac{\rho v^2}{2} \tag{4.9}$$

where l/d is the length-diameter ratio. The friction factor (f) is calculated from the following relationships:

Laminar:	$f = 64/N_{Re}$	$N_{Re} \leq 2000$
Transition:	$f = 0.0243 + 3.85\times10^{-6}\cdot N_{Re}$	$2000 < N_{Re} < 4000$
Turbulent:	$f = 0.316/N_{Re}$	$N_{Re} \geq 4000$

Since the thermosyphon mass flow rate is constant throughout the system, at any particular time, Equation 4.9 can be rewritten in terms the flow rate as follows:

$$\Delta H = \frac{\dot{m}^2}{2}.\Sigma\left[f.\frac{(l)}{d}.\frac{1}{\rho A^2}\right], \tag{4.10}$$

when

$$\Sigma\left[f.\frac{(l)}{d}.\frac{1}{\rho A^2}\right] = f.\frac{(l)}{d}.\frac{1}{\rho A^2}\Big|_{\text{collector}} + f.\frac{(l)}{d}.\frac{1}{\rho A^2}\Big|_{\text{riser}} + f.\frac{(l)}{d}.\frac{1}{\rho A^2}\Big|_{\text{down-comer}} + \Sigma \text{ losses from fittings.} \tag{4.11}$$

Then, the thermosyphon mass flow rate at any particular time is given by

$$\dot{m} = \sqrt{\frac{2\,(\Delta H)}{\Sigma\,[\,f.\,\frac{(l)}{d}\,.\,\frac{1}{\rho A^2}\,]}}\quad . \tag{4.12}$$

Fig.4.4 shows the computer program flow chart that used to determine the thermosyphon mass flow rate.

4.3.2.1 Friction Losses from Valves and Fittings [30].

The losses from fittings in Equation 4.11 were determined from the losses through valve and fittings in the experimental systems. The losses which are generally given in terms of resistance coefficient (K) and indicated static head losses through a valve or fitting in terms of velocity head or equivalent length in pipe-diameters (l/d) that will cause the same head loss as the fittings.

From Darcy's formula, head loss through a pipe is

$$h = f.\,\frac{(l)}{d}\,.\,\frac{V^2}{2g} \tag{4.13}$$

and loss through a valve is

$$h = K\,\frac{V^2}{2g}\quad . \tag{4.14}$$

Therefore

$$K = f\,\frac{(l)}{d} \tag{4.15}$$

Then the term, losses, in Equation 4.11 can be determined by Equation 4.16 below

$$\Sigma\,\text{losses} = \sum_{\text{fitting}}\,[f.\,\frac{(l)}{d}\,.\,\frac{1}{\rho A^2}\,] \quad \underline{\text{OR}} \quad \sum_{\text{fitting}}\,[\,K\,\frac{1}{\rho A^2}\,]\quad . \tag{4.16}$$

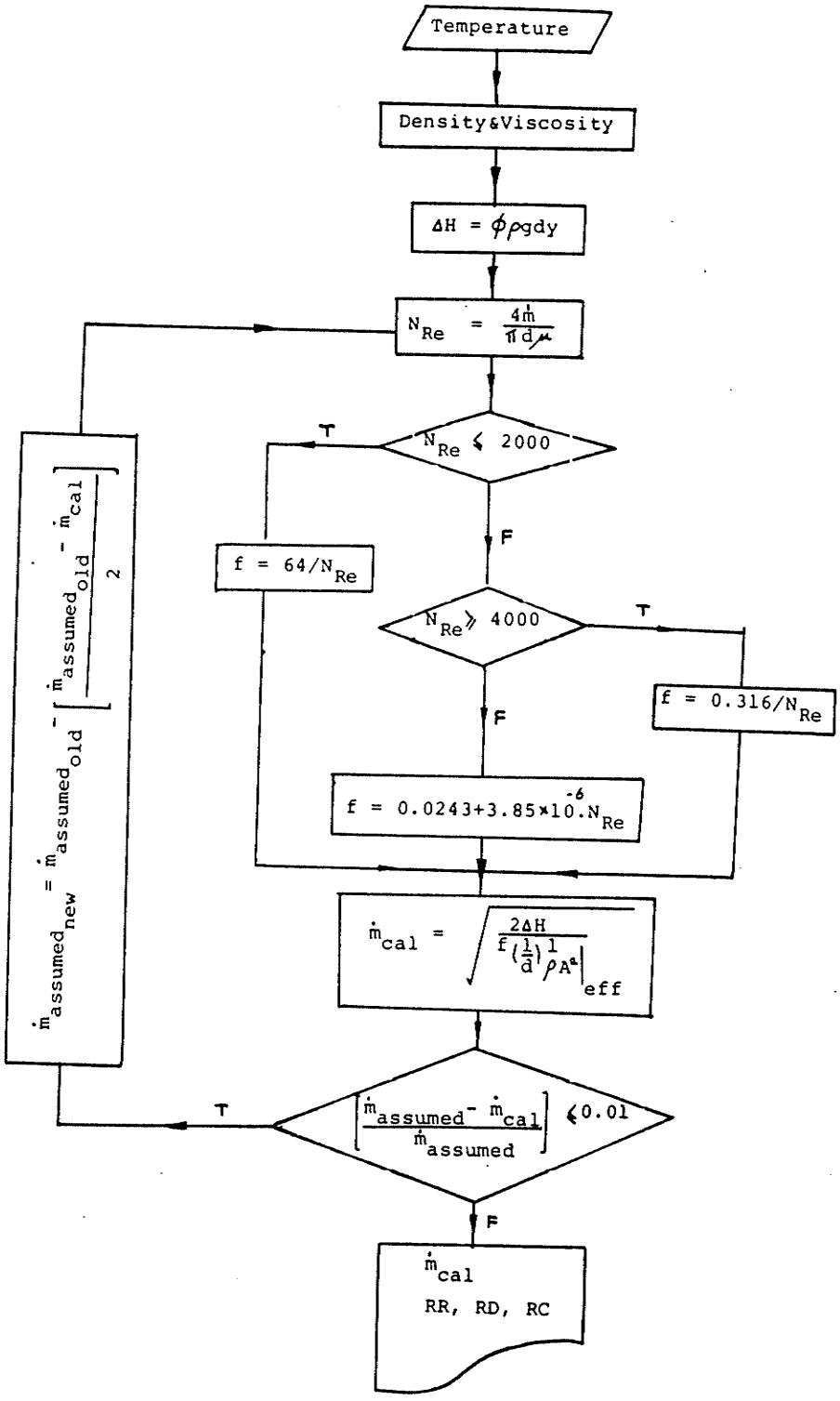

Fig.4.4 The Computer Flow Chart used to determine Thermosyphon Mass Flow Rate.

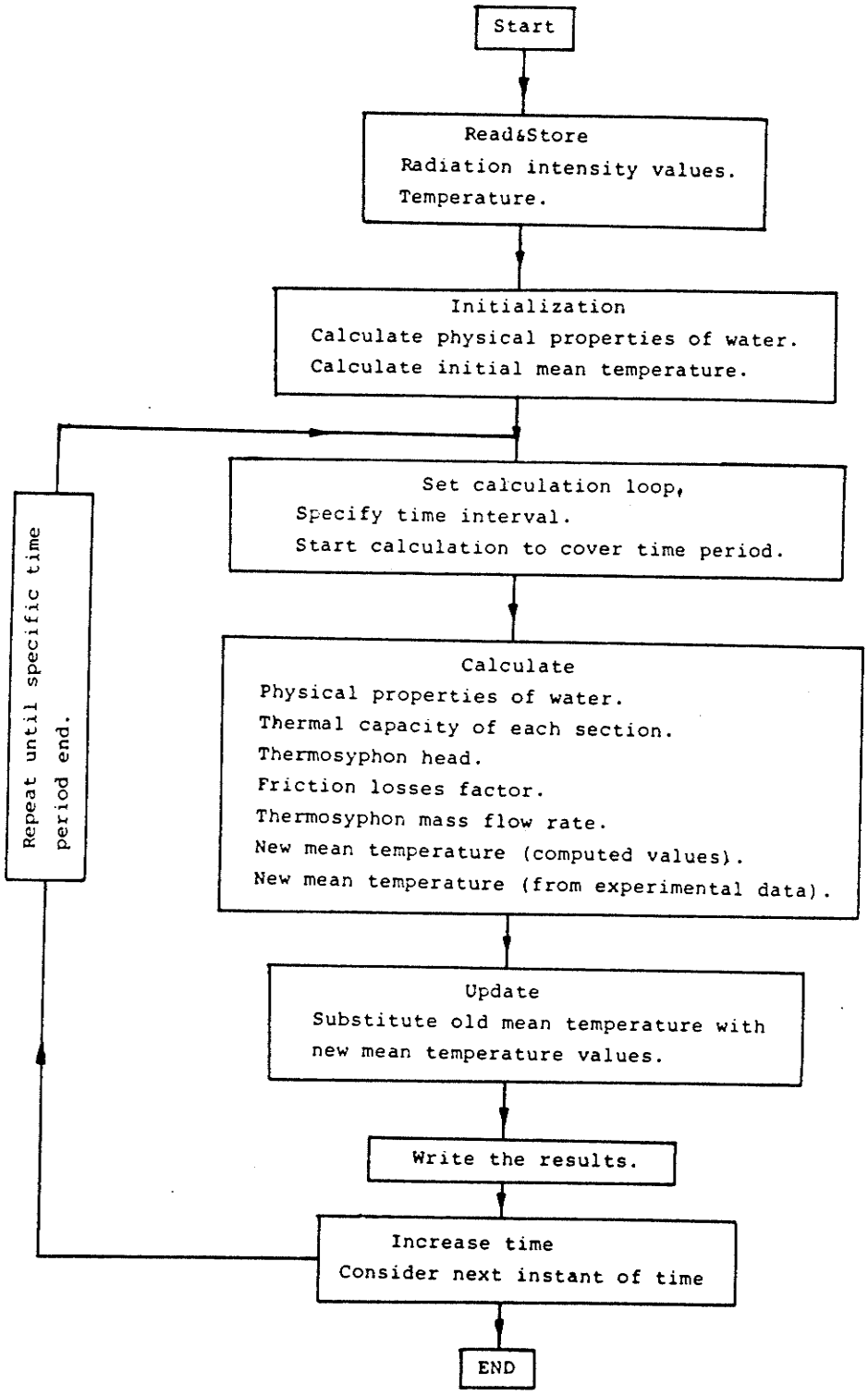

Fig.4.5 The Flow Chart of The Computer Program used to determine The Mean Storage Temperatures.

4.4 Experimental Results.

The thermosyphon SDHW systems, Type A and Type B as shown in Fig.4.1 and 4.2, were located on the south side of the engineering building at The University of Manitoba. The experiments were operated during the months of August-September 1987, under no-load conditions. Operating the thermosyphon system without a load allowed the mass flow rate to be evaluated without complexities. Operating at no-load condition allows the optimum time period for the water draw to be determined and a high degree of stratification to be maintained.

Three experimental investigations were conducted, namely, Experiment A, B1, and B2. Each experimental result is described separately and the following performance characteristics were investigated in each experiment:

- thermosyphon mass flow rate,
- mean storage temperature,
- vertical storage tank temperature profile changes,
- collector inlet/outlet temperature,
- degree of stratification, and
- collector efficiency.

In this section, one set of data for each experiment is shown as a representative sample of each investigation. The rest of the experimental data are shown in Appendix C.

4.4.1 Results of Experiment - Type A.

Experiment A was conducted using a domestic water heating storage tank as illustrated in Fig.4.1 with the details of the tank shown in Appendix A. The data were collected in August,1987. System performance characteristics of experiment A are shown in Fig.4.6 to 4.8.

4.4.2 Results of Experiments - Type B1 and B2.

Experiment B was conducted by connecting an extension tank directly to the top of the storage tank of type A. Inside the extension tank, horizontal baffles were mounted (see Fig.A2 Appendix A) in order to investigate the effects of the horizontal baffles on stratification. Experiment B was conducted using two different methods, namely, Experiments B1 and B2 described as follows:

Experiment B1: operated with the uniform temperature of water at the starting time.

Experiment B2: operated with the stratified temperature of water at the starting time.

Results of Experiments B1 and B2 are shown in Fig.4.9 to 4.14. Also Fig.4.15 shows a plot of all experimental data sets in order to indicate the degree of stratification, the slope of the temperature gradient as the time-dependent characteristics. The collector efficiencies for Experiments A, B1, and B2 are plotted in the same graph as shown in Fig.4.16.

The performance characteristics for the three different experiments are shown in the Figures and these performance characteristics are discussed in Chapter 5.

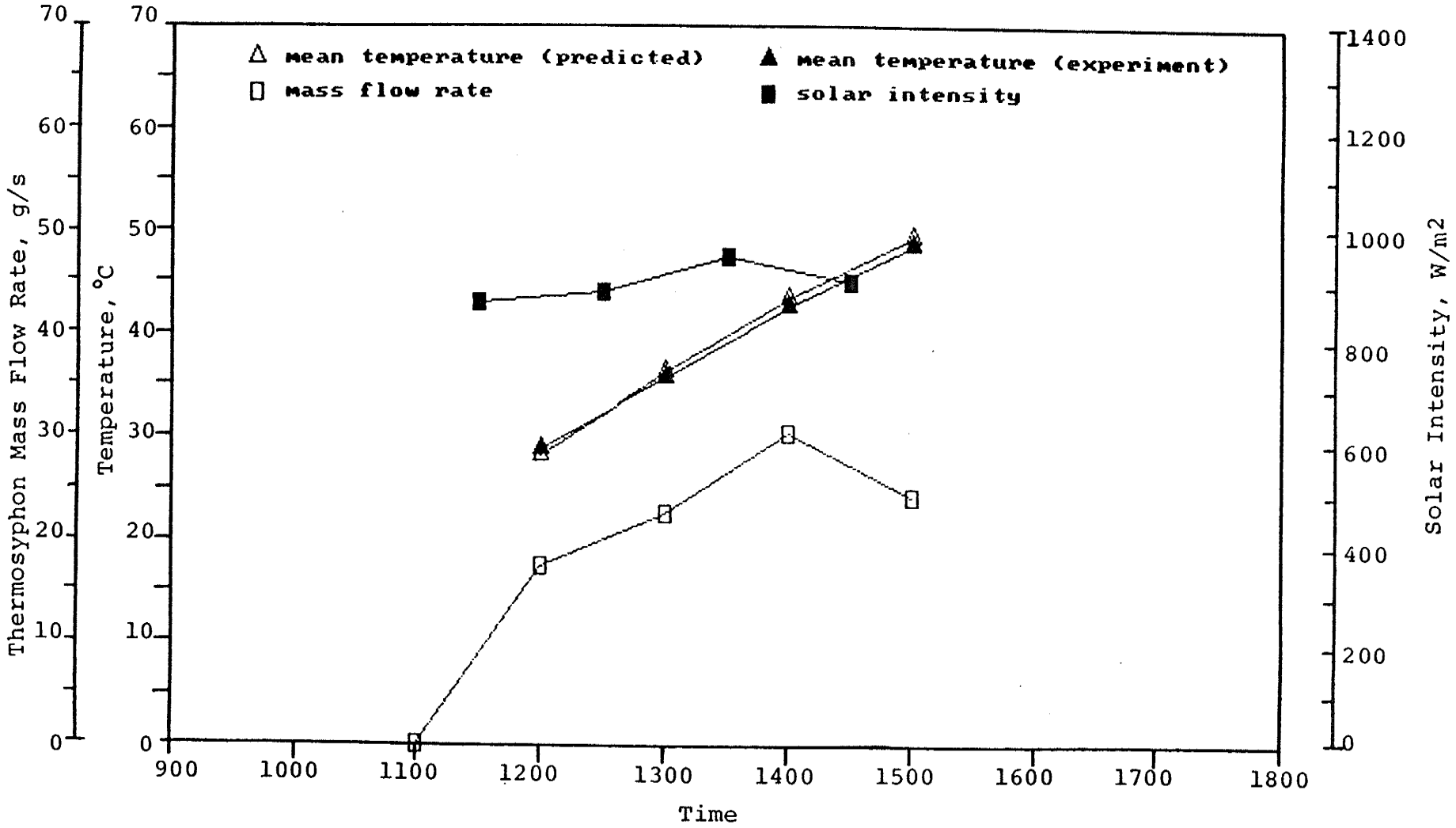

Fig. 4.6 Performance Characteristics; Mean Storage Temperatures, Thermosyphon Mass Flow Rate, and Solar Intensity. From Experiment A.

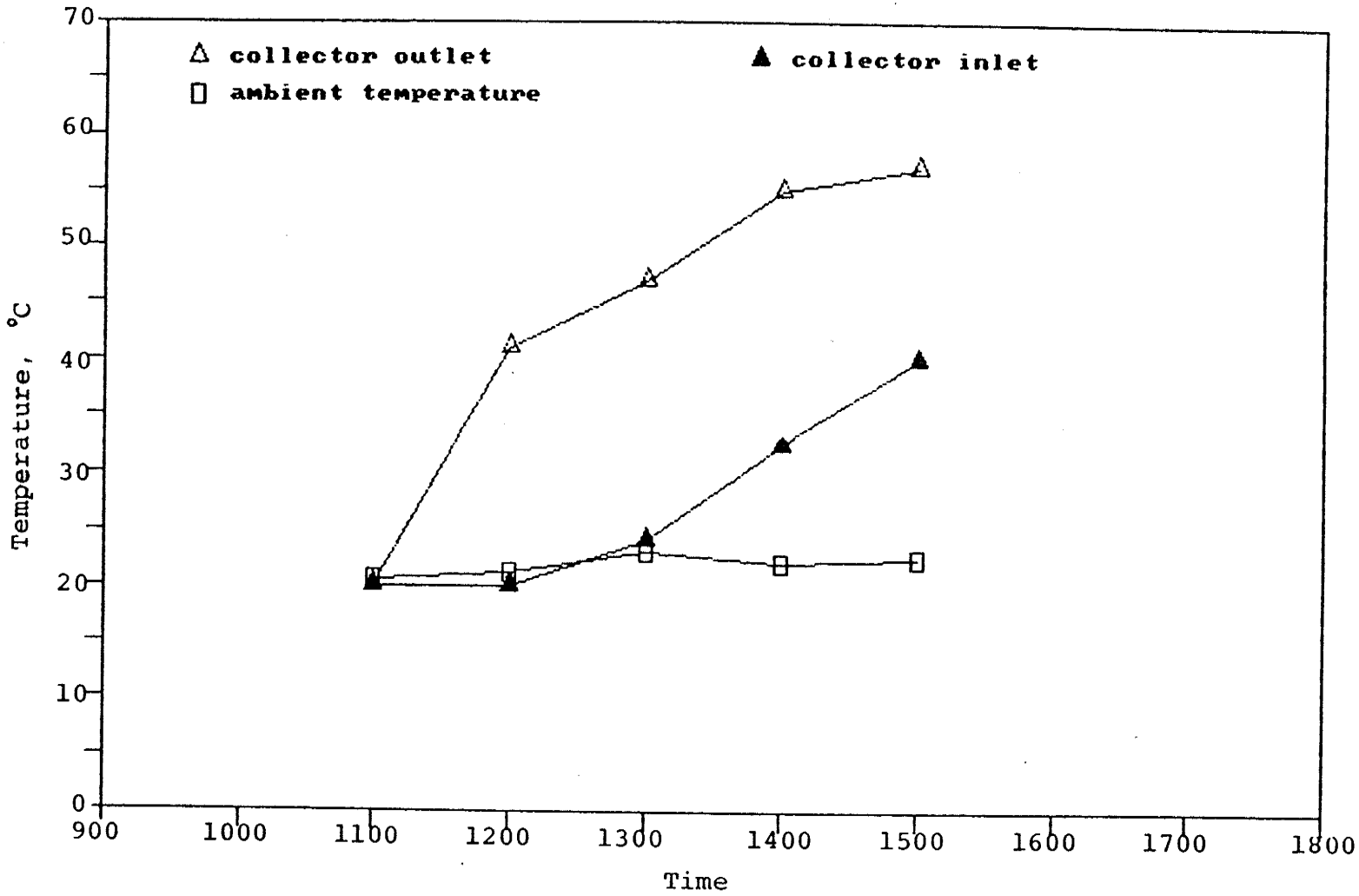

Fig.4.7 Collector Input/Output, and Ambient Temperatures. From Experiment A.

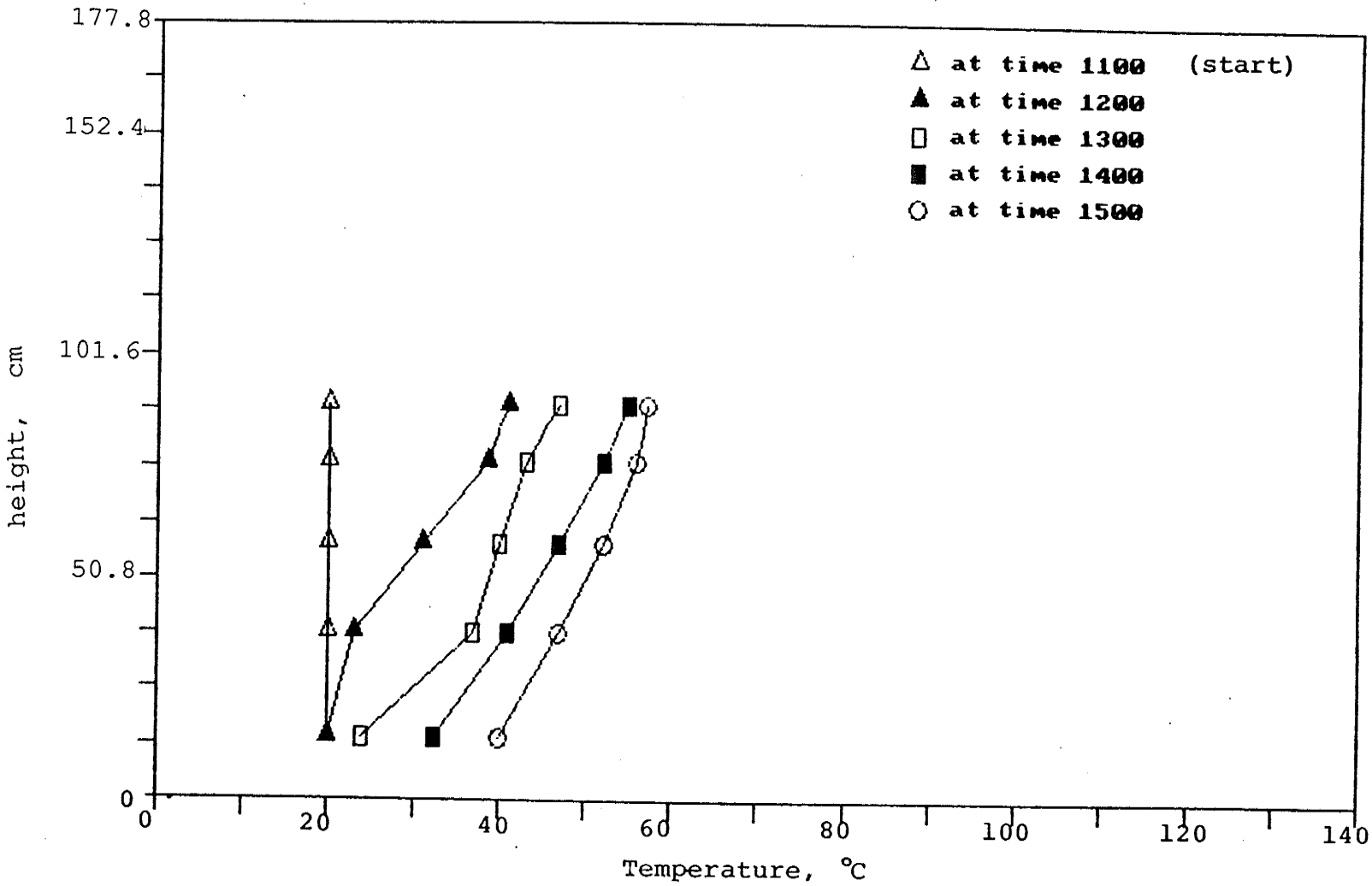

Fig.4.8 Vertical Temperature Profile Changes. From Experiment A.

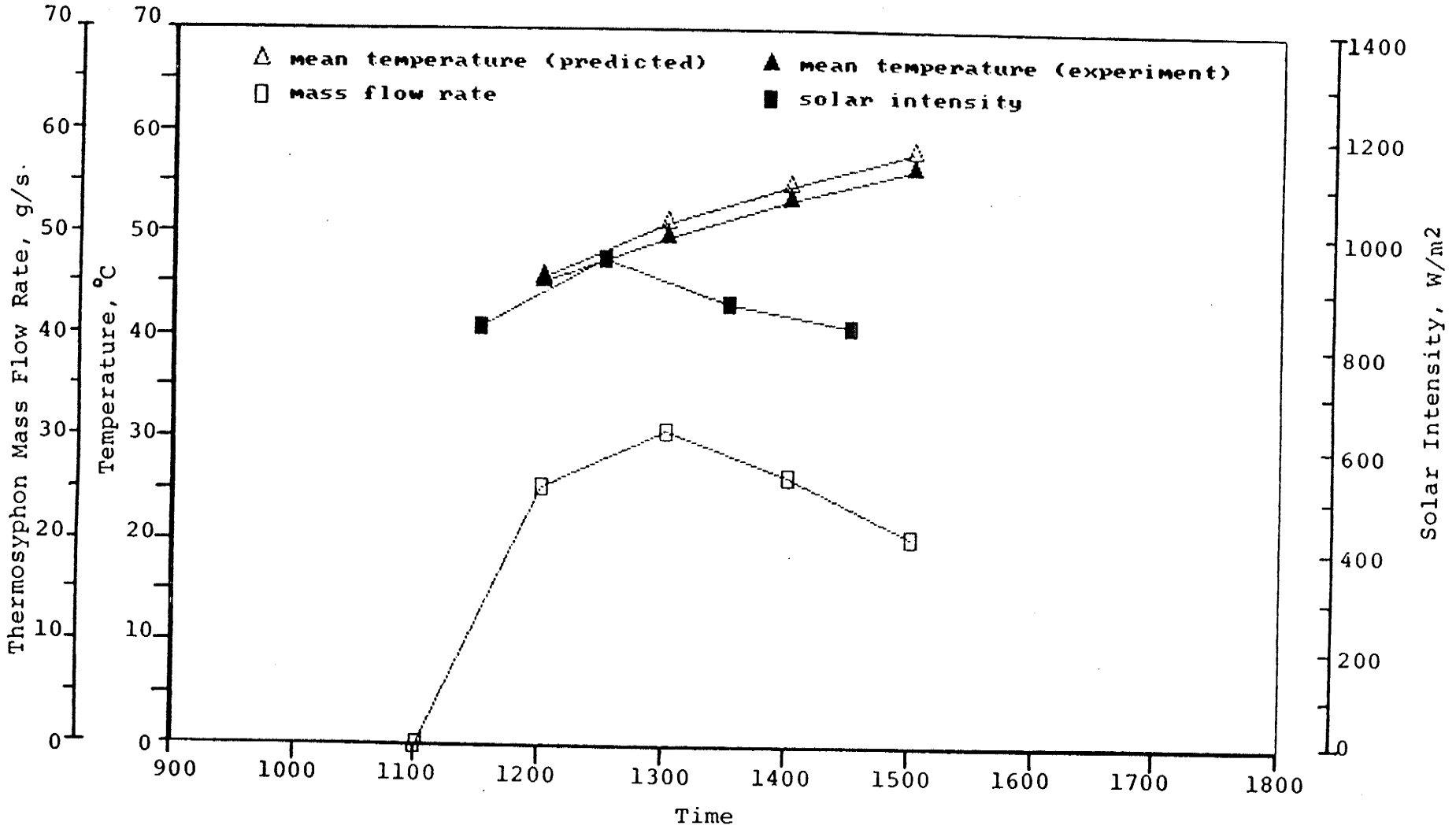

Fig.4.9 Performance Characteristics; Mean Storage Temperature, Thermosyphon Mass Flow Rate, and Solar Intentsity. From Experiment B1

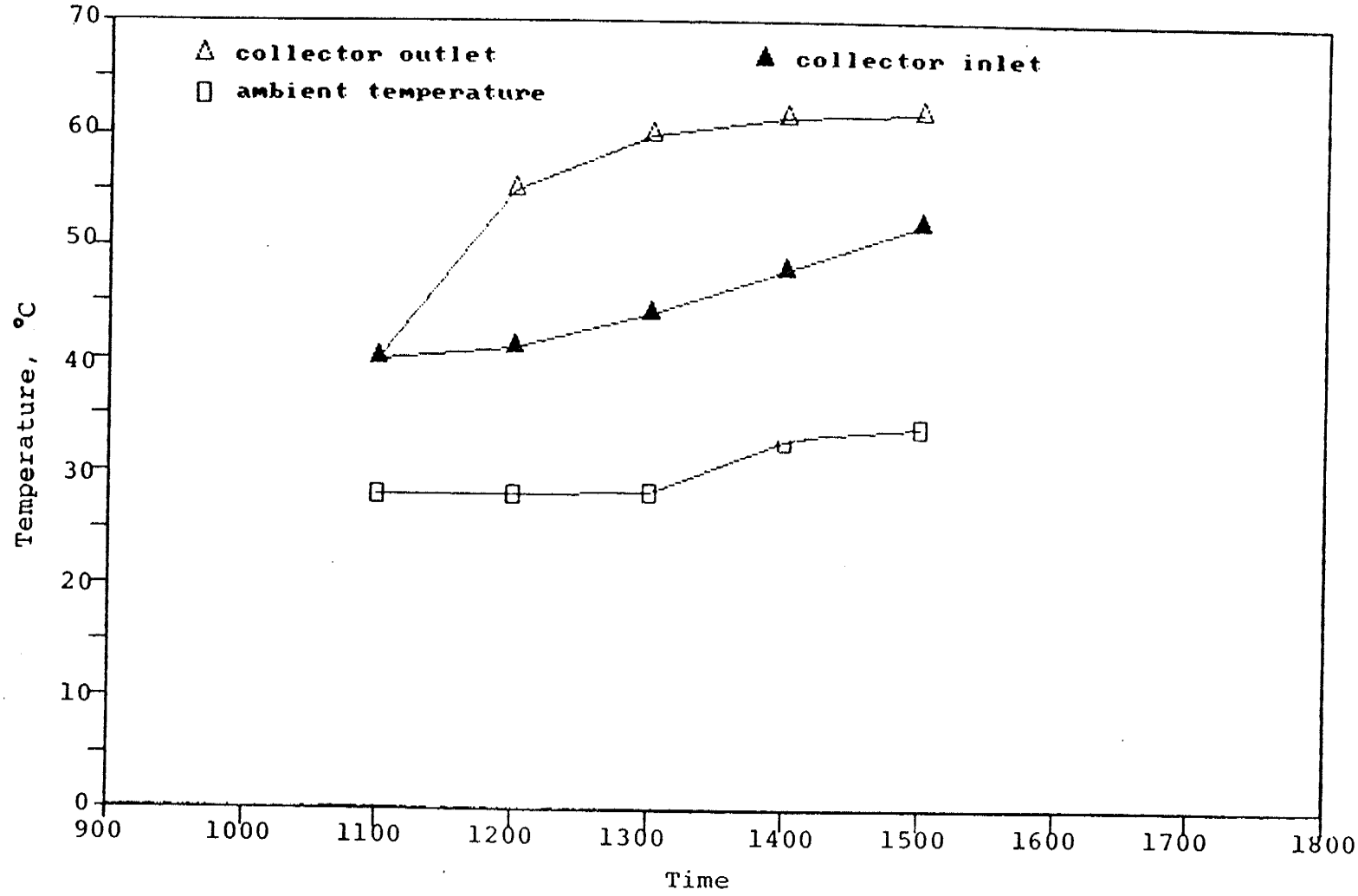

Fig.4.10 Collector Inlet/Outlet, and Ambient Temperature. From Experiment B1

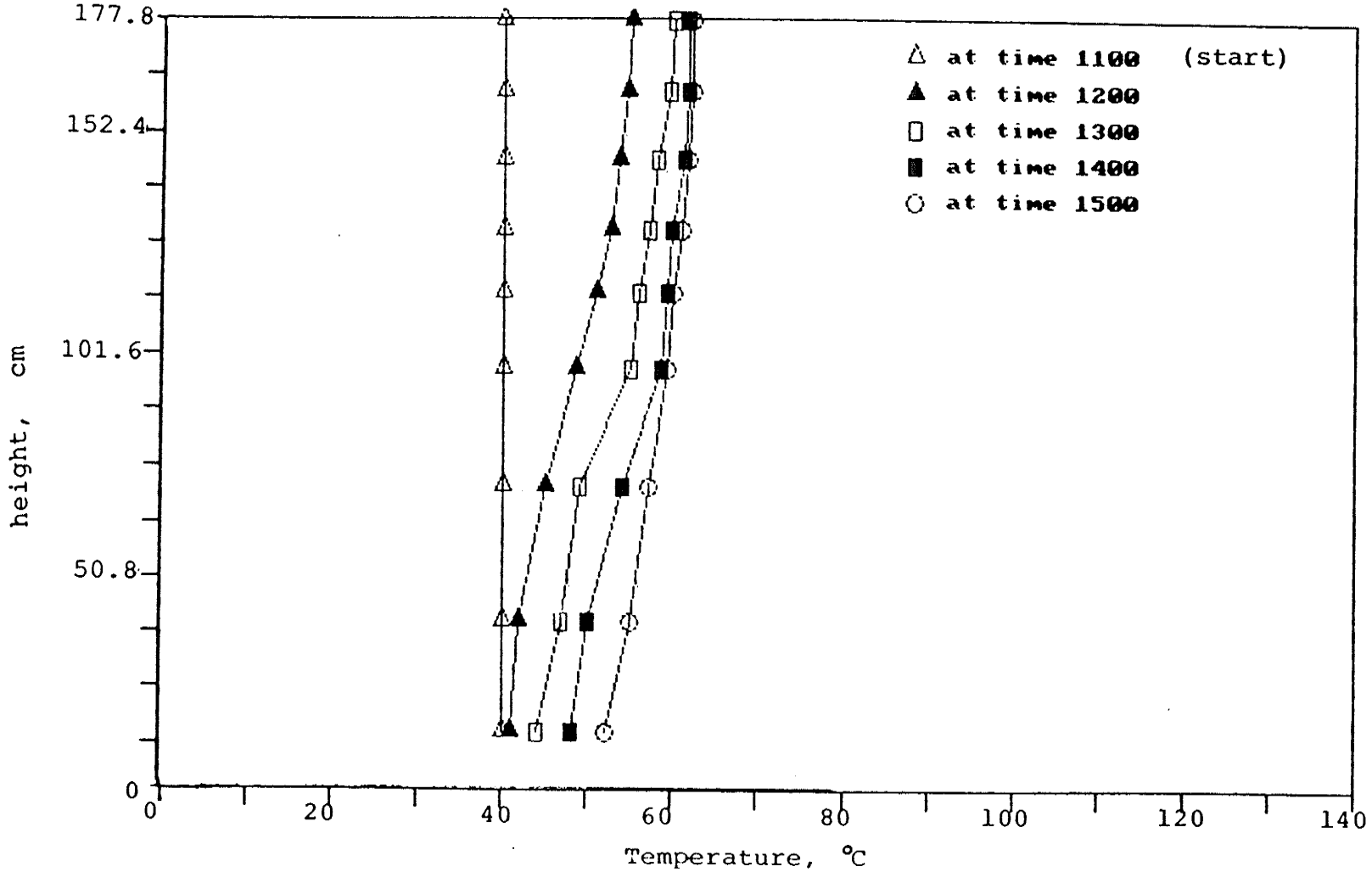

Fig.4.11 Vertical Temperature Profile Changes. From Experiment B1

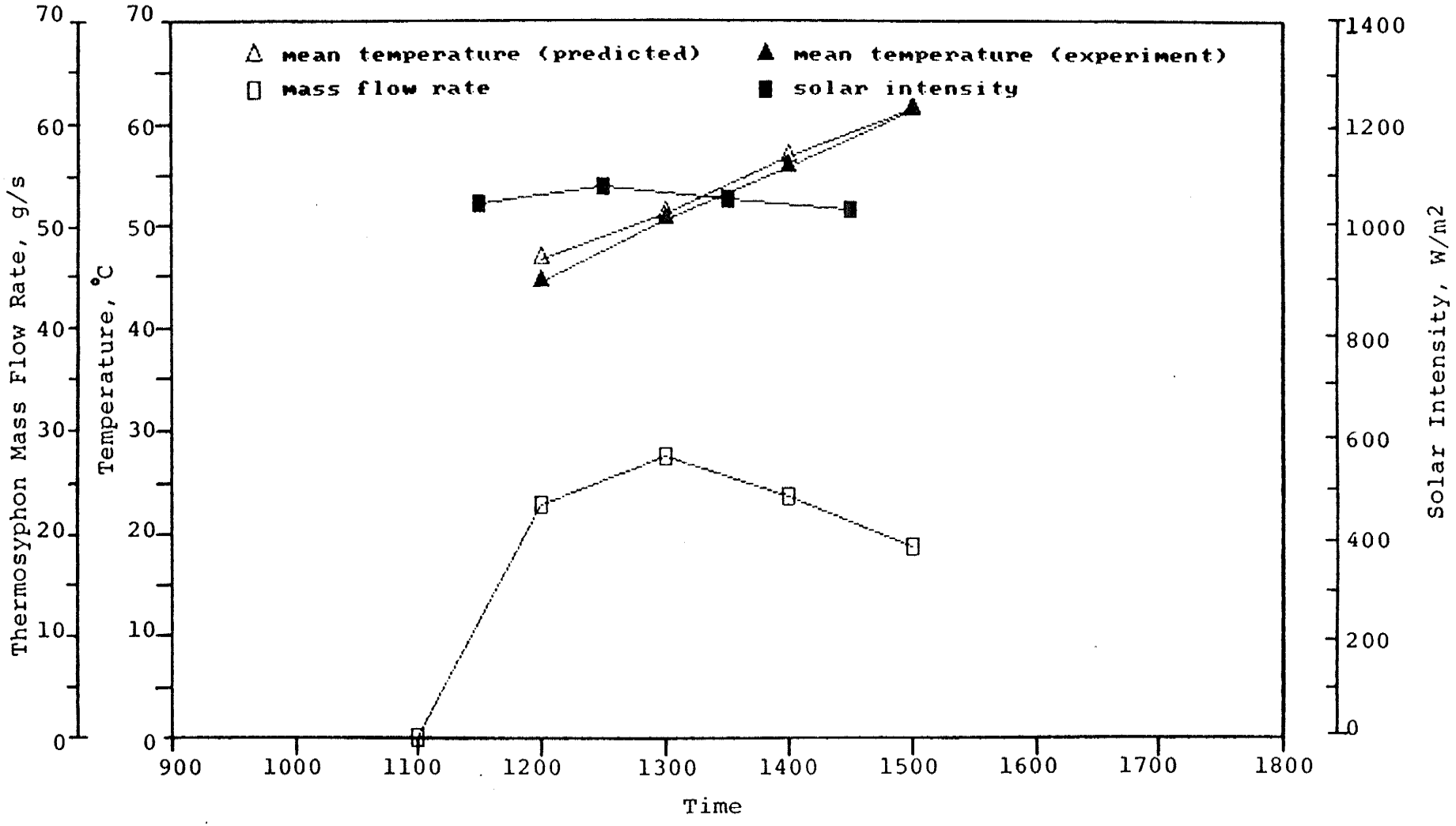

Fig.4.12 Performance Characteristics; Mean Storage Temperatures, Thermosyphon Mass Flow Rate, and Solar Intensity. From Experiment B2

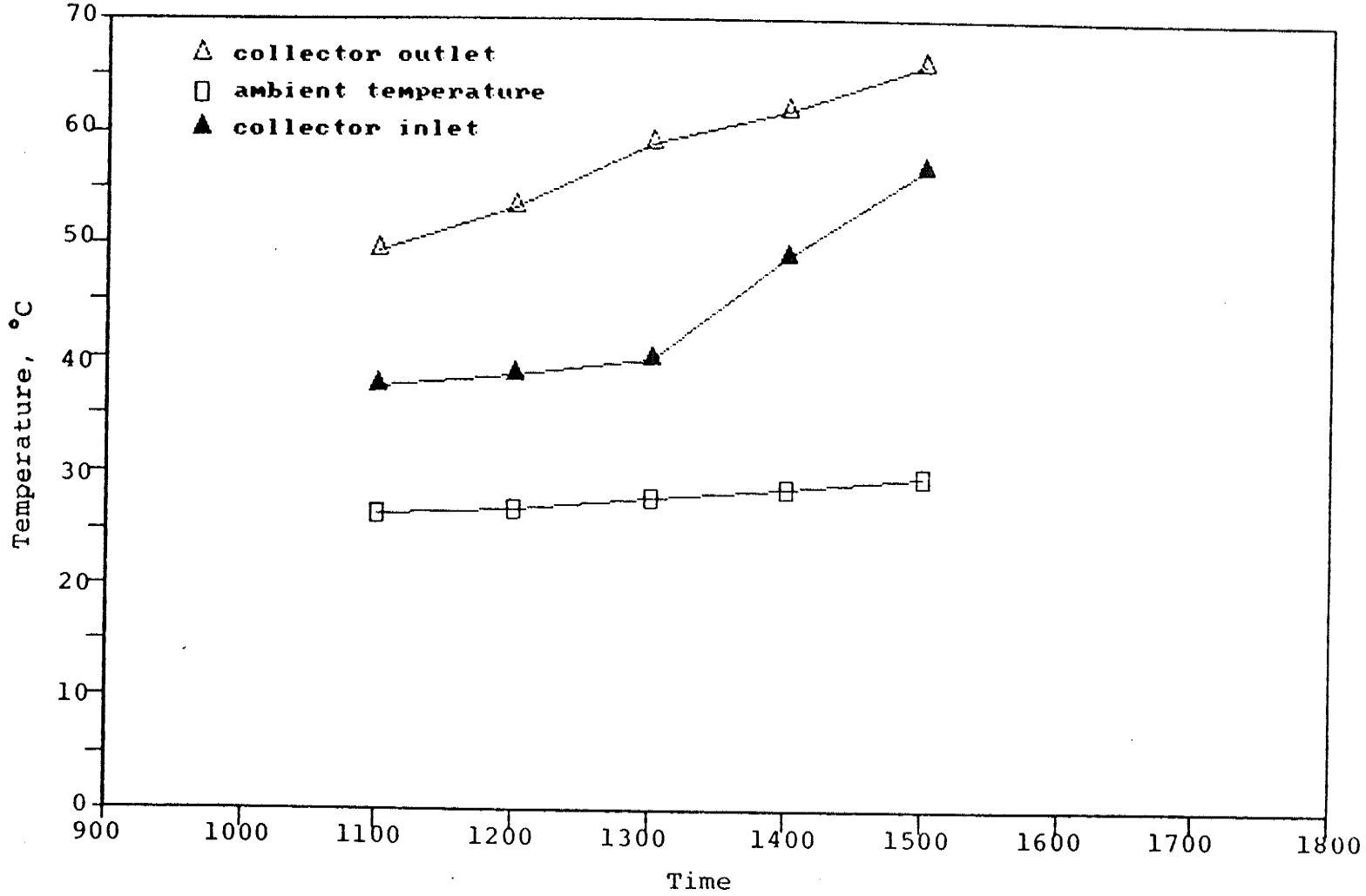

Fig.4.13 Collector Input/Output, and Ambient Temperatures. From Experiment B2

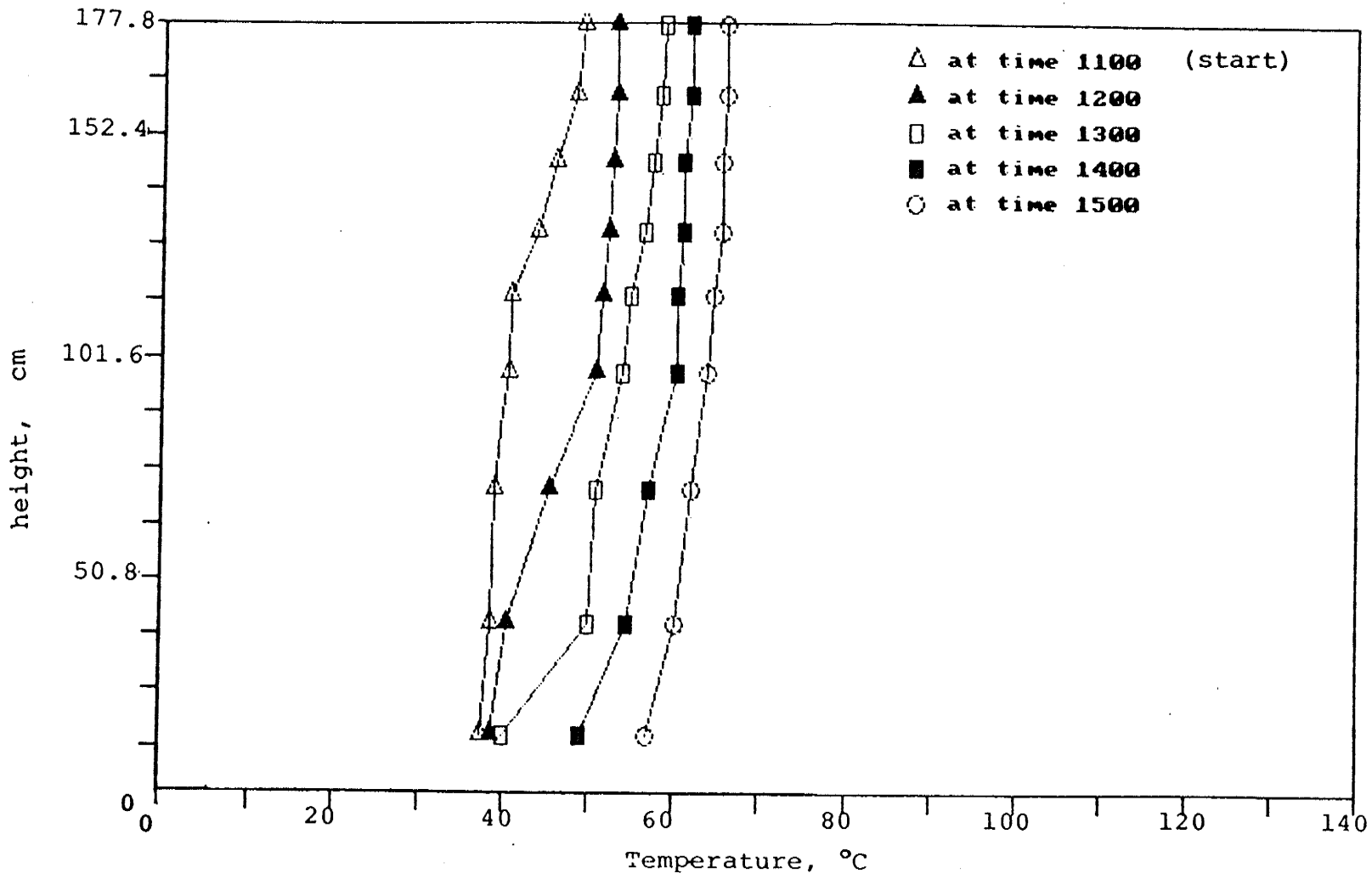

Fig.4.14 Vertical Temperature Profile Changes. From Experiment B2

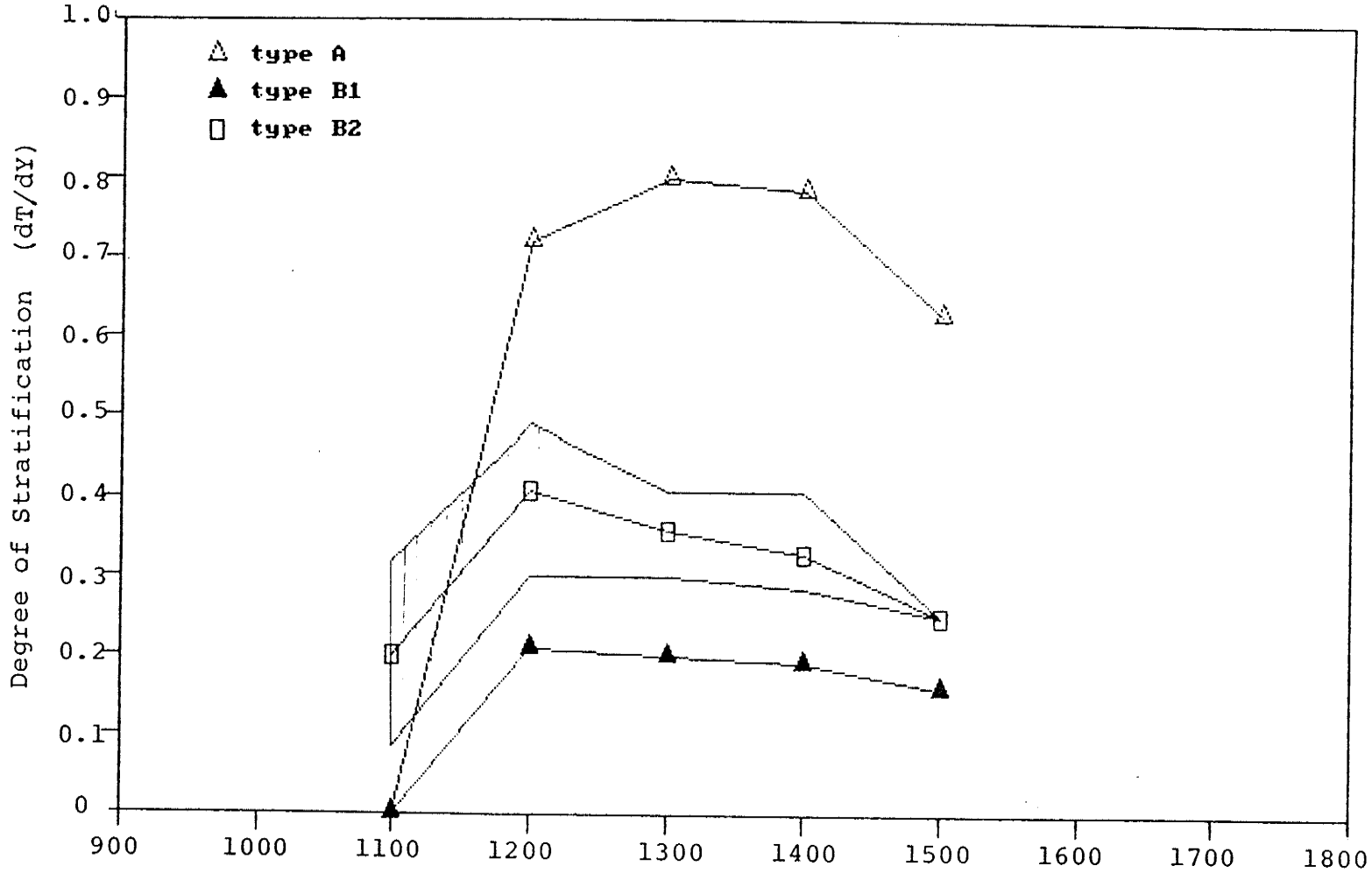

Fig.4.15 The Time-Dependent Behavior of Stratification of Experiment A, B1, and B2.

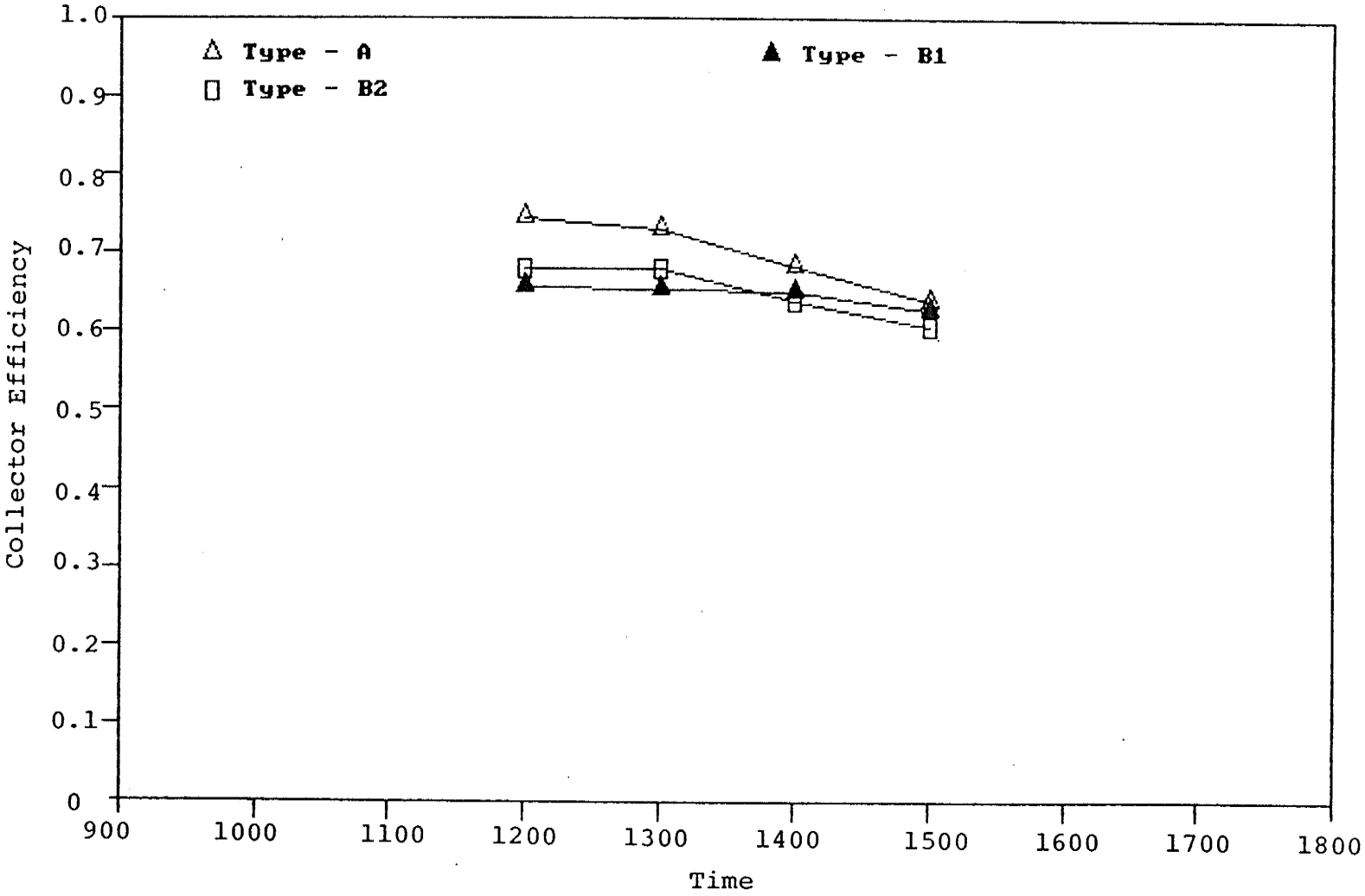

Fig.4.16 The Time-Dependent Behavior of Collector Efficiency.

Chapter 5

Discussion of Results and Conclusions

In section 4.5, the system performance characteristics of Experiments A, B1, and B2 are shown. In this chapter, section 5.1, these characteristics are interpreted and discussed. Conclusions drawn from the results of the investigation are enumerated in section 5.2.

5.1 Discussion of Experimental Results

5.1.1 Thermosyphon Mass Flow Rate

The thermosyphon mass flow rate of Experiments A, B1, and B2 demonstrated the same behavior and depends on the solar intensity. The maximum flow rate of each experiment was 30 g/s (108 kg/h). In Experiment A, the flow rate approached the maximum at the end of the third hour of operation. Whereas in Experiments B1 and B2 the flow rate approached the maximum at the end of the second hour.

After the maximum stratification had been obtained the hydrostatic head decreased and thus also the flow rate. For example, consider Fig.5.1, the system temperature-height distribution of Experiment B1 is shown. The thermosyphon head causing flow is equivalent to the shaded area shown in the system temperature-height distribution relationships. The shaded area is zero at the starting time because the fluid densities throughout the system were the same numerical values. When the solar intensity increased causing the temperature distribution throughout the system to rise, the shaded area became larger, increasing the thermosyphon mass flow rate. This phenomenon continued until the end of second hour of operation. After that, the temperature-height distribution decreased indicating a reduction in stratification due to the no drain off condition.

This indicated that the required water should be drawn off after the second hour (for Experiment B1) to maintain the high degree of stratification.

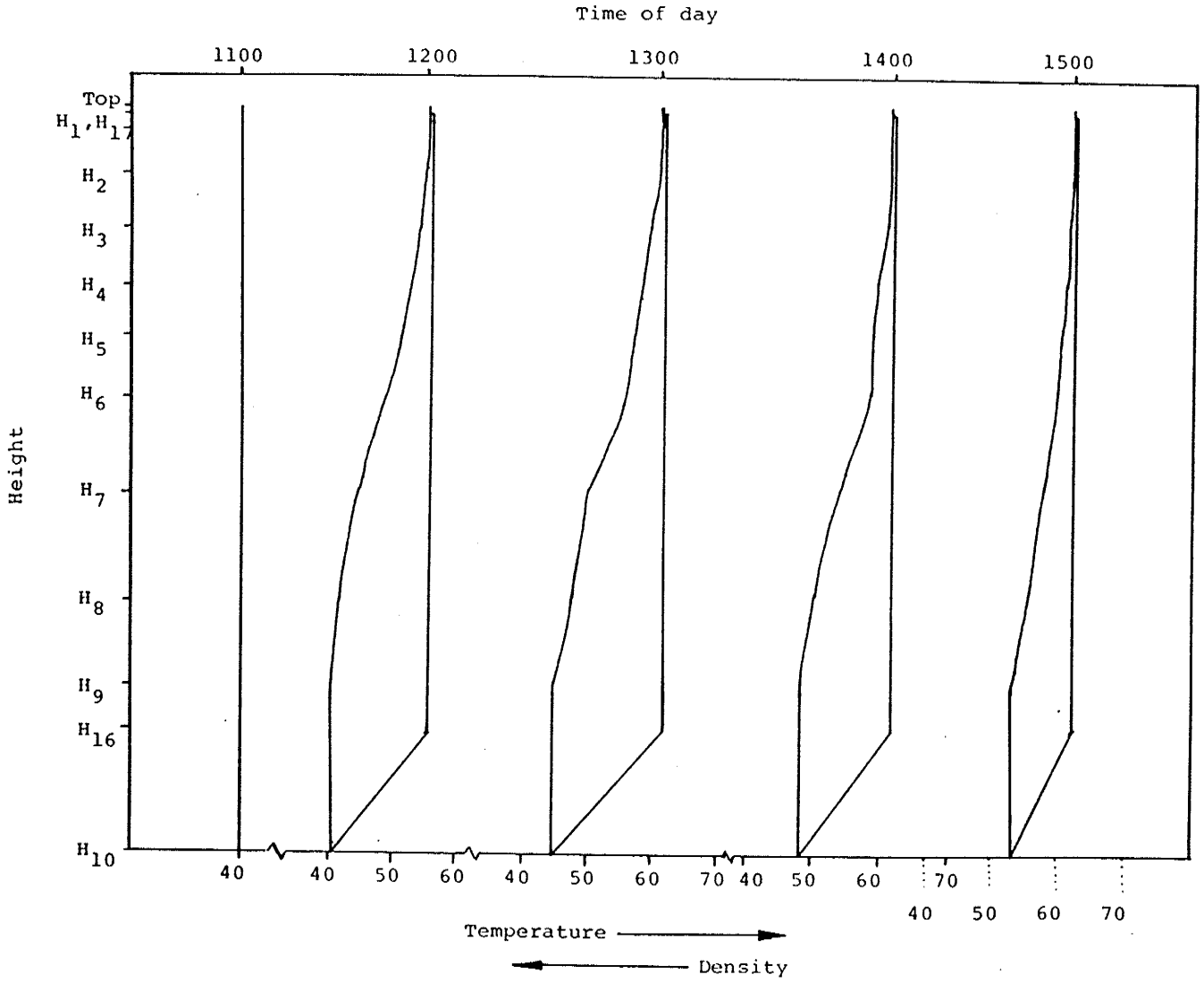

Fig.5.1 System Temperature-Height Distribution, results from Experiment B1.

5.1.2 The Mean Storage Temperatures.

The mean storage temperatures of Experiments A, B1, and B2 were linear. The mean temperatures from Experiments B1 and B2 were higher than from Experiment A because the temperatures of the water for Experiments B1 and B2 were 40°C at the starting time whereas for Experiment A the temperature was 20°C at the start.

The measured mean storage temperatures were up to 3.8 percent lower than that computed by using mathematical analyses because of unpredictable thermal loss from the system to the surroundings. However, the small discrepancy between computed values and measured values indicated that the analytical methods were accurate.

The results also showed that if the temperature of the required water is not important, then the water can be drawn off when the stratification is high in order to keep the storage highly stratified.

5.1.3 Collector Inlet/Outlet Temperatures.

The temperature rise in the fluid across the solar collector in Experiments A, B1, and B2 was nearly constant. The temperature rise was approximately 20°C for Experiment A and 15°C for Experiments B1 and B2. The reason for the higher temperature rise across the collector in Experiment A compared to Experiments B1 and B2 was because the collector inlet temperature in Experiment A was less than in Experiments B1 and B2. Thus, the collector efficiency of Experiment A was higher and the temperature rise greater.

During the last hour of each experiment the temperature rise across the collector decreased due to the decreasing of collector efficiency caused by a higher inlet water temperature. According to Fig.4.7, 4.10, and 4.13, at the end of second hour any required water should be drawn off to maintain the high temperature rise across the collector.

5.1.4 Vertical Storage Tank Temperature Profile Changes.

In Experiment A, the temperature in the entire tank was constant at the start and gradually the degree of stratification increased till 1300 h and after that the temperature gradient tended to become uniform (Fig.4.8). The results indicated that to maintain a high degree of stratification any required water should be drawn off at the second hour for Experiment A.

Experiments B1 and B2 involved the extended system with the added baffled tank. In experiment B1 the temperature at the start was also uniform and the degree of stratification increased till 1200 h when the temperature profile gradually became nearly uniform again at 1500 h. This occured because no water was used throughout the operation period. In Experiment B2 the water was stratified at the start. At 1200 h the temperature of the water in the upper baffled tank became uniform whereas the water in the lower tank remained stratified. This occured because the hot water from the collector transfered heat to the colder water at the bottom of upper tank due to mixing promoted by the perforated horizontal baffles. This mixing caused by the perforated baffles had not been reported previously in the literature. After 1200 h the temperature profile behaved as in Experiment B1 and gradaully became uniform because no water was used.

Considering experiments B1 and B2, there was more advantage in drawing the required water from the upper tank after the end of first hour because:

1. the water at the bottom of the lower tank was still cooler than in Experiment B1, thus the collector efficiency of Experiment B2 was higher than that of Experiment B1,
2. the temperature gradient in the lower tank of Experiment B2 was greater than that of Experiment B1, because of stratification at the start, thus, the thermosyphon mass flow rate of Experiment B2 was higher than that of Experiment B1.

5.1.5 Degree of Stratification.

Fig.4.15 was plotted from all of data sets (as shown in Appendix C). Results showed that the highest degree of stratification occured at the end of the third hour for Experiment A and at the end of the first hour for Experiments B1 and B2.

The degree of stratification in Experiments B1 and B2 was not as great as in Experiment A. This was due to the horizontal baffles which promoted mixing in the upper storage tank. The connecting pipes between the upper and lower storage tanks also promoted mixing due to pluming effects in the lower storage tank.

However, comparing Experiment B1 and B2, it was obvious that the use of the stratified temperature distribution at starting time gave better performance than using the uniform temperature distribution at the starting time.

5.1.6 Collector Efficiency.

Experiment A gave a higher daily performance than Experiments B1 and B2, because the temperature of fluid at the collector inlet was lower than that in Experiments B1 and B2.

According to the collector efficiencies for Experiments B1 and B2 shown in Fig.4.16, the results showed that the best operating time was the first two hours. After that the required water should be drawn off, providing a better operating condition as in Experiment B2.

5.2 Conclusions.

A number of conclusions were drawn from the results of the present investigation. These conclusions are as follows:

1. It was observed that the temperature rise in the fluid across the solar collector in the thermosyphon SDHW system was constant. The temperature rises were approximately 20 °C for the system configuration that used the domestic hot water storage tank

(and approximately 15 °C because of the increased mixing due to the horizontal baffles mounted inside). The constant temperature rise across the collector agrees with the previous investigations studied by Close, Gupta and Garg, and Morrison and Braun.

2. The thermosyphon mass flow rate varied with the solar insolation. The estimated flow rate reached a maximum of 109 kg/h. It was higher than that in Morrison and Braun's results (97.2 kg/h). This higher flow could be attributed to:
    a) the collector tracked the sun, and
    b) the distance between tank bottom and collector top in the present investigation was higher than that in Morrison and Braun's investigation.
3. The temperature profiles in the storage tank were not linear (as indicated by Ong's investigation).
4. The type of horizontal interior baffles used promoted mixing.
5. Operating the system with a stratified temperature of the fluid at the starting time gave better performance compared to operating with a uniform temperature of the fluid at starting time in terms of:
    a) collector efficiency, and
    b) degree of stratification.
6. The required hot water should be drawn off after the degree of stratification reaches a maximum in order to maintain high stratification and high thermosyphon mass flow rate.

5.3 Recommendations.

Like many investigations reported in the literature, the results were difficult to interpret due to the fluctuating solar insolation, varying surrounding conditions, etc. However, this study led to several recommendations for additional research efforts for an

increased understanding of the mechanisms involved in liquid storage tanks. Recommendations are:

1. In order to reduce the thermal capacity of the storage tank, a thin walled tank sould be used.
2. A low thermal conductive material should be used in order to reduce the wall conduction effect.
3. The effect of other baffle arrangements on mixing in the storage tank should be investigated.
4. The doughnut or segmental baffles should be tried to try to reduce the mixing condition in the storage tank.

REFERENCES

1. Lighstone, M. et al., " Effect of Plume Entrainment in the Storage tank on Calculated Solar System Performance, " Proceedings of the 14th Annual Conference of the Solar Energy Society of Canada Inc., 1988.
2. Wuestling, M.D. et al., " Promisinf Control Alternatives for Solar Water Heating Systems, " Journal of Solar Energy Engineering, Vol.107, p 215-221, 1985.
3. Hollands, K.G.T. et al., " A Review of Low Flow, Stratified-Tank Solar Water Heating System, " Proceedings of Solar'87, Portland, Oregon (1987).
4. Duffie, J.A. and Beckman, W.A., " Solar Engineering of Thermal Processes, " John Wiley & Sons, New York, 1980.
5. Dickinson, W.C. and Dheremisinoff, P.N., " Solar Energy Technology Handbook, " Marcel Dekker, Inc., 1980.
6. Carpenter, S.C., " Design of Thermosyphon Solar Domestic Heating Water System for Canadian Climate, " Proceedings 10th Annual National Conference of Solar Engineering Society of Canada, 1984.
7. Close, D.J., " The Performance of Solar Water Heaters with Natural Circulation, " Solar Energy 6, 33 (1962).
8. Desa, V.G., " Solar Energy Utilization at Dacca, " Solar Energy 8, 84 (1964).
9. Gupta, C.L. and Garg, H.P., " System Design in Solar Water Heater with Natural Circulation, " Solar Energy 12, 163 (1968).
10. Ong, K.S., " A Finite - Difference Method to evaluate The Thermal Performance of a Solar Water Heater, " Solar Energy 16, 137 (1974).
11. Ong, K.S., " An Improved Computer Program for The Thermal Performance of A Solar Water Heater, " Solar Energy 18, 1976.
12. Klien, S.A. et al., " TRNSYS, A Transient Simulation Program, " Engineering Experiment Station Report#38, University of Wisconsin - Madison, 1974.

13. Morrison, G.L. and Ranatunga, D.B.J., " Thermosyphon Circulation in Solar Collector, " Solar Energy 24, 1980.

14. Young, M.F. and Bergquam, J.B., " Performance Characteristics of a Thermosyphon Solar Domestic Hot Water System, " Journal of Solar Energy Engineering, Vol.13, 1981.

15. Cabelli, A., " Storage Tank - A Numerical Experiment, " Solar Energy 19, 1977.

16. Sharp, M.K. and Loehrke, R.I., " Stratified versus Well-Mixed Sensible Heat Storage in a Solar Space Heating Application, an ASME Publication, 78 - HT - 49, 1978.

17. Loehrke, R.I. et al., " A Passive Technique for Enhancing Thermal Stratification in Liquid Storage Tanks, " an ASME Publication, 78 - HT - 50, 1978.

18. Young, M.F. and Baughn, J.W., " An Investigation of Thermal Stratification in Horizontal Storage Tank, " Transaction of the ASME, Vol.103, Nov. 1981.

19. Veltkamp, W.B., " Thermal Stratification in Heat Storages, " Thermal Storage of Solar Energy, Martinus Nijhaff Publishers, 1981.

20. Jaluria, Y. and Gupta, S.K., " Decay of Thermal Stratification in A Water Body for Solar Energy Storage, " Solar Energy 28, 1982.

21. Phillips, W.F. and Dave, R.N., " Effects of Stratification on Performance of Liquid -Based Solar Heating Systems, " Solar Energy 29, 1982.

22. Jesch, L.F. and Braun, J.E., " Variable Volume Storage And Stratified Storage for Improved Water Heater Performance, " technical note, Solar Energy 33, 1984.

23. Briggs, R.J. and Ferguson, J.E., " Effects of Stratification Enhancement on Performance of A Solar DHW System, " proceedings, 10th Annual National Conference of The Solar Energy Society of Canada; Calgary, Alberta. 1984.

24. Kenneth Rush, C., " Stratified Storage Tanks for Solar Water Heaters, " Proceedings, 10th Annaul National Conference of The Solar Energy Society of Canada; Calgary, Alberta. 1984.

25. Den Braven, K., " An Analytical Model of Stratification for Liquid-Based Solar System, " Journal of Solar Energy Engineering, Vol.108, May 1986.

26. Shyu, R.J. and Hsieh, C.K., " Unsteady Natural Convection in Enclosures with Stratified Medium, " Journal of Solar Energy Engineering, Vol.109, May 1987.

27. Petro - Sun Inc., " Thermo Solar STM & CIM-1 Liquid Flat Plate, " data sheet.

28. Lavan, Z. and Thompson, T., " Experiment Study of Thermally Stratified Hot Water Storwge Tanks, " Solar Energy, 19, p 519, 1977.

29. Beckman, W.A., " Duct and Pipe Losses in Solar Energy Systems, " Solar Energy, 21, p 531, 1978.

30. CRANE company, " Flow of Fluid Through Valves, Fittings, and Pipes, " Technical paper No. 410.

31. Morrison, G.L. and Braun, J.E., " System Modeling and Operation Characteristics of Thermosyphon Solar Water Heaters, " Solar Energy, 34, p 389, 1985.

Appendix A

Description of Storage Units

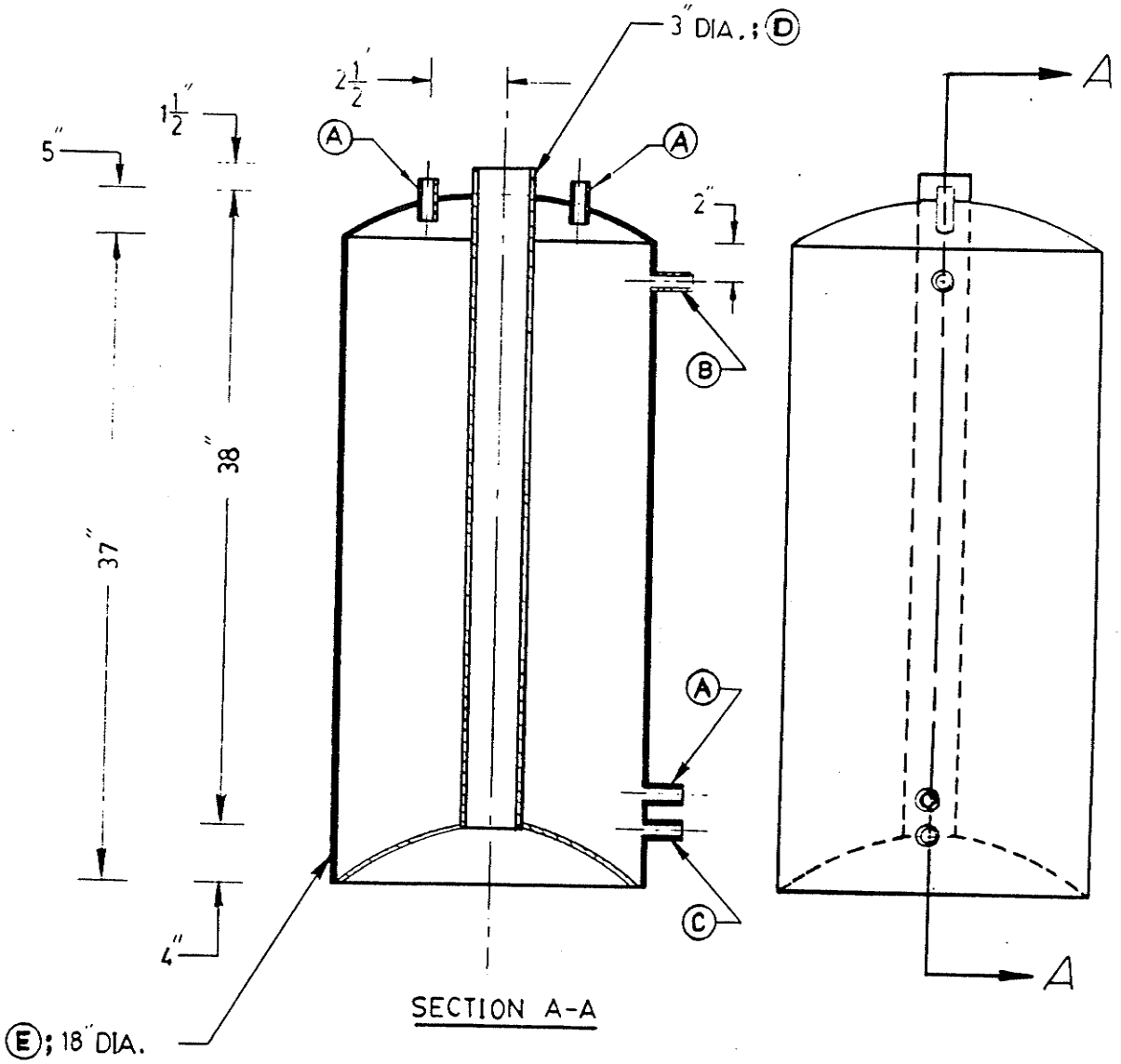

Fig.A1 A Commercial Domestic Hot Water Storage Tank.

Parts	Functions	Details
A	connecting pipe	3/4″ coupling
B	inlet port	3/4″ coupling
C	outlet port	3/4″ coupling
D	hot air path	3″ ID pipe
E	tank body	18″ ID cylinder

Table A1 Details for Fig.A1.

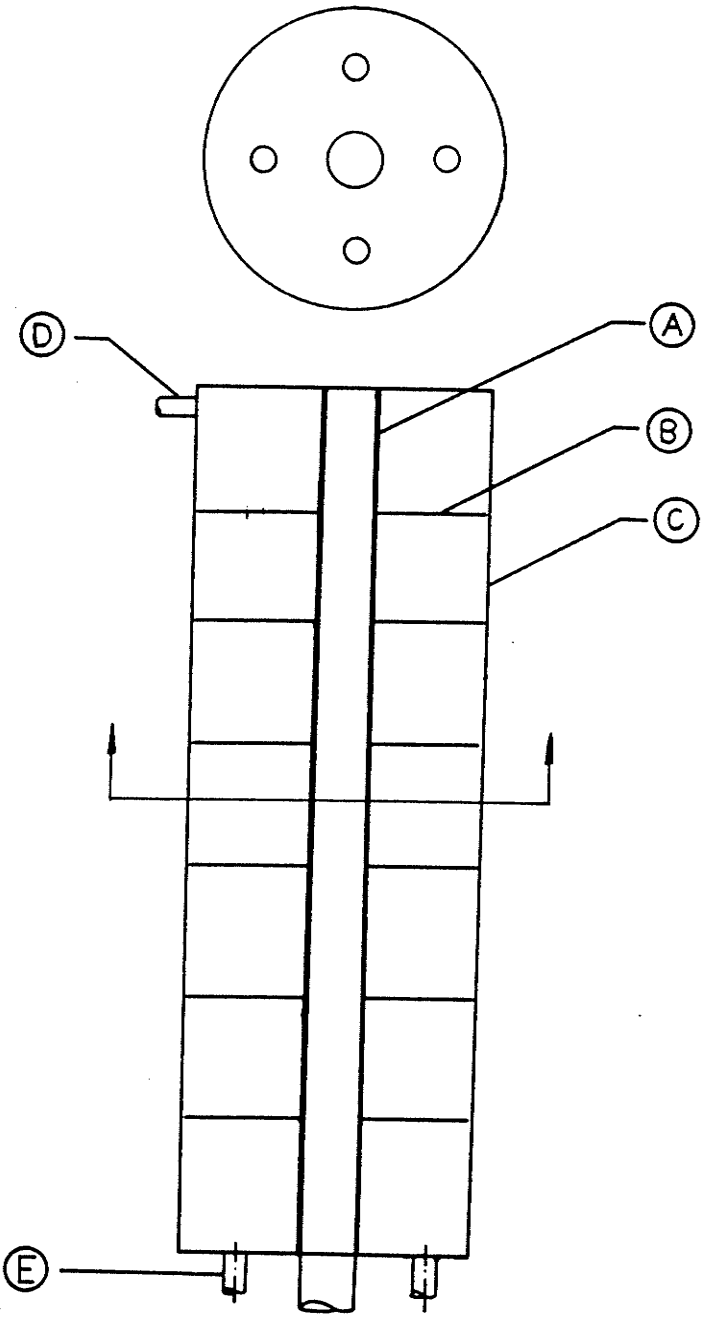

Fig.A2 The Upper Tank with Baffles mounted inside used in Experiment B.

Parts	Functions	Details
A	support	3″ OD pipe
B	baffle	1.7″ OD (metal sheet)
C	tank body	17.5″ ID cylinder
D	inlet port	3/4″ coupling
E	connecting pipe	3/4″ coupling

Table A2 Details for Fig.A2.

Appendix B

Computer Programs

Computer Program used in Experiment A

```
10  REM
**************************************************************
*******
20  REM       This programme has been written in order to
evaluate the
30  REM       mean temperatures (computed and experimental
values )                              and the thermosyphon mass
flow rate throug the system                                  of
experiment A. The system confriguration is shown in Fig.4.1.
40  REM
**************************************************************
*******
50  REM
60  REM                                  Read & Store
70  REM
80  REM
**************************************************************
*******
90  DIM
T(30),DY(30),RW(30),VW(30),D(30),H(30),C(30),V(5),M(5),CW(30
),                    KW(30),Z(10),WW(30)
100 MM     = 0
110 DY(1)  = .0254
120 DY(2)  = .1778
130 DY(3)  = .2032
140 DY(4)  = .2032
150 DY(5)  = .2286
160 DY(6)  = 2.057486
170 DY(7)  = .2642788
180 DY(8)  = .2642788
190 DY(9)  = .2642788
200 DY(10) = .2642788
210 DY(11) = .2642788
220 DY(12) = 1.574292
230 D(6)   = .01905
240 D(7)   = .0095
250 D(12)  = .01905
260 W      = 3
270 LC     = .42672
280 V(1)   = .0121625
290 V(2)   = .0283792
300 V(3)   = .032433
310 V(4)   = .032433
320 V(5)   = .0445958
330 REM
340 REM
**************************************************************
**********
```

```
350 REM            Initialization of the mean storage
temperature
360 REM
************************************************************
***********
370 GOSUB 3580
380 GOSUB 3460
390 T(14) = T(19)
400 PRINT "The starting mean storage temperature ",T(14)
410 PRINT
420 REM
************************************************************
***********
430 REM
440 REM    Prediction mean temperature of storage by using
energy balance
450 REM
460 REM
************************************************************
***********
470 GOSUB 3580
480 T(16) =  (.736-4.98*(T(6)-T(13))/T(15))*(8475.08*T(15))
490 T(17) =  24439*T(13)+6.38793*(10^5)*T(14)
500 T(18) =  (T(16)+T(17))/(6.63232*(10^5))
510 REM PRINT "Old mean storage temperature ",T(14)
520 REM PRINT "New mean storage temperature ",T(18)
530 REM
************************************************************
**********
540 REM
550 REM      The evaluation of mean storage temperature from
experiment
560 REM
570 REM
************************************************************
**********
580 REM
590 GOSUB 3460
600 FOR I = 1 TO 5
610 TW    = T(I)
620 GOSUB 2050
630 RW(I) = RW
640 VW(I) = (VW/10^6)
650 CW(I) = (CW*1000)
660 WW(I) = V(I)*CW(I)*RW(I)
670 NEXT I
680 Z(1)  =
WW(1)*T(1)+WW(2)*T(2)+WW(3)*T(3)+WW(4)*T(4)+WW(5)*T(5)
690 Z(2)  = WW(1)+WW(2)+WW(3)+WW(4)+WW(5)
700 T(19) = Z(1)/Z(2)
710 REM
************************************************************
*********
720 REM
```

```
730 REM            Comparison mean storage temperature
between
740 REM                      prediction and experiment
750 REM
760 REM
*************************************************************
*********
770 REM PRINT "Mean storage temperature (last hour ) ",T(14)
780 REM PRINT "Mean storage temperature (prediction) ",T(18)
790 REM PRINT "Mean storage temperature (experiment) ",T(19)
800 REM
*************************************************************
**********
810 REM
820 REM   Process to evaluate mass flow rate by using the
method of total
830 REM                      hydrostatic pressure head
840 REM
850 REM
*************************************************************
**********
860 T(7)  = T(6) + (T(12) - T(6))*1/10
870 T(8)  = T(6) + (T(12) - T(6))*3/10
880 T(9)  = T(6) + (T(12) - T(6))*5/10
890 T(10) = T(6) + (T(12) - T(6))*7/10
900 T(11) = T(6) + (T(12) - T(6))*9/10
910 FOR I = 1 TO 12
920 TW    = T(I)
930 GOSUB 2050
940 RW(I) =RW
950 VW(I) = (VW/10^6)
960 H(I)  = RW(I)*9.810001*DY(I)
970 NEXT I
980 H     = H(1)+H(2)+H(3)+H(4)+H(5)+H(6)-H(7)-H(8)-H(9)-
H(10)-H(11)-H(12)
990   WC = W/10
1000  RR = (4*W)/(VW(12)*D(12)*3.141592)
1010  RD = (4*W)/(VW(6)*D(6)*3.141592)
1020  RC = (4*WC)/(VW(11)*D(7)*3.141592)
1030  IF RR<2000 THEN GOTO 1070
1040  IF RR>4000 THEN GOTO 1090
1050  FR = .0243+(3.85*RR/10^6)
1060  GOTO 1270
1070  FR = 64/RR
1080  GOTO 1270
1090  FR = .316/RR
1100  GOTO 1270
1110  IF RD <2000 THEN GOTO 1150
1120  IF RD>4000 THEN GOTO 1170
1130  FD = .0243+(3.85*RD/10^6)
1140  GOTO 1290
1150  FD = 64/RD
1160  GOTO 1290
1170  FD = .316/RD
```

```
1180  GOTO 1290
1190  IF RC<2000 THEN GOTO 1230
1200  IF RC>4000 THEN GOTO 1250
1210  FC = .0243+(3.85*RC/10^6)
1220  GOTO 1310
1230  FC = 64/RC
1240  GOTO 1310
1250  FC = .316/RC
1260  GOTO 1310
1270  A  =
(FR*DY(12))/(D(12)*RW(12)*(3.141593*(D(12)^2)/4)^2)
1280  GOTO 1110
1290  B  = (FD*DY(6))/(D(6)*RW(6)*(3.141593*(D(6)^2)/4)^2)
1300  GOTO 1190
1310  FOR I = 7 TO 11
1320  C(I) = (FC*LC)/(D(7)*RW(I)*(3.141593*(D(7)^2)/4)^2)
1330  NEXT I
1340  D  = A+B+C(7)+C(8)+C(9)+C(10)+C(11)
1350  G1 = .78/(RW(6)*(3.141593*(.01905^2)/4)^2)
1360  G2 = (FD*13*.025)/(RW(6)*(3.141593*(.01905^2)/4)^2)
1370  G3 = (.1936)/(RW(6)*(3.141593*(.01588^2)/4)^2)
1380  G4 = (FD*30*.025)/(RW(6)*(3.141593*(.01588^2)/4)^2)
1390  G5 = (.3713)/(RW(6)*(3.141593*(.01588^2)/4)^2)
1400  G6 = (FC*60*.025)/(RW(6)*(3.141593*(.0095^2)/4)^2)
1410  G7 = (FC*60*.025)/(RW(12)*(3.141593*(.0095^2)/4)^2)
1420  G8 = (FR*30*.025)/(RW(12)*(3.141593*(.0254^2)/4)^2)
1430  G9 = (.6049)/(RW(12)*(3.141593*(.01905^2)/4)^2)
1440  J1 = (1.563)/(RW(12)*(3.141593*(.0127^2)/4)^2)
1450  J2 = (1)/(RW(1)*(3.141593*(.0127^2)/4)^2)
1460  J9 = G1+G2+G3+G4+G5+G6+G7+G8+G9+J1+J2
1470  E  = D+J9
1480  WCAL = (2*H/E)^(.5)
1490  Z  = (WCAL - W)/W
1500  Y  = ABS(Z)
1510  IF Y<(.01) THEN GOTO 1550
1520  W  = W - ((W-WCAL)/2)
1530  GOTO 990
1540  REM ******************* SHOWING THE RESULTS
**********************
1550  FOR  I =1 TO 12
1560  REM PRINT
1570  REM PRINT
1580  PRINT "POINT No.",I
1590  PRINT "TEMP. (C) ",T(I)
1600  PRINT "DENSITY (kg/m^3)",RW(I)
1610  REM PRINT "VISCOSITY (N.s/m^2)",VW(I)
1620  NEXT I
1630  PRINT
1640  PRINT
1650  PRINT "Mean storage temperature (last hour ) ",T(14)
1660  PRINT "Mean storage temperature (prediction) ",T(18)
1670  PRINT "Mean storage temperature (experiment) ",T(19)
1680  REM PRINT "TOTAL HYDROSTATIC PRESSURE (pascal)",H
1690  REM PRINT "FLOW RATE (assumed);kg/s",W
```

```
1700  REM PRINT "FLOW RATE (calculated);kg/s",WCAL
1710  REM PRINT "FLOW RATE THROUGH COLLECTOR;kg/s",WC
1720  REM PRINT" REYNOLD NO. IN DOWN COMER",RD
1730  REM PRINT" REYNOLD NO. IN COLLECTER",RC
1740  REM PRINT" REYNOLD NO. IN RISER    ",RR
1750  REM LPRINT "TOTAL HYDROSTATIC PRESSURE (pascal)",H
1760  REM LPRINT "FLOW RATE (assumed);kg/s",W
1770  REM LPRINT "FLOW RATE (calculated);kg/s",WCAL
1780  REM LPRINT "FLOW RATE THROUGH COLLECTOR;kg/s",WC
1790  REM LPRINT" REYNOLD NO. IN DOWN COMER",RD
1800  REM LPRINT" REYNOLD NO. IN COLLECTER",RC
1810  REM LPRINT" REYNOLD NO. IN RISER    ",RR
1820  REM
**********************************************************
**********
1830  REM
1840  REM       Calculating mass flow rate by using the
energy balance
1850  REM                              at the collector
1860  REM
1870  REM
**********************************************************
*********
1880  TC  =  (T(6)+T(12))/2
1890  TW  =  TC
1900  GOSUB 2050
1910  M(1)= ((.725-5.37*(T(6)-
T(13))/T(14))*2.3419*T(14))/(CW*1000*(T(12)-T(6)))
1920  REM
**********************************************************
*********
1930  REM
1940  REM    Comparison mass flow between the method of
energy balance and
1950  REM                total hydrostatic pressure head
1960  REM
1970  REM
**********************************************************
*********
1980  PRINT"FLOW RATE (by energy balance)  ",M(1)
1990  PRINT"FLOW RATE (by hydro static head)  ",W
2000  T(14) = T(19)
2010  IF MM = 3 GOTO 2040
2020  MM    = MM+1
2030  GOTO 470
2040  END
2050  O = TW +273.15
2060  IF O<273.15 THEN GOTO 3380
2070  IF O>275 THEN GOTO 2140
2080  B1=0        :B2=1
2090  B3=-.0012   :B4=4.217
2100  B5=19.6     :B6=1750
2110  B7=1        :B8=569
2120  B9=.154     :C1=12.99          :01=O-273.15
```

```
2130  GOTO 3320
2140  IF O>280 THEN GOTO 2210
2150  B1=0          :B2=1
2160  B3=-.0026 :B4=4.211
2170  B5=46         :B6=1652
2180  B7=1.6        :B8=574
2190  B9=.392       :C1=12.22          :O1=O-275
2200  GOTO 3320
2210  IF O>285 THEN GOTO 2280
2220  B1=0          :B2=1
2230  B3=-.0018   :B4=4.198
2240  B5=39.4       :B6=1422
2250  B7=1.6        :B8=582
2260  B9=.29        :C1=10.26          :O1=O-280
2270  GOTO 3320
2280  IF O>290 THEN GOTO 2350
2290  B1=.0002    :B2=1
2300  B3=-.001  :B4=4.189
2310  B5=29       :B6=1225
2320  B7=1.6      :B8=590
2330  B9=.25      :C1=8.810001            :O1=O-285
2340  GOTO 3320
2350  IF O>295 THEN GOTO 2420
2360  B1=.0002    :B2=1.001
2370  B3=-6.000001E-04:B4=4.184
2380  B5=24.2     :B6=1080
2390  B7=1.6      :B8=598
2400  B9=.188     :C1=7.56           :O1=O-290
2410  GOTO 3320
2420  IF O>300 THEN GOTO 2490
2430  B1=.0002    :B2=1.002
2440  B3=-.0004:B4=4.181
2450  B5=20.8     :B6=959
2460  B7=1.4      :B8=606
2470  B9=.158     :C1=6.62           :O1=O-295
2480  GOTO 3320
2490  IF O>305 THEN GOTO 2560
2500  B1=.0004    :B2=1.003
2510  B3=-.0002:B4=4.179
2520  B5=17.2     :B6=855
2530  B7=1.4      :B8=613
2540  B9=.126     :C1=5.83           :O1=O-300
2550  GOTO 3320
2560  IF O>310 THEN GOTO 2630
2570  B1=.0004    :B2=1.005
2580  B3=0        :B4=4.178
2590  B5=14.8     :B6=769
2600  B7=1.6      :B8=620
2610  B9=.116     :C1=5.2            :O1=O-305
2620  GOTO 3320
2630  IF O>315 THEN GOTO 2700
2640  B1=.0004    :B2=1.007
2650  B3=.0002    :B4=4.178
2660  B5=12.8     :B6=695
```

```
2670  B7=1.2     :B8=628
2680  B9=.092    :C1=4.62            :O1=O-310
2690  GOTO 3320
2700  IF O>320 THEN GOTO 2770
2710  B1=.0004   :B2=1.009
2720  B3=.0002   :B4=4.179
2730  B5=10.8    :B6=631
2740  B7=1.2     :B8=634
2750  B9=.078    :C1=4.16            :O1=O-315
2760  GOTO 3320
2770  IF O>325 THEN GOTO 2840
2780  B1=.0004   :B2=1.011
2790  B3=.0004   :B4=4.18
2800  B5=9.8     :B6=577
2810  B7=1       :B8=640
2820  B9=.07     :C1=3.77            :O1=O-320
2830  GOTO 3320
2840  IF O>330 THEN GOTO 2910
2850  B1=6.000001E-04  :B2=1.013
2860  B3=.0004   :B4=4.182
2870  B5=7.8     :B6=528
2880  B7=1       :B8=645
2890  B9=.054    :C1=3.42            :O1=O-325
2900  GOTO 3320
2910  IF O>335 THEN GOTO 2980
2920  B1=.0004   :B2=1.016
2930  B3=.0004   :B4=4.184
2940  B5=7.2     :B6=489
2950  B7=1.2     :B8=650
2960  B9=.054    :C1=3.15            :O1=O-330
2970  GOTO 3320
2980  IF O>340 THEN GOTO 3050
2990  B1=6.000001E-04  :B2=1.018
3000  B3=.0004   :B4=4.186
3010  B5=6.6     :B6=453
3020  B7=.8      :B8=656
3030  B9=.044    :C1=2.88            :O1=O-335
3040  GOTO 3320
3050  IF O>345 THEN GOTO 3120
3060  B1=6.000001E-04  :B2=1.021
3070  B3=6.000001E-04  :B4=4.188
3080  B5=6.2     :B6=420
3090  B7=1.6     :B8=660
3100  B9=.042    :C1=2.66            :O1=O-340
3110  GOTO 3320
3120  IF O> 350 THEN GOTO 3190
3130  B1=6.000001E-04  :B2=1.024
3140  B3=.0008   :B4=4.191
3150  B5=4.8     :B6=389
3160  B7=0       :B8=668
3170  B9=.032    :C1=2.45            :O1=O-345
3180  GOTO 3320
3190  IF O>355 THEN GOTO 3260
3200  B1=6.000001E-04  :B2=1.027
```

```
3210  B3=.0008   :B4=4.195
3220  B5=4.4     :B6=365
3230  B7=.6      :B8=668
3240  B9=.03     :C1=2.29          :O1=O-350
3250  GOTO 3320
3260  IF O>360 THEN GOTO 3380
3270  B1=.0008   :B2=1.03
3280  B3=.0008   :B4=4.199
3290  B5=3.8     :B6=343
3300  B7=.6      :B8=671
3310  B9=.024    :C1=2.14          :O1=O-355
3320  RW=(1/((B1*O1+B2)*10^-3))
3330  CW = B3*O1+B4
3340  VW = (-B5*O1+B6)
3350  KW = B7*O1+B8
3360  PW = (-B9*O1+C1)
3370  GOTO 3390
3380  PRINT "ERROR IN PROPERTY LIMITS"
3390  PRINT
3400  REM PRINT "PROPERTIES OF LIQUID WATER AT
",TW+273.15,"KELVIN"
3410  REM PRINT "Density ",RW,"kg/m^3","    Specific ht.
",CW,"kj/kg.K"
3420  REM PRINT "Viscosity * 10^6 ",VW,"N.s/m^2","
Conductivity ",KW,"W/m.K"
3430  REM PRINT "Pr No. ",PW
3440  REM PRINT "***ERROR***THIS PROGRAM HAS NO CORRELATIONS
TO PREDICT NUSSELT                    NUMBER WHEN THE
REYNOLDS NUMBER IS LESS THAN 1000 AND WHEN
GREATER THAN 2000000."
3450  RETURN
3460  FOR I = 1 TO 5
3470  TW    = T(I)
3480  GOSUB 2050
3490  RW(I) = RW
3500  VW(I) = (VW/10^6)
3510  CW(I) = (CW*1000)
3520  WW(I) = V(I)*CW(I)*RW(I)
3530  NEXT I
3540  Z(1)  =
WW(1)*T(1)+WW(2)*T(2)+WW(3)*T(3)+WW(4)*T(4)+WW(5)*T(5)
3550  Z(2)  = WW(1)+WW(2)+WW(3)+WW(4)+WW(5)
3560  T(19) = Z(1)/Z(2)
3570  RETURN
3580  INPUT "Ambient temperature      ",T(13)
3590  INPUT "Temperature at point 1 ? ",T(1)
3600  INPUT "Temperature at point 2 ? ",T(2)
3610  INPUT "Temperature at point 3 ? ",T(3)
3620  INPUT "Temperature at point 4 ? ",T(4)
3630  INPUT "Temperature at point 5 ? ",T(5)
3640  INPUT "Temperature in down comer ? ",T(6)
3650  INPUT "Temperature in riser ? ",T(12)
3660  INPUT"Solar intensity  (instantaneous) ",T(15)
3670  RETURN
```

Computer Program used in Experiment B

```
10  REM
************************************************************
************
20  REM   This program has been written in order to evaluate
mean temperatures (computed and experimental values) and the
thermosyphon mass flow rates through the system of
Experiment B. The system confrigura
30  REM   tion is shown in Fig.4.2.
40  REM
50  REM
************************************************************
************
60  DIM
T(30),DY(30),RW(30),VW(30),D(30),H(30),C(30),V(15),M(5),CW(3
0),                    KW(30),Z(10),WW(30)
70   MM     = 0
80   DY(1)  = .13546
90   DY(2)  = .16086
100  DY(3)  = .16086
110  DY(4)  = .16086
120  DY(5)  = .16086
130  DY(6)  = .16086
140  DY(7)  = .4064
150  DY(8)  = .2667
160  DY(9)  = .2667
170  DY(10) = 2.05749
180  DY(11) = .262715
190  DY(12) = .262715
200  DY(13) = .262715
210  DY(14) = .262715
220  DY(15) = .262715
230  DY(16) = 2.62346
240  D(6)  = .01905
250  D(7)  = .0095
260  D(12) = .01905
270  W = 3
280  LC = .42672
290  V(1) = 8.151001E-03
300  V(2) = 8.151001E-03
310  V(3) = 8.151001E-03
320  V(4) = 8.151001E-03
330  V(5) = 8.151001E-03
340  V(6) = 8.151001E-03
350  V(7) = .06672
360  V(8) = .043785
370  V(9) = .043785
380
REM************************************************************
************
```

```
390  REM
400  REM              Initialization of mean storage
temperature
410  REM
420
REM************************************************************
************
430  GOSUB 3370
440  GOSUB 3510
450  T(18) = T(23)
460  PRINT " Mean storage temperature at starting
time",T(18)
470  REM
************************************************************
********
480  REM
490  REM   Prediction of mean temperature by using energy
balance method
500  REM
510  REM
************************************************************
********
520  GOSUB 3370
530  T(20) = (.736-4.98*(T(10)-T(17))/T(19))*(8475.08*T(19))
540  T(21) = 8451.504*T(17)+875287.5*T(18)
550  T(22) = (T(20)+T(21))/(8.83739*10^5)
560  REM    New mean temp. (by energy method) = T(22)
570  REM    Old mean temp.                    = T(18)
580  REM
************************************************************
********
590  REM
600  REM         The evaluation of mean temperature by
experiment
610  REM
620  REM
************************************************************
********
630  GOSUB 3510
640  REM
************************************************************
********
650  REM
660  REM    Comparison of mean temperatures between by
energy balance and
by experiment
670  REM
680  REM
************************************************************
*******
690  REM Old mean temperature   = T(18)
700  REM New mean temperature (by energy balance) = T(22)
710  REM New mean temperature (by experiment)     = T(23)
```

```
720  REM
**************************************************************
*******
730  REM
740  REM        Evaluating mass flow rate by using total
hydrostatic
750  REM                                  pressure head
760  REM
770  REM
**************************************************************
*******
780  T(11) = T(10) + (T(16) - T(10))*1/10
790  T(12) = T(10) + (T(16) - T(10))*3/10
800  T(13) = T(10) + (T(16) - T(10))*5/10
810  T(14) = T(10) + (T(16) - T(10))*7/10
820  T(15) = T(10) + (T(16) - T(10))*9/10
830  FOR I = 1 TO 16
840  TW = T(I)
850  GOSUB 1960
860  RW(I) = RW
870  VW(I) = VW/10^6
880  H(I)  = RW(I)*9.810001*DY(I)
890  NEXT I
900  H = H(1)+H(2)+H(3)+H(4)+H(5)+H(6)+H(7)+H(8)+H(9)+H(10)-
H(11)-H(12)-H(13)-H(14)-H(15)-H(16)
910  WC = W/10
920  RR = (4*W)/(VW(16)*D(12)*3.141592)
930  RD = (4*W)/(VW(10)*D(6)*3.141592)
940  RC = (4*WC)/(VW(15)*D(7)*3.141592)
950  IF RR<2000 THEN GOTO 990
960  IF RR>4000 THEN GOTO 1010
970  FR = .0243+(3.85*RR/10^6)
980  GOTO 1190
990  FR = 64/RR
1000 GOTO 1190
1010 FR = .316/RR
1020 GOTO 1190
1030 IF RD <2000 THEN GOTO 1070
1040 IF RD>4000 THEN GOTO 1090
1050 FD = .0243+(3.85*RD/10^6)
1060 GOTO 1210
1070 FD = 64/RD
1080 GOTO 1210
1090 FD = .316/RD
1100 GOTO 1210
1110 IF RC<2000 THEN GOTO 1150
1120 IF RC>4000 THEN GOTO 1170
1130 FC = .0243+(3.85*RC/10^6)
1140 GOTO 1230
1150 FC = 64/RC
1160 GOTO 1230
1170 FC = .316/RC
1180 GOTO 1230
1190 A = (FR*DY(16))/(D(12)*RW(16)*(3.141593*(D(12)^2)/4)^2)
```

```
1200 GOTO 1030
1210 B = (FD*DY(10))/(D(6)*RW(10)*(3.141593*(D(6)^2)/4)^2)
1220 GOTO 1110
1230 FOR I = 11 TO 15
1240 C(I) = (FC*LC)/(D(7)*RW(I)*(3.141593*(D(7)^2)/4)^2)
1250 NEXT I
1260 D = A+B+C(11)+C(12)+C(13)+C(14)+C(15)
1270 G1 = (.78)/(RW(10)*(3.14159*(.01905^2)/4)^2)
1280 G2 = (FD*13*.025)/(RW(10)*(3.14159*(.01905^2)/4)^2)
1290 G3 = (.1936)/(RW(10)*(3.14159*(.01588^2)/4)^2)
1300 G4 = (FD*30*.025)/(RW(10)*(3.14159*(.01588^2)/4)^2)
1310 G5 = (.3713)/(RW(10)*(3.14159*(.01588^2)/4)^2)
1320 G6 = (FC*60*.025)/(RW(10)*(3.14159*(.0095^2)/4)^2)
1330 G7 = (FC*60*.025)/(RW(16)*(3.14159*(.0095^2)/4)^2)
1340 G8 = (FR*30*.025)/(RW(16)*(3.14159*(.0254^2)/4)^2)
1350 G9 = (.6049)/(RW(16)*(3.14159*(.01905^2)/4)^2)
1360 J1 = (1.563)/(RW(16)*(3.14159*(.0127^2)/4)^2)
1370 J2 = (1)/(RW(1)*(3.14159*(.0127^2)/4)^2)
1380 E  = D+G1+G2+G3+G4+G5+G6+G7+G8+G9+J1+J2
1390 WCAL = (2*H/E)^(.5)
1400 Z = (WCAL - W)/W
1410 Y = ABS(Z)
1420 IF Y<(.01) THEN GOTO 1460
1430 W = W - ((W-WCAL)/2)
1440 GOTO 910
1450 REM ******************** SHOWING THE RESULTS
**********************
1460 FOR  I =1 TO 16
1470 PRINT
1480 PRINT
1490 PRINT "POINT No.",I
1500 PRINT "TEMP. (C) ",T(I)
1510 PRINT "DENSITY (kg/m^3)",RW(I)
1520 PRINT "VISCOSITY (N.s/m^2)",VW(I)
1530 NEXT I
1540 REM PRINT
1550 REM PRINT
1560 PRINT "TOTAL HYDROSTATIC PRESSURE (pascal)",H
1570 REM PRINT "FLOW RATE (assumed);kg/s",W
1580 REM PRINT "FLOW RATE (calculated);kg/s",WCAL
1590 REM PRINT "FLOW RATE THROUGH COLLECTOR;kg/s",WC
1600 REM PRINT" REYNOLD NO. IN DOWN COMER",RD
1610 REM PRINT" REYNOLD NO. IN COLLECTER",RC
1620 REM PRINT" REYNOLD NO. IN RISER    ",RR
1630 REM LPRINT "TOTAL HYDROSTATIC PRESSURE (pascal)",H
1640 REM LPRINT "FLOW RATE (assumed);kg/s",W
1650 REM LPRINT "FLOW RATE (calculated);kg/s",WCAL
1660 REM LPRINT "FLOW RATE THROUGH COLLECTOR;kg/s",WC
1670 REM LPRINT" REYNOLD NO. IN DOWN COMER",RD
1680 REM LPRINT" REYNOLD NO. IN COLLECTER",RC
1690 REM LPRINT" REYNOLD NO. IN RISER    ",RR
1700
REM************************************************************
************
```

```
1710 REM
1720 REM          Calculating mass flow by using energy
balance
1730 REM
1740 REM
**********************************************************
*********
1750 TC = (T(10)+T(16))/2
1760 TW = TC
1770 GOSUB 1960
1780 M(1) = (.736-4.98*(T(10)-
T(17))/T(19))*(2.3419*T(19))/(CW*1000*(T(16)-T(10)))
1790
REM**********************************************************
*************
1800 REM
1810 REM  Comparison of mass flow rates between the method
of energy balance
1820 REM      and total hydrostatic pressure head
1830 REM
1840
REM**********************************************************
**************
1850 PRINT "Mass flow rate (by energy balance)        ",M(1)
1860 PRINT "Mass flow rate (by static pressure head) ",W
1870 PRINT
1880 PRINT"Old mean temperature                       ",T(18)
1890 PRINT"New mean temperature (energy balance)  ",T(22)
1900 PRINT"New mean temperature (experiment)      ",T(23)
1910 T(18) = T(23)
1920 IF MM = 3 GOTO 1950
1930 MM = MM+1
1940 GOTO 520
1950 END
1960 O = TW +273.15
1970 IF O<273.15 THEN GOTO 3290
1980 IF O>275 THEN GOTO 2050
1990 B1=0        :B2=1
2000 B3=-.0012   :B4=4.217
2010 B5=19.6     :B6=1750
2020 B7=1        :B8=569
2030 B9=.154     :C1=12.99        :O1=O-273.15
2040 GOTO 3230
2050 IF O>280 THEN GOTO 2120
2060 B1=0        :B2=1
2070 B3=-.0026 :B4=4.211
2080 B5=46       :B6=1652
2090 B7=1.6      :B8=574
2100 B9=.392     :C1=12.22        :O1=O-275
2110 GOTO 3230
2120 IF O>285 THEN GOTO 2190
2130 B1=0        :B2=1
2140 B3=-.0018   :B4=4.198
2150 B5=39.4     :B6=1422
```

```
2160 B7=1.6      :B8=582
2170 B9=.29      :C1=10.26          :O1=O-280
2180 GOTO 3230
2190 IF O>290 THEN GOTO 2260
2200 B1=.0002   :B2=1
2210 B3=-.001 :B4=4.189
2220 B5=29       :B6=1225
2230 B7=1.6      :B8=590
2240 B9=.25      :C1=8.810001           :O1=O-285
2250 GOTO 3230
2260 IF O>295 THEN GOTO 2330
2270 B1=.0002   :B2=1.001
2280 B3=-6.000001E-04:B4=4.184
2290 B5=24.2     :B6=1080
2300 B7=1.6      :B8=598
2310 B9=.188     :C1=7.56           :O1=O-290
2320 GOTO 3230
2330 IF O>300 THEN GOTO 2400
2340 B1=.0002   :B2=1.002
2350 B3=-.0004:B4=4.181
2360 B5=20.8     :B6=959
2370 B7=1.4      :B8=606
2380 B9=.158     :C1=6.62           :O1=O-295
2390 GOTO 3230
2400 IF O>305 THEN GOTO 2470
2410 B1=.0004   :B2=1.003
2420 B3=-.0002:B4=4.179
2430 B5=17.2     :B6=855
2440 B7=1.4      :B8=613
2450 B9=.126     :C1=5.83           :O1=O-300
2460 GOTO 3230
2470 IF O>310 THEN GOTO 2540
2480 B1=.0004   :B2=1.005
2490 B3=0        :B4=4.178
2500 B5=14.8     :B6=769
2510 B7=1.6      :B8=620
2520 B9=.116     :C1=5.2            :O1=O-305
2530 GOTO 3230
2540 IF O>315 THEN GOTO 2610
2550 B1=.0004   :B2=1.007
2560 B3=.0002   :B4=4.178
2570 B5=12.8     :B6=695
2580 B7=1.2      :B8=628
2590 B9=.092     :C1=4.62           :O1=O-310
2600 GOTO 3230
2610 IF O>320 THEN GOTO 2680
2620 B1=.0004   :B2=1.009
2630 B3=.0002   :B4=4.179
2640 B5=10.8     :B6=631
2650 B7=1.2      :B8=634
2660 B9=.078     :C1=4.16           :O1=O-315
2670 GOTO 3230
2680 IF O>325 THEN GOTO 2750
2690 B1=.0004   :B2=1.011
```

```
2700 B3=.0004   :B4=4.18
2710 B5=9.8     :B6=577
2720 B7=1       :B8=640
2730 B9=.07     :C1=3.77            :O1=O-320
2740 GOTO 3230
2750 IF O>330 THEN GOTO 2820
2760 B1=6.000001E-04   :B2=1.013
2770 B3=.0004   :B4=4.182
2780 B5=7.8     :B6=528
2790 B7=1       :B8=645
2800 B9=.054    :C1=3.42            :O1=O-325
2810 GOTO 3230
2820 IF O>335 THEN GOTO 2890
2830 B1=.0004   :B2=1.016
2840 B3=.0004   :B4=4.184
2850 B5=7.2     :B6=489
2860 B7=1.2     :B8=650
2870 B9=.054    :C1=3.15            :O1=O-330
2880 GOTO 3230
2890 IF O>340 THEN GOTO 2960
2900 B1=6.000001E-04   :B2=1.018
2910 B3=.0004   :B4=4.186
2920 B5=6.6     :B6=453
2930 B7=.8      :B8=656
2940 B9=.044    :C1=2.88            :O1=O-335
2950 GOTO 3230
2960 IF O>345 THEN GOTO 3030
2970 B1=6.000001E-04   :B2=1.021
2980 B3=6.000001E-04   :B4=4.188
2990 B5=6.2     :B6=420
3000 B7=1.6     :B8=660
3010 B9=.042    :C1=2.66            :O1=O-340
3020 GOTO 3230
3030 IF O> 350 THEN GOTO 3100
3040 B1=6.000001E-04   :B2=1.024
3050 B3=.0008   :B4=4.191
3060 B5=4.8     :B6=389
3070 B7=0       :B8=668
3080 B9=.032    :C1=2.45            :O1=O-345
3090 GOTO 3230
3100 IF O>355 THEN GOTO 3170
3110 B1=6.000001E-04   :B2=1.027
3120 B3=.0008   :B4=4.195
3130 B5=4.4     :B6=365
3140 B7=.6      :B8=668
3150 B9=.03     :C1=2.29            :O1=O-350
3160 GOTO 3230
3170 IF O>360 THEN GOTO 3290
3180 B1=.0008   :B2=1.03
3190 B3=.0008   :B4=4.199
3200 B5=3.8     :B6=343
3210 B7=.6      :B8=671
3220 B9=.024    :C1=2.14            :O1=O-355
3230 RW=(1/((B1*O1+B2)*10^-3))
```

```
3240 CW = B3*O1+B4
3250 VW = (-B5*O1+B6)
3260 KW = B7*O1+B8
3270 PW=(-B9*O1+C1)
3280 GOTO 3300
3290 PRINT "ERROR IN PROPERTY LIMITS"
3300 PRINT
3310 REM PRINT "PROPERTIES OF LIQUID WATER AT
",TW+273.15,"KELVIN"
3320 REM PRINT "Density ",RW,"kg/m^3","    Specific ht.
",CW,"kj/kg.K"
3330 REM PRINT "Viscosity * 10^6 ",VW,"N.s/m^2","
Conductivity ",KW,"W/m.K"
3340 REM PRINT "Pr No. ",PW
3350 REM PRINT "***ERROR***THIS PROGRAM HAS NO CORRELATIONS
TO PREDICT NUSSELT NUMBER WHEN THE   REYNOLDS NUMBER IS LESS
THAN 1000 AND WHEN GREATER THAN 2000000."
3360 RETURN
3370 INPUT "Ambient temperature      ",T(17)
3380 INPUT "Temperature at point 1 ? ",T(1)
3390 INPUT "Temperature at point 2 ? ",T(2)
3400 INPUT "Temperature at point 3 ? ",T(3)
3410 INPUT "Temperature at point 4 ? ",T(4)
3420 INPUT "Temperature at point 5 ? ",T(5)
3430 INPUT "Temperature at point 6 ? ",T(6)
3440 INPUT "Temperature at point 7 ? ",T(7)
3450 INPUT "Temperature at point 8 ? ",T(8)
3460 INPUT "Temperature at point 9 ? ",T(9)
3470 INPUT "Temperature in down comer ? ",T(10)
3480 INPUT "Temperature in riser ? ",T(16)
3490 INPUT "Solar intensity (instantaneous) ",T(19)
3500 RETURN
3510 FOR I = 1 TO 9
3520 TW = T(I)
3530 GOSUB 1960
3540 RW(I) = RW
3550 VW(I) = VW/10^6
3560 CW(I) = CW*1000
3570 WW(I) = V(I)*RW(I)*CW(I)
3580 NEXT I
3590 Z(1) =
WW(1)*T(1)+WW(2)*T(2)+WW(3)*T(3)+WW(4)*T(4)+WW(5)*T(5)+WW(6)
*T(6)+              WW(7)*T(7)+WW(8)*T(8)+WW(9)*T(9)
3600 Z(2) =
WW(1)+WW(2)+WW(3)+WW(4)+WW(5)+WW(6)+WW(7)+WW(8)+WW(9)
3610 T(23) = Z(1)/Z(2)
3620 RETURN
```

Appendix C

Experimental Data

August 17,1987
conventional system

Time	Intensity	T1	T2	T3	T4	T5	Flow	T(predc)	T(exper)
1100		19.5	19.5	19.5	19.5	19.5	0		
1200	920	40	37.5	30	22.5	21	0.0016	28	27.85
1300	940	49	46	40.3	31.5	24	0.0027	36.2	35.3
1400	910	55	53	48.7	42.2	30.1	0.0032	43.1	43
1500	910	59.5	58.5	54	49.7	39.5	0.0029	50.1	50

August 18,1987
conventional system

Time	Intensity	T1	T2	T3	T4	T5	Flow	T(predc)	T(exper)
1100		20	20	20	20	20	0		
1200	860	41	38.5	31	23	20	0.0018	28.2	28.2
1300	880	47	43	40	37	24	0.0027	36.2	35.7
1400	950	55	52	47	41	32.5	0.0031	43.5	42.8
1500	900	57	56	52	47	40	0.0024	49.4	48.5

September 8,1987
system with baffles

Time	Intensity	T1	T2	T3	T4	T5	T6	T7	T8	T9	Flow	T(predc)	T(exper)
1100		20.2	19.6	17.2	16.8	16.6	16	15.2	15.1	14.9	0		
1200	975	41	40	37.7	36.2	34.1	30	22	15.5	15	0.0025	22.9	22.5
1300	1010	43	42	41.5	40.9	40	38.8	33.5	23	16.7	0.0024	30.9	29.4
1400	1100	50	49	48.5	47.8	47	46.5	38.5	33	22	0.0032	37.3	36
1500	1010	50.5	50	49.7	49	47.5	47	42.2	40.17	32.8	0.0023	42.7	41.3

September 14,1987
system with baffles

Time	Intensity	T1	T2	T3	T4	T5	T6	T7	T8	T9	Flow	T(predc)	T(exper)
1100		40	40	40	40	40	40	40	40	40	0		
1200	820	55	54.5	53.5	52.5	51	48.5	45	42	41	0.0025	45.75	45.3
1300	950	60	59.5	58	57.2	56	55	49	47	44	0.0031	51	49.5
1400	860	61.5	61.5	61	59.8	59.2	58.4	54	50	48	0.0026	54.8	53.3
1500	820	62	62	61.5	60.8	60	59.2	57	55	52	0.002	58.1	56.4

September 15,1987
system with baffles

Time	Intensity	T1	T2	T3	T4	T5	T6	T7	T8	T9	Flow	T(predc)	T(exper)
1100		49.5	48.5	46.3	44	41	40.7	39	38.5	37.5	0		
1200	1045	53.4	53.4	52.75	52.3	51.6	51	45.5	40.5	38.5	0.0023	46.7	44.6
1300	1080	59	58.5	57.45	56.6	55	54	51	50	40	0.0028	51.2	50.7
1400	1050	62	62	61.2	61	60.5	60.5	57	54.5	49	0.0026	56.9	55.7
1500	1035	66	66	65.7	65.6	64.7	64	62	60.2	56.8	0.0019	61.49	61.3

September 21,1987
system with baffles

Time	Intensity	T1	T2	T3	T4	T5	T6	T7	T8	T9	Flow	T(predc)	T(exper)
1100		38	38	38	38	38	38	38	38	38	0		
1200	777	51.2	50.2	49	46	46.8	45	42.5	39.8	38	0.0029	42.7	42.3
1300	690	53	52.6	52	51.7	51	49	47	44.5	40	0.0019	46.2	46
1400	860	57.5	56.6	55.7	54.9	54.6	53.3	51.1	49.1	44	0.0027	50.9	50
1500	700	60	59.5	58.9	57.9	57	56	53.5	51	50.2	0.0021	53.6	53.3

September 22,1987
system with baffles

Time	Intensity	T1	T2	T3	T4	T5	T6	T7	T8	T9	Flow	T(predc)	T(exper)
1100		40	40	40	40	40	40	40	40	40	0		
1200	950	56	54.2	53.1	52.3	50.5	48.3	43.8	41	40	0.003	45.8	44.4
1300	950	59	58.2	57.3	56.6	55.5	54.7	48.7	45.1	42.7	0.0031	50.2	49
1400	930	60.3	59.7	59.5	59.4	58.9	58.2	54	53.2	48.7	0.0022	54.1	53.8
1500	900	63	63	62.5	62.5	61.5	60.5	56.7	55	53.5	0.002	58.8	57.1

September 24,1987
system with baffles

Time	Intensity	T1	T2	T3	T4	T5	T6	T7	T8	T9	Flow	T(predc)	T(exper)
1100		49	48.5	47.2	46.75	44.75	43.9	32.2	31.7	31.7	0		
1200	1120	60	59	58	57.5	56.5	55	46	32.7	31.7	0.00484	43.1	42.8
1300	1120	63	62	61.5	61	60.7	60.2	51	43.2	40.3	0.0042	49.6	49.4
1400	1120	66	65.5	65	65	63	61	55	49	48.5	0.0039	56.2	54.5
1500	1120	69	69	68.8	68.3	68	67	62	58	52	0.0038	61	60.5

September 25,1987
system with baffles

Time	Intensity	T1	T2	T3	T4	T5	T6	T7	T8	T9	Flow	T(predc)	T(exper)
1100		39.35	38.75	38	38	38	38	37.78	30	30	0		
1200	950	50.5	49	48	47.2	46	44	38	33	33	0.0027	40.2	38.1
1300	960	54	53	50	49	47.6	46.5	42	38.2	35	0.0031	43.9	42
1400	960	58.2	57.4	56.2	56	55	54.3	48	42	42	0.003	47.5	47.3
1500	915	60.7	59.9	59	58.2	57.6	56.5	51	47.4	46	0.0029	52.4	51.1

September 26,1987
system with baffles

Time	Intensity	T1	T2	T3	T4	T5	T6	T7	T8	T9	Flow	T(predc)	T(exper)
1100		44.45	44	43.1	42.6	42.2	42.2	41.3	39.8	37.2	0		
1200	1035	53.2	53	52.1	51.8	51	50	48	44.2	40.1	0.0019	46.85	46.3
1300	1035	60.4	59.8	59	58.6	58.3	56.2	52.4	49	44	0.003	52.5	51.4
1400	990	63	62.5	62	61.2	60.8	60	57.4	52.6	50.6	0.0026	56.9	55.9
1500	950	65	65	64.4	63.9	63	62.5	61	58.4	54	0.0022	60.9	59.6

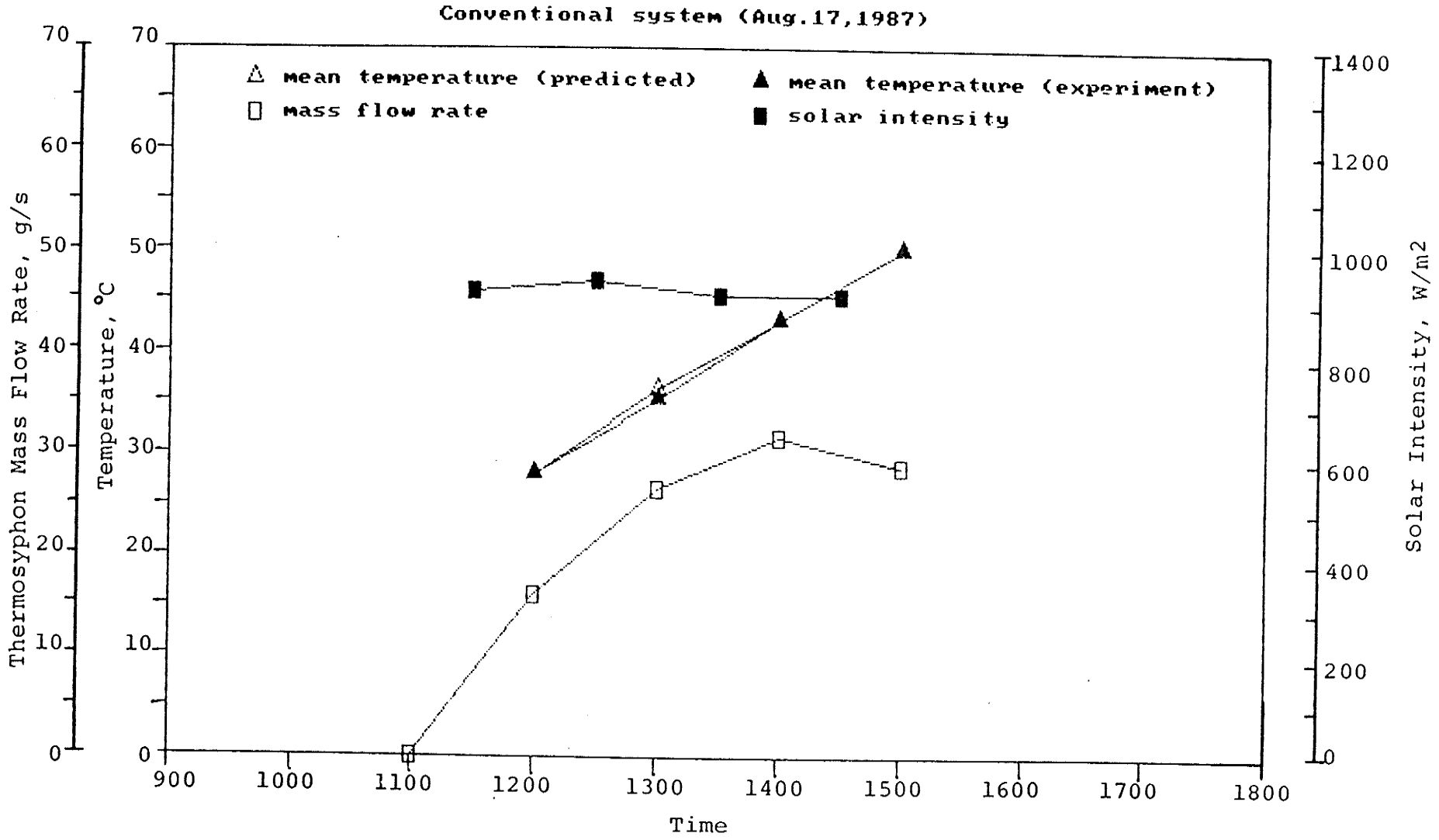

Performance Characteristics; Mean Storage Temperatures, Thermosyphon Mass Flow Rate, and Solar Intensity. From Experiment A.

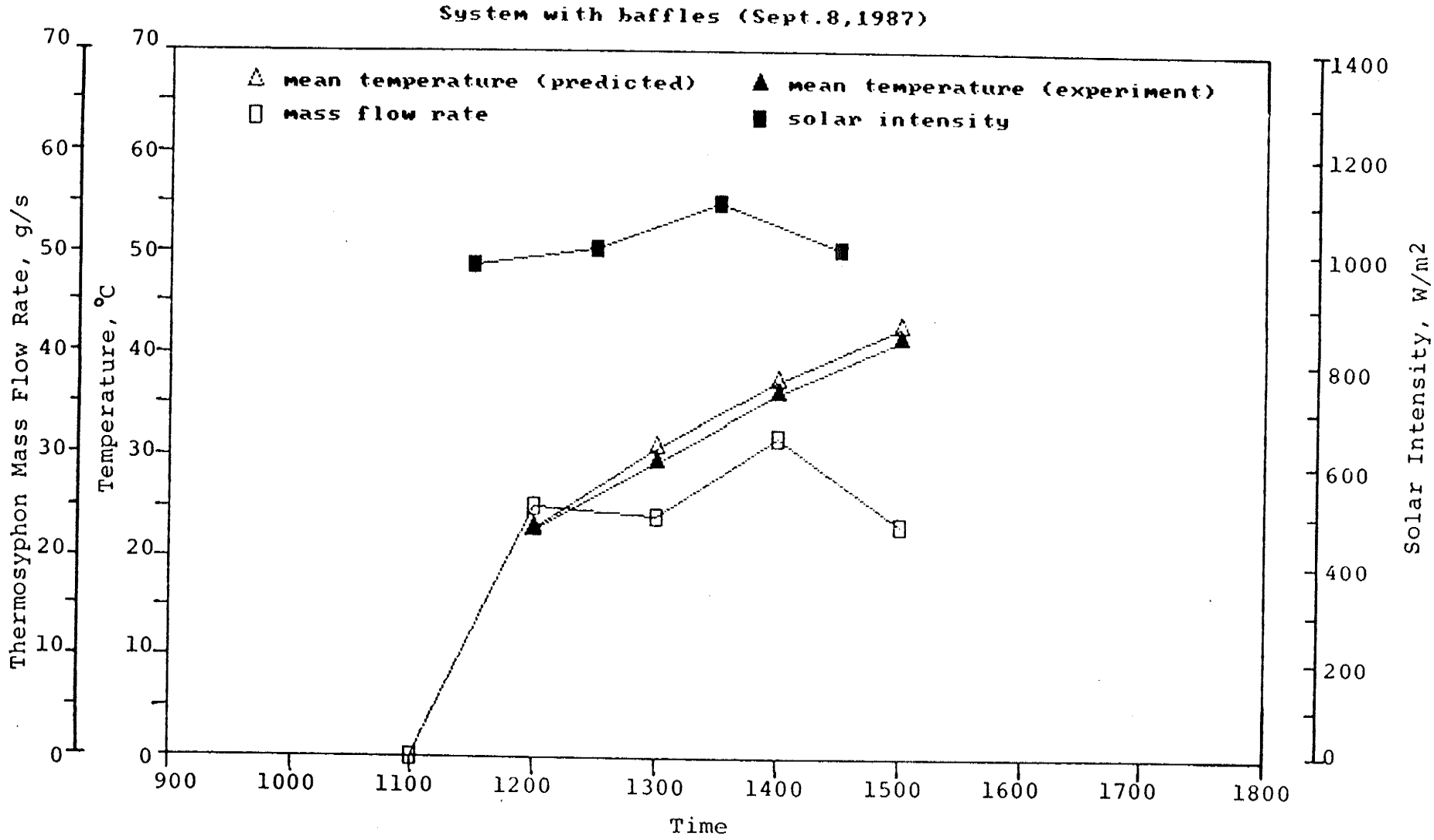

Performance Characteristics; Mean Storage Temperatures, Thermosyphon Mass Flow Rate, and Solar Intensity. From Experiment B2.

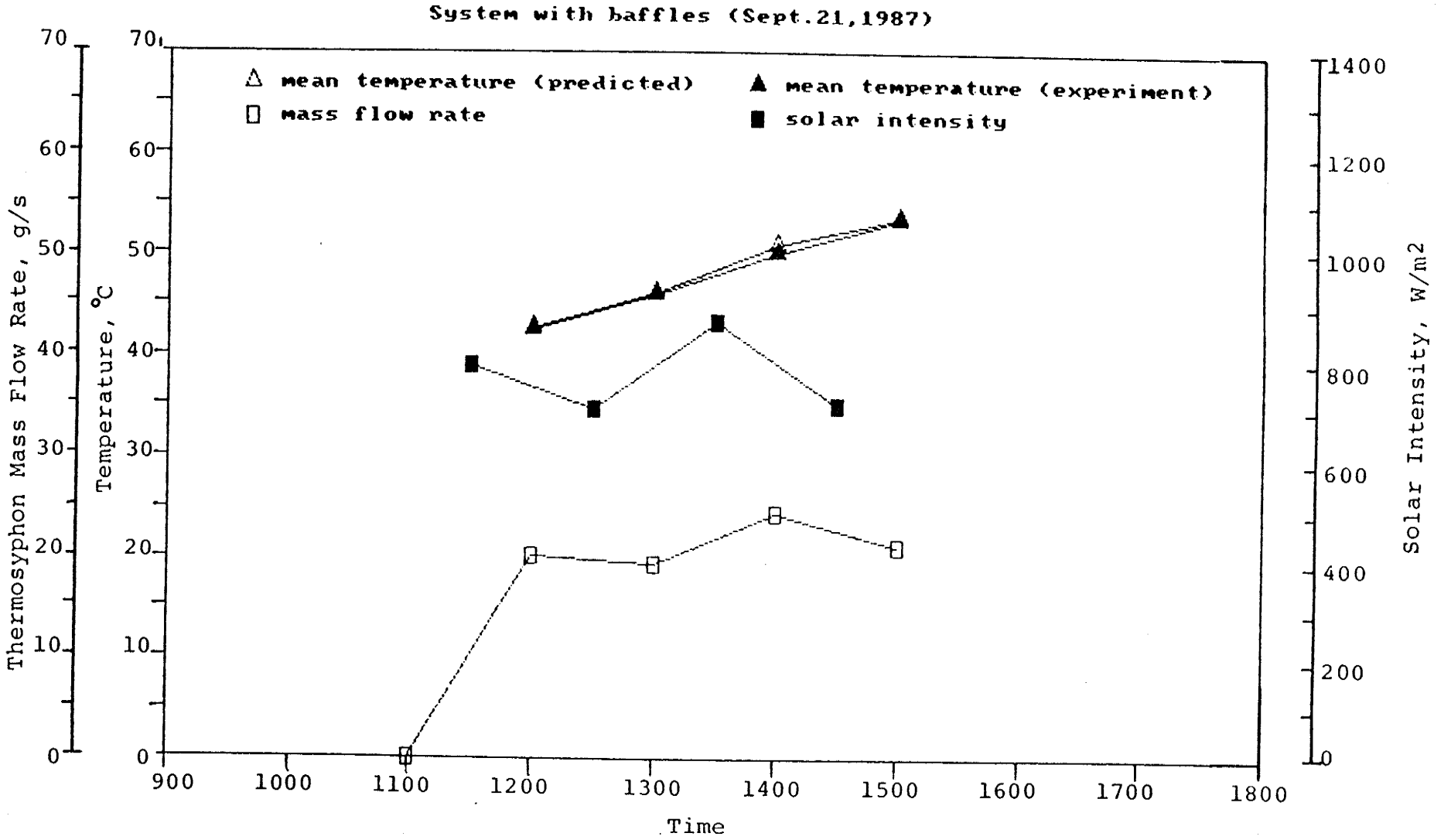

Performance Characteristics; Mean Storage Temperatures, Thermosyphon Mass Flow Rate, and Solar Intensity. From Experiment B1.

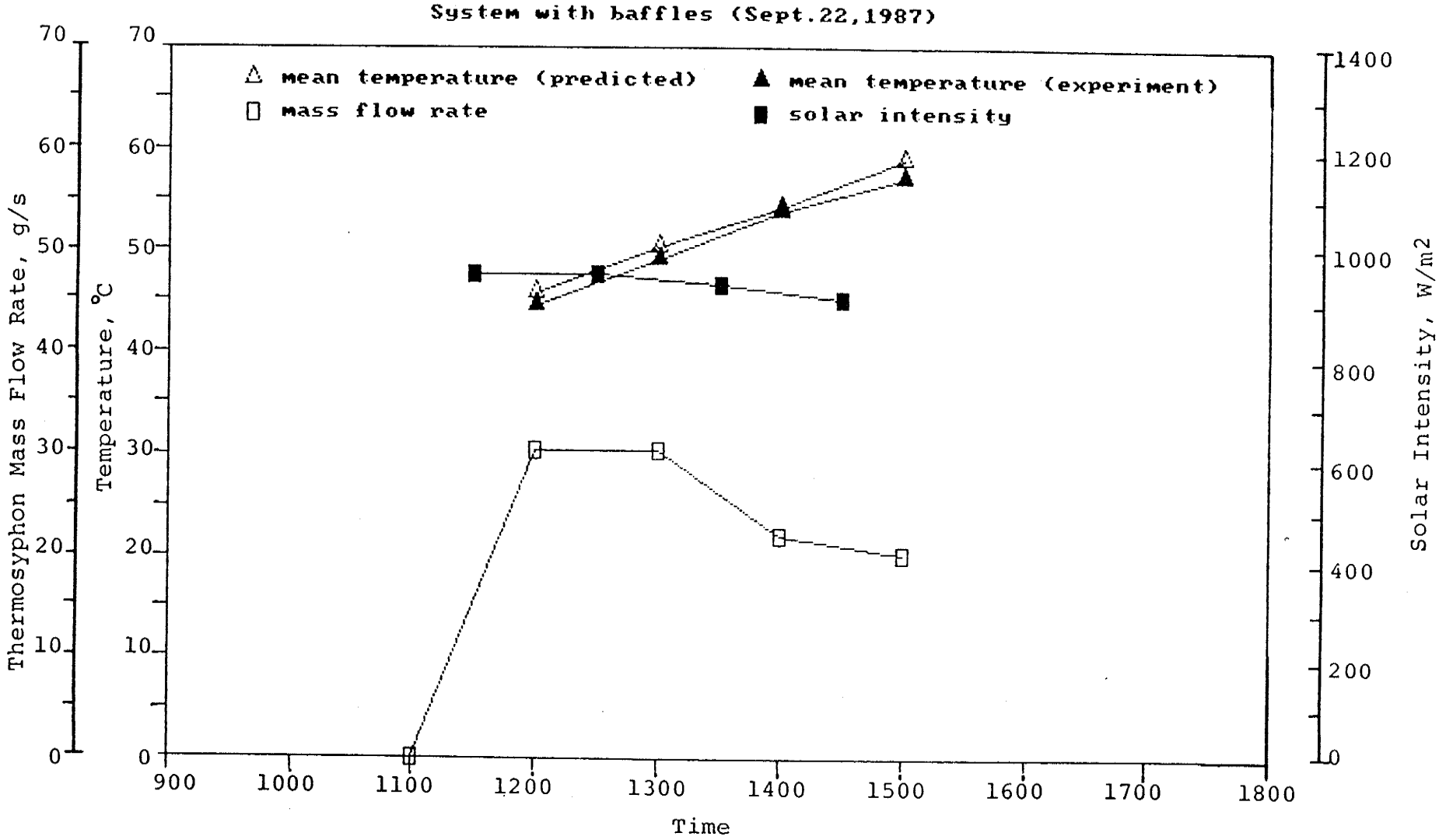

Performance Characteristics; Mean Storage Temperatures, Thermosyphon Mass Flow Rate, and Solar Intensity. From Experiment B1.

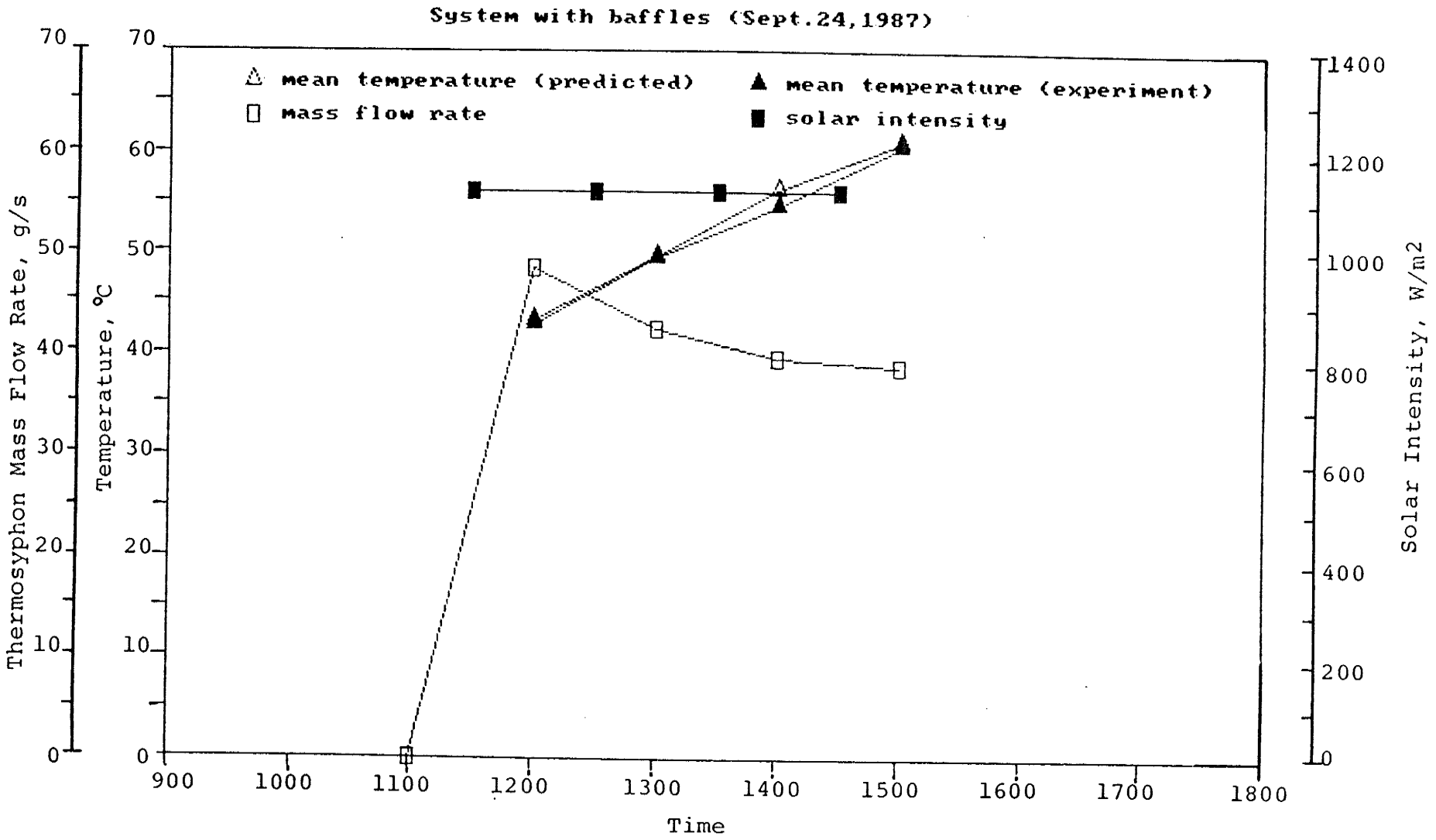

Performance Characteristics; Mean Storage Temperatures, Thermosyphon Mass Flow Rate, and Solar Intensity. From Experiment B2.

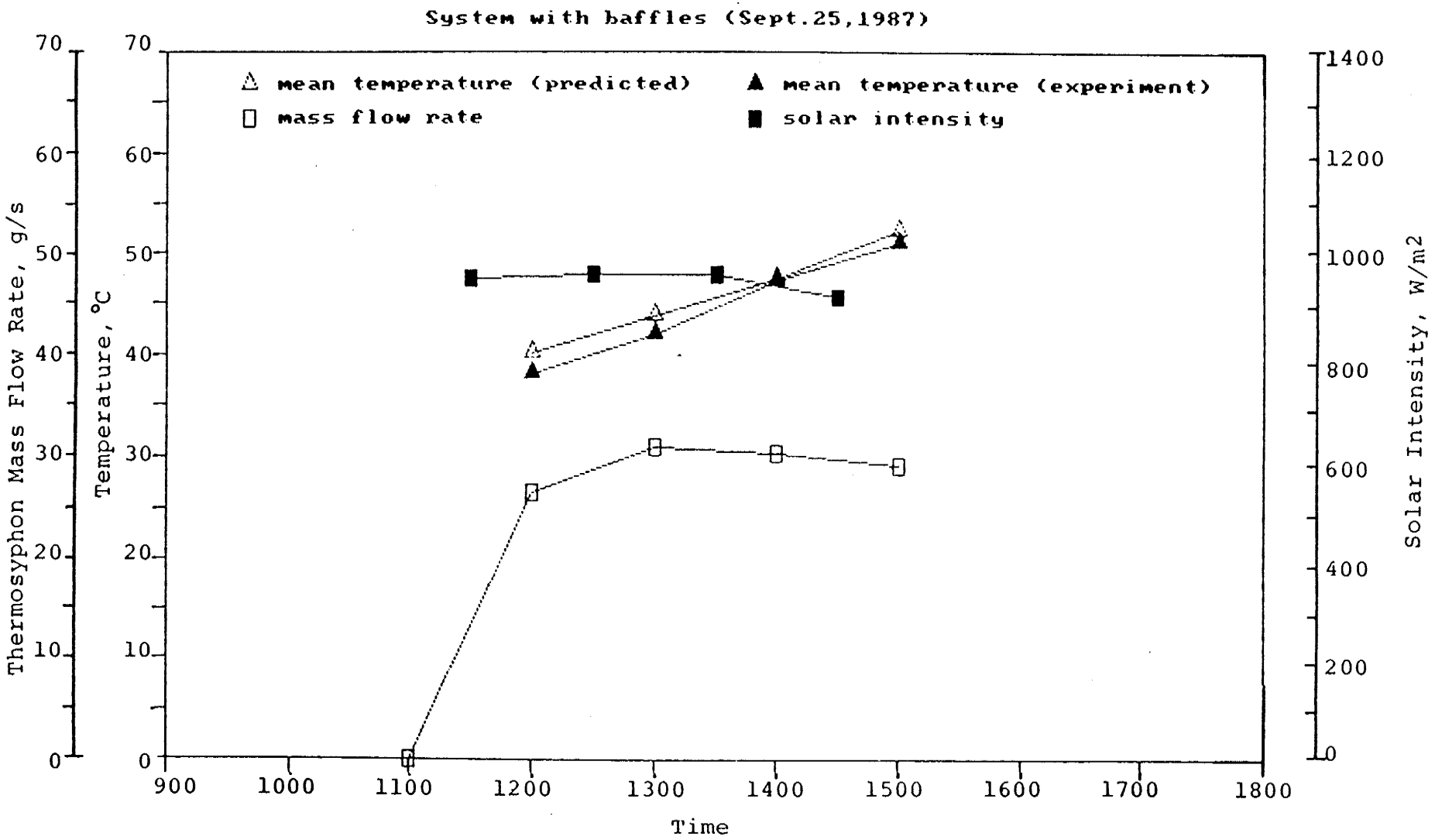

Performance Characteristics; Mean Storage Temperatures, Thermosyphon Mass Flow Rate, and Solar Intensity. From Experiment B2.

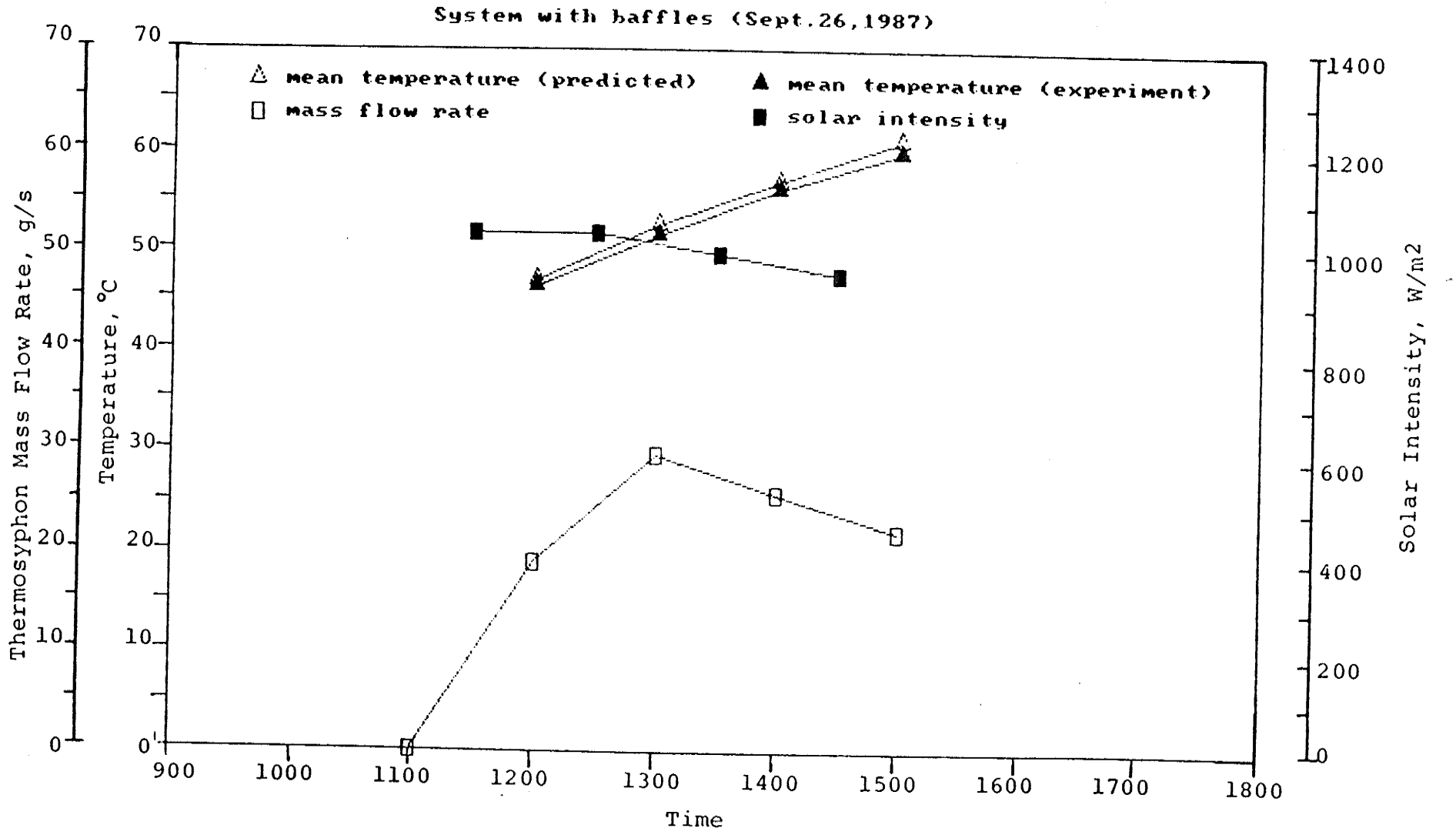

Performance Characteristics; Mean Storage Temperatures, Thermosyphon Mass Flow Rate, and Solar Intensity. From Experiment B2.

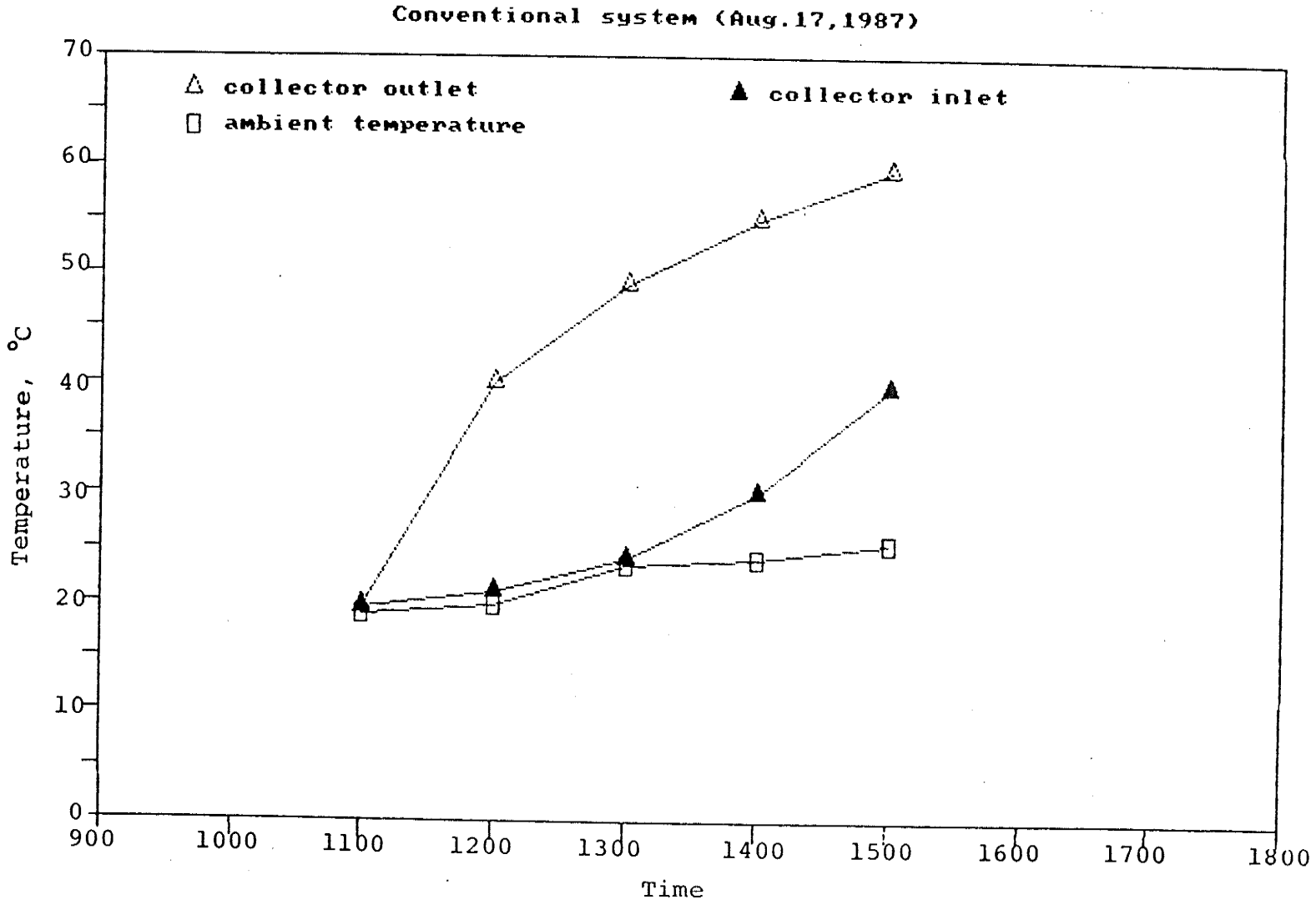

Collector Input/Output, and Ambient Temperatures. From Experiment A.

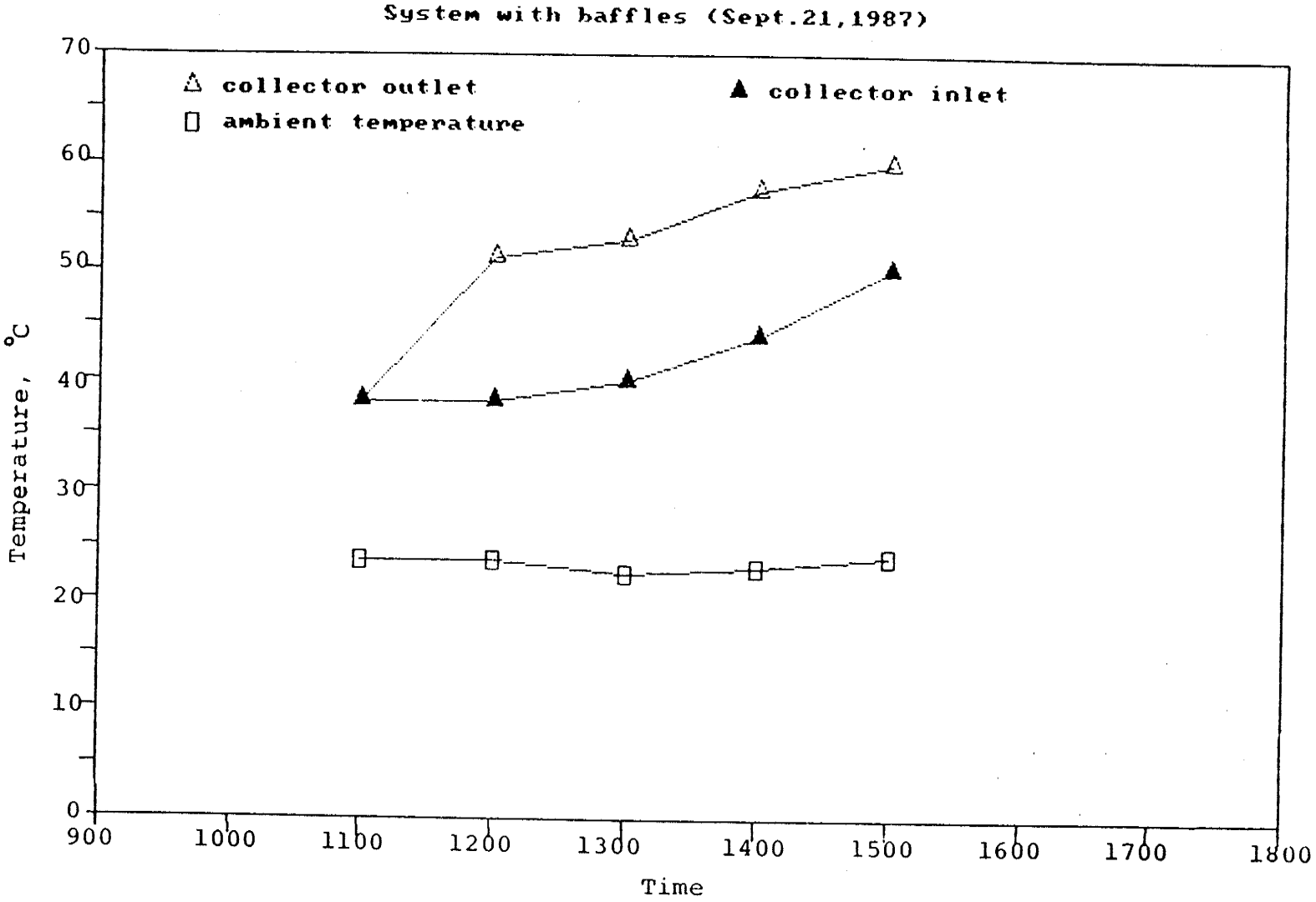

Collector Input/Output, and Ambient Temperatures. From Experiment B1.

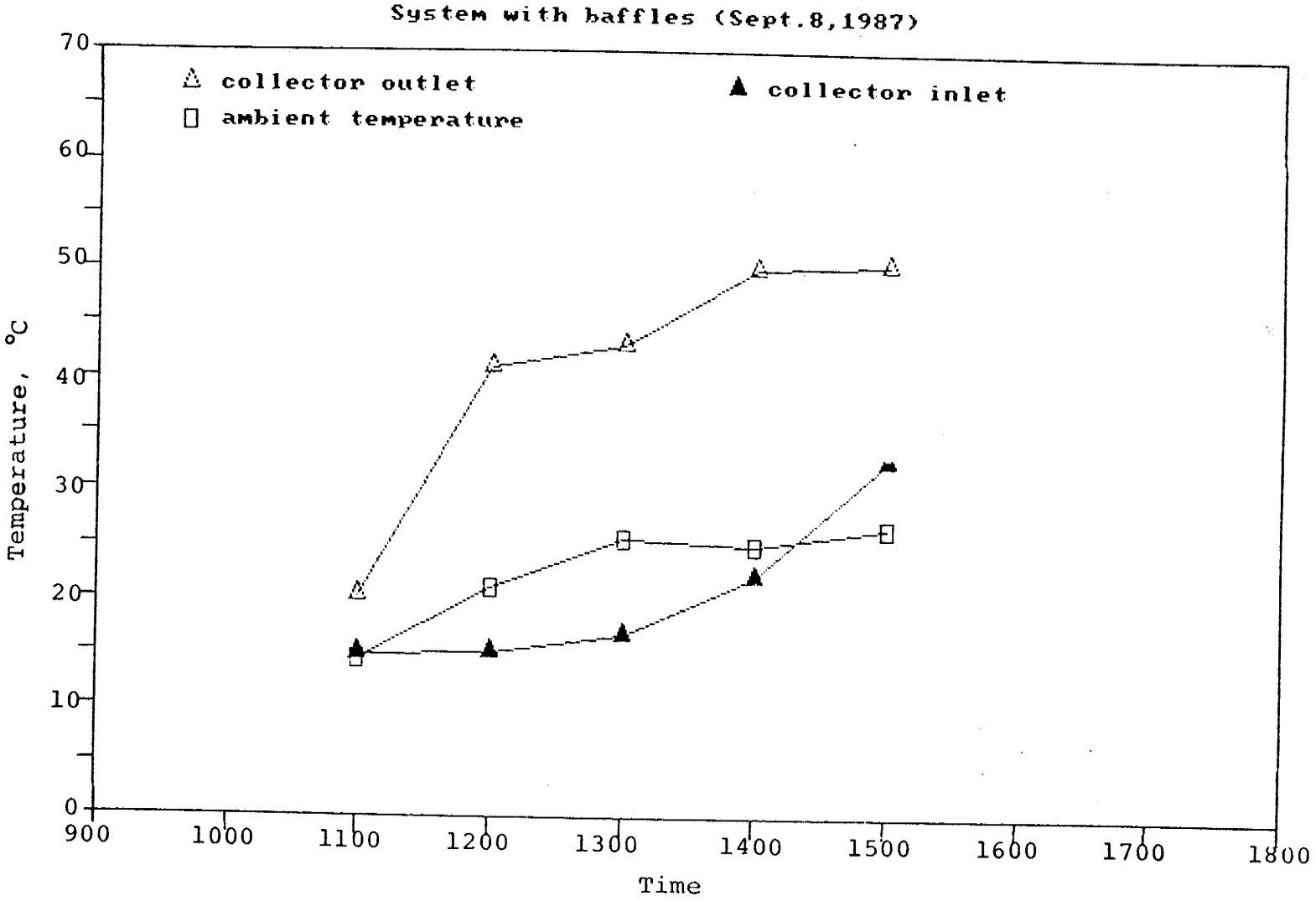

Collector Input/Output, and Ambient Temperatures. From Experiment B2.

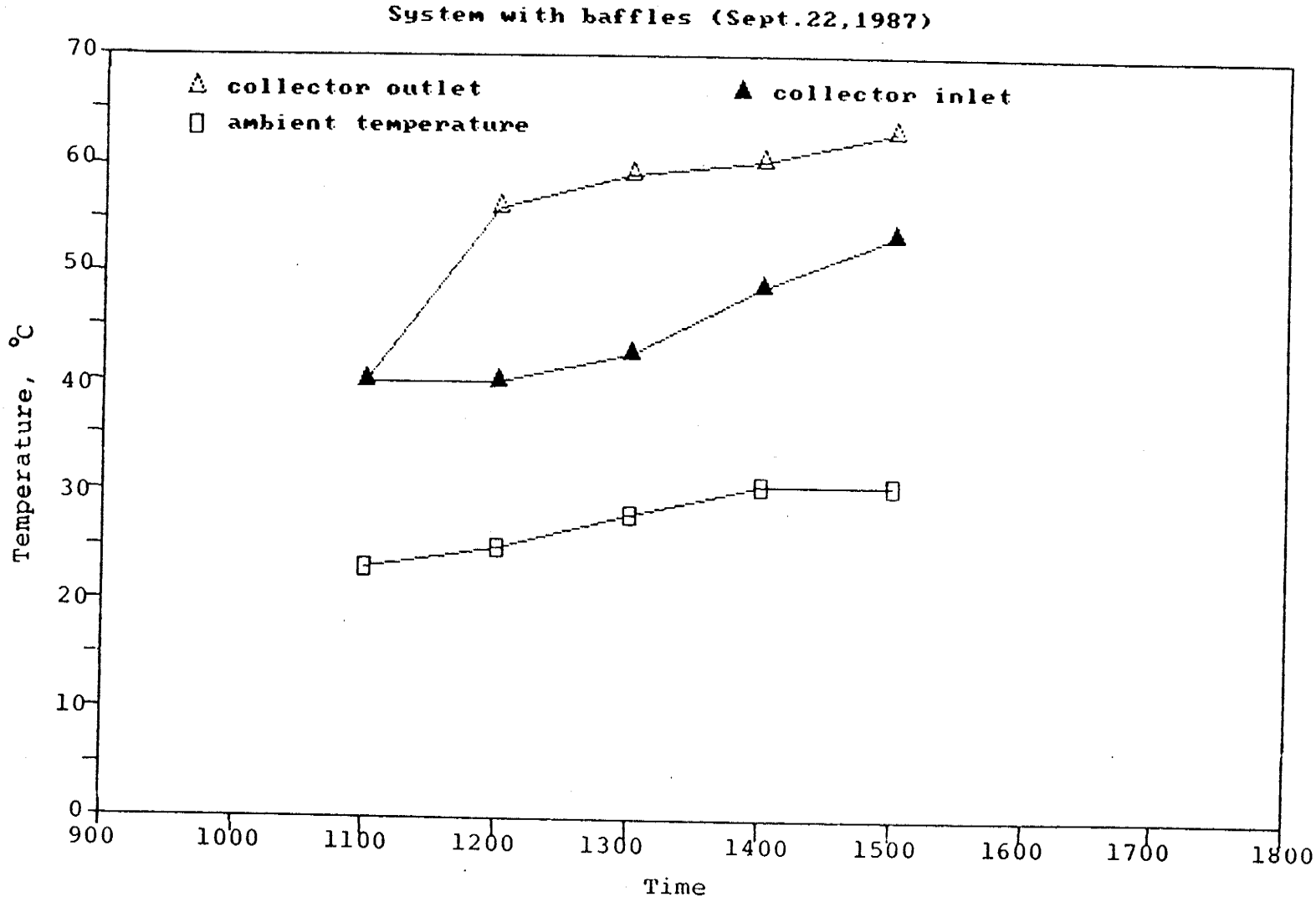

Collector Input/Output, and Ambient Temperatures. From Experiment B1.

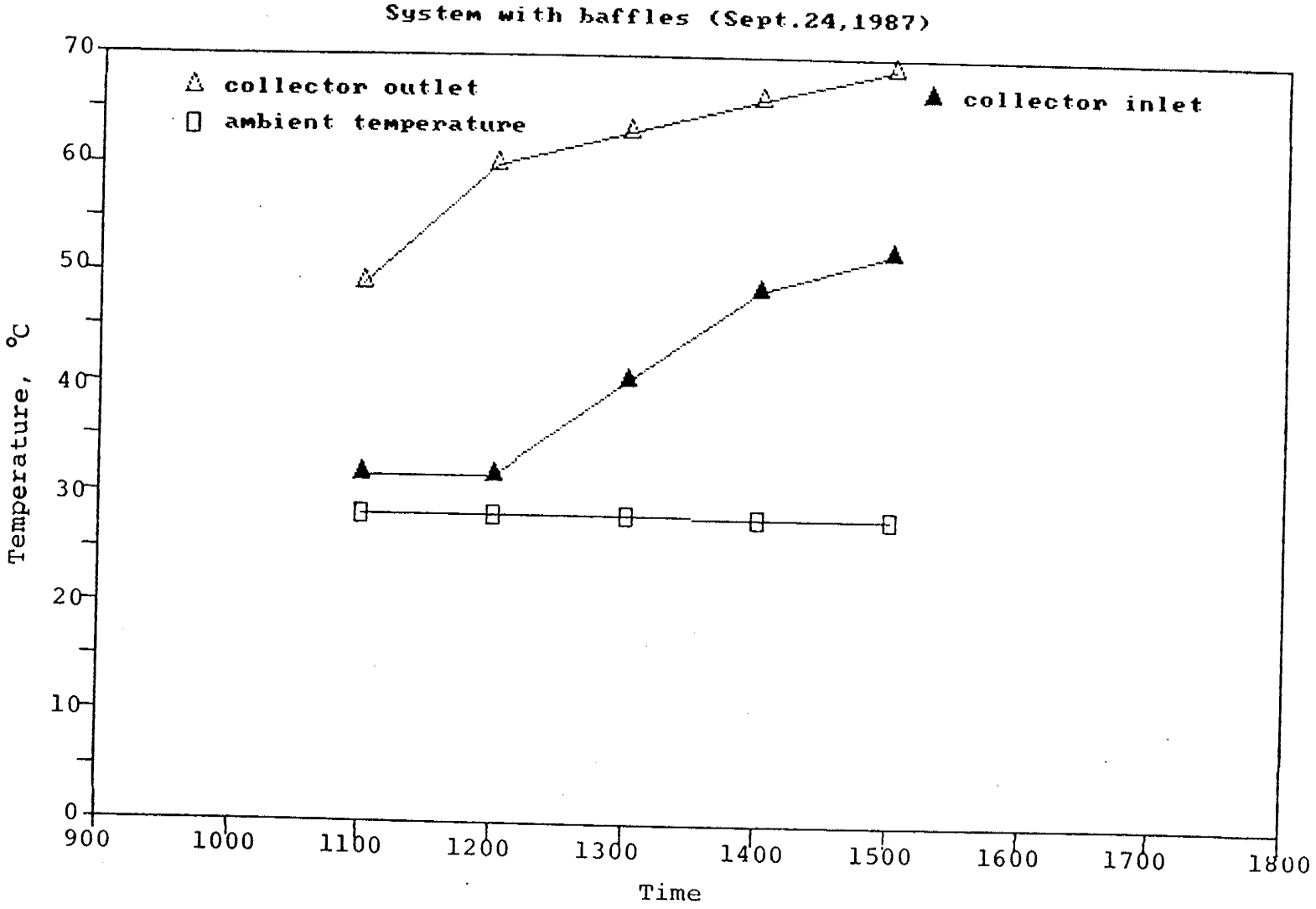

Collector Input/Output, and Ambient Temperatures. From Experiment B2.

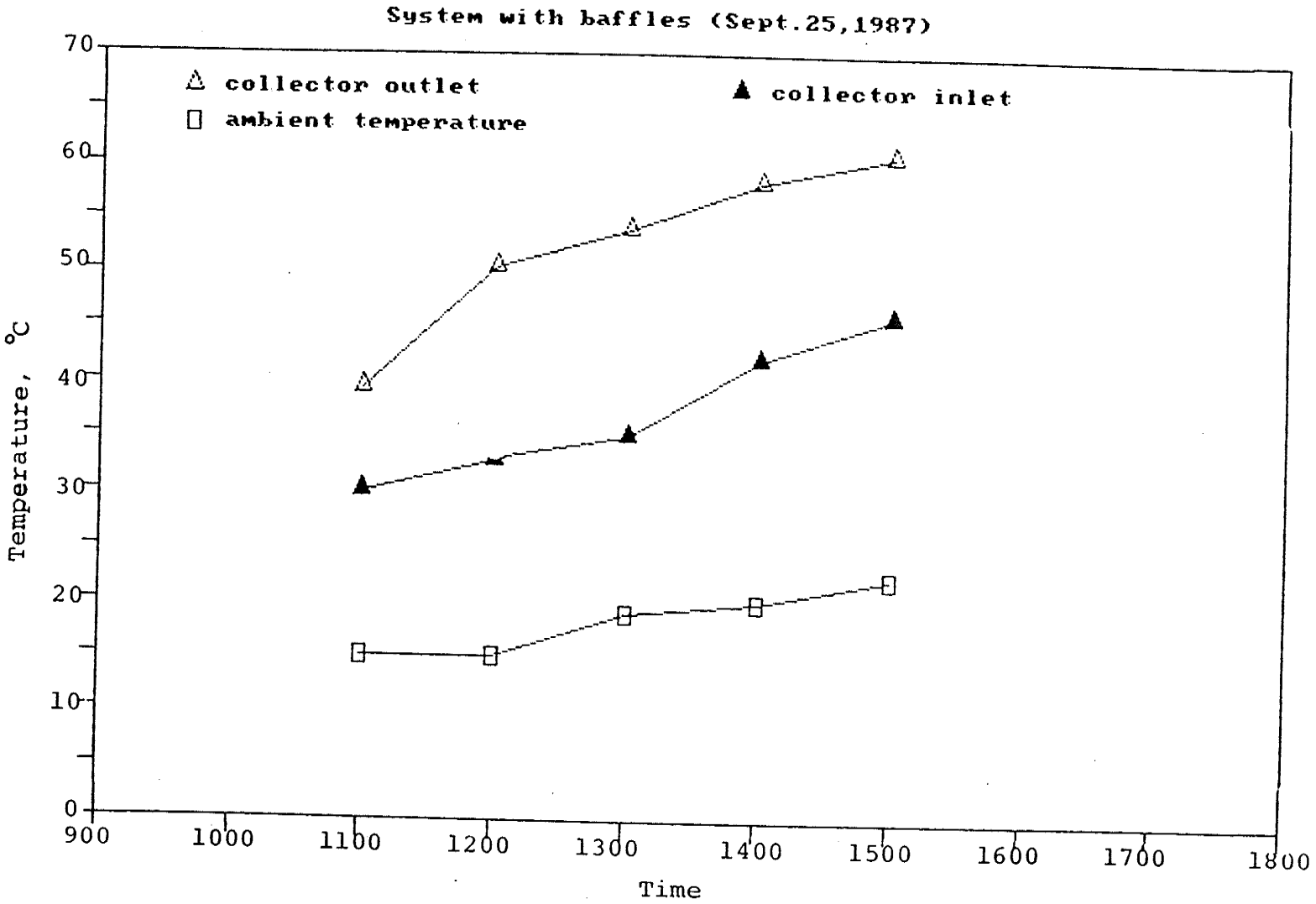

Collector Input/Output, and Ambient Temperatures. From Experiment B2.

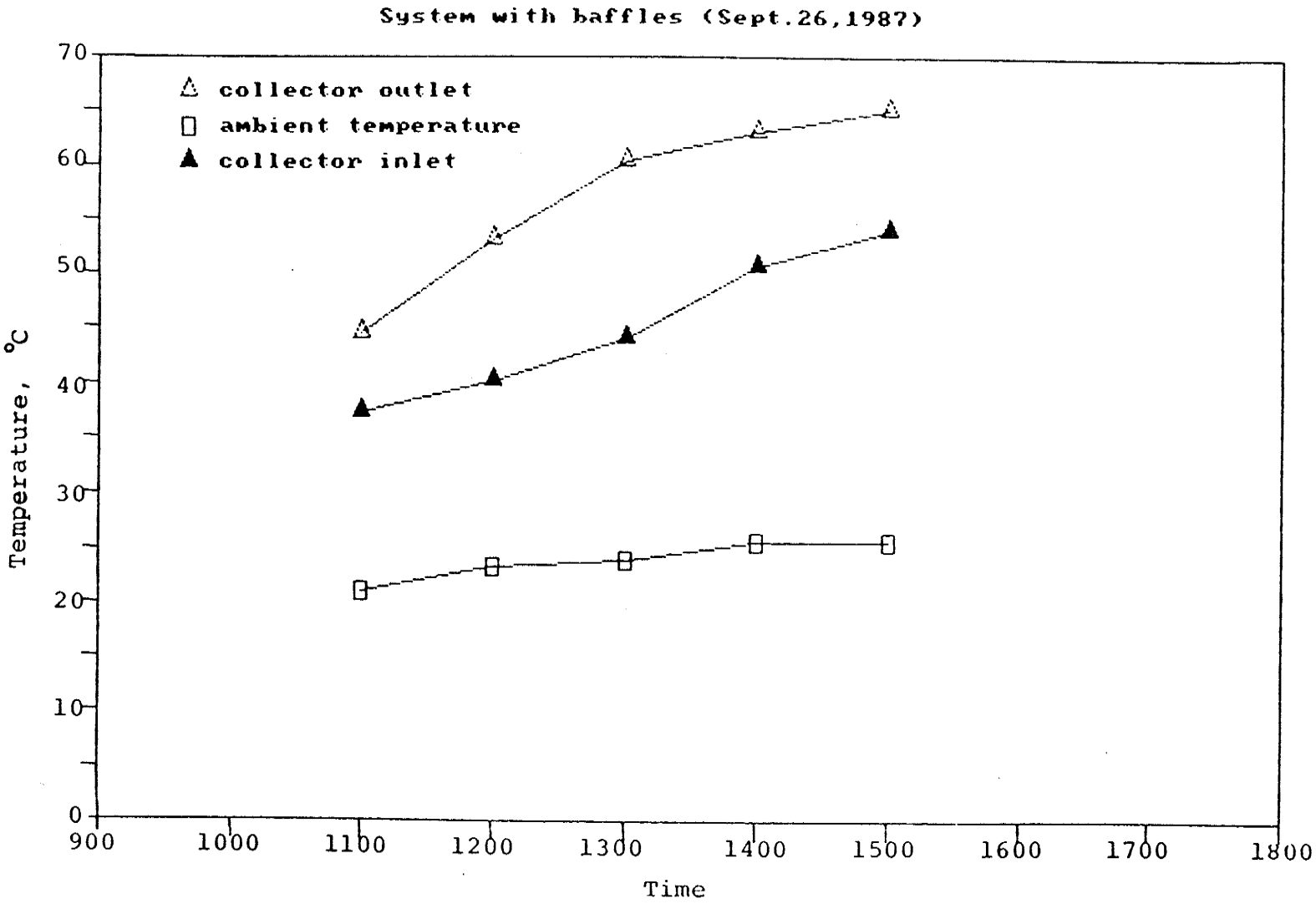

Collector Input/Output, and Ambient Temperatures. From Experiment B2.

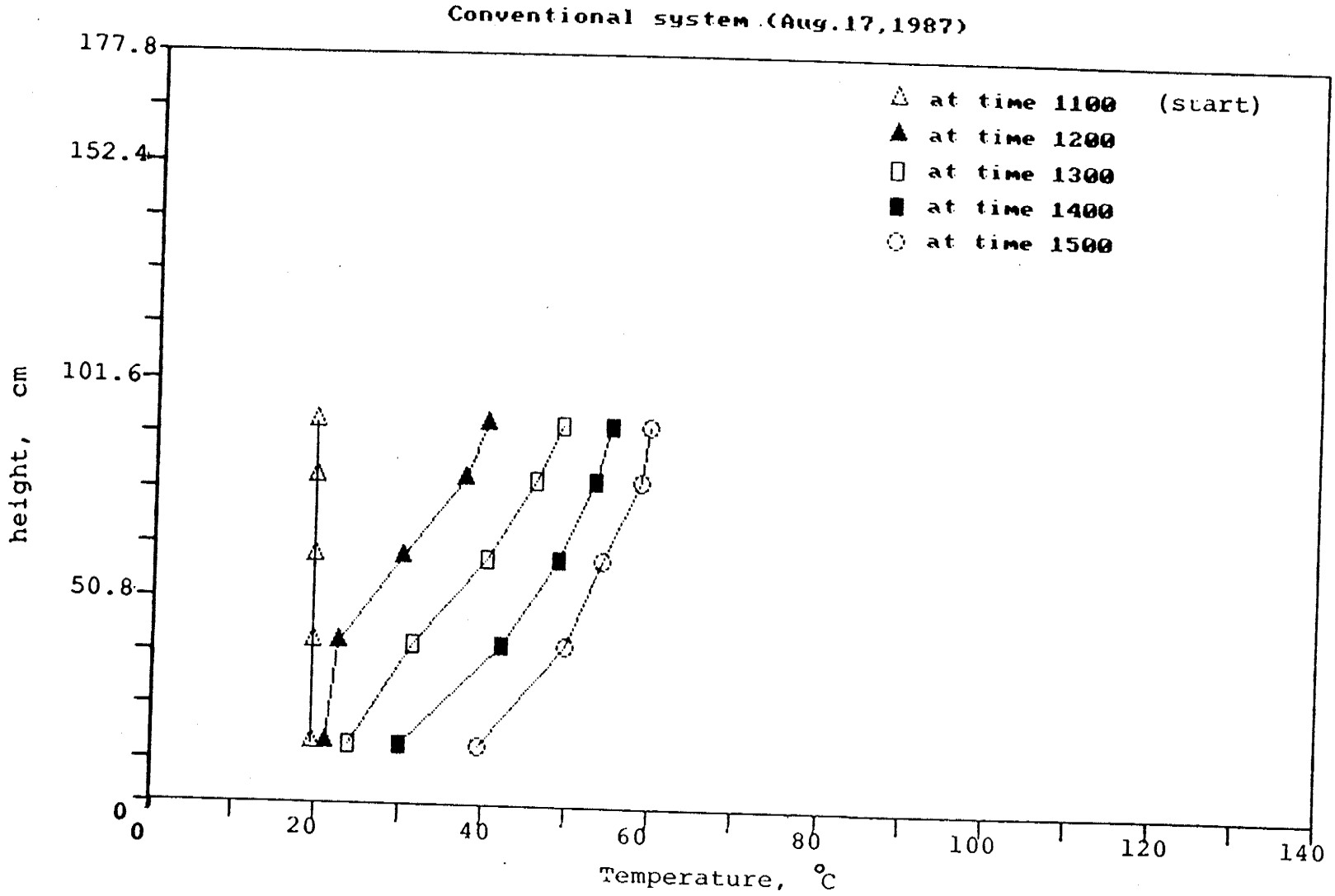

Vertical Temperature Profile Changes. From Experiment A.

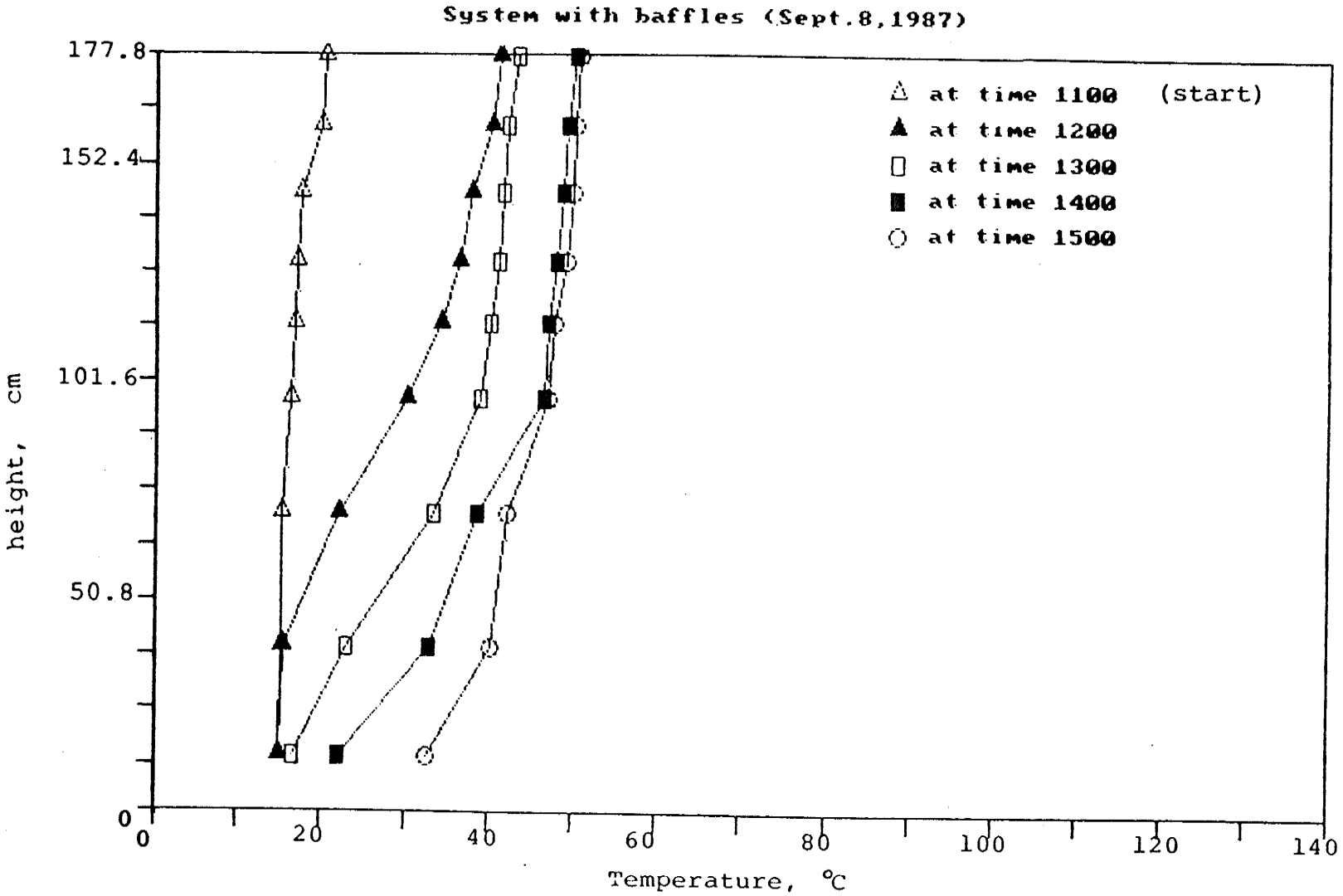

Vertical Temperature Profile Changes. From Experiment B2.

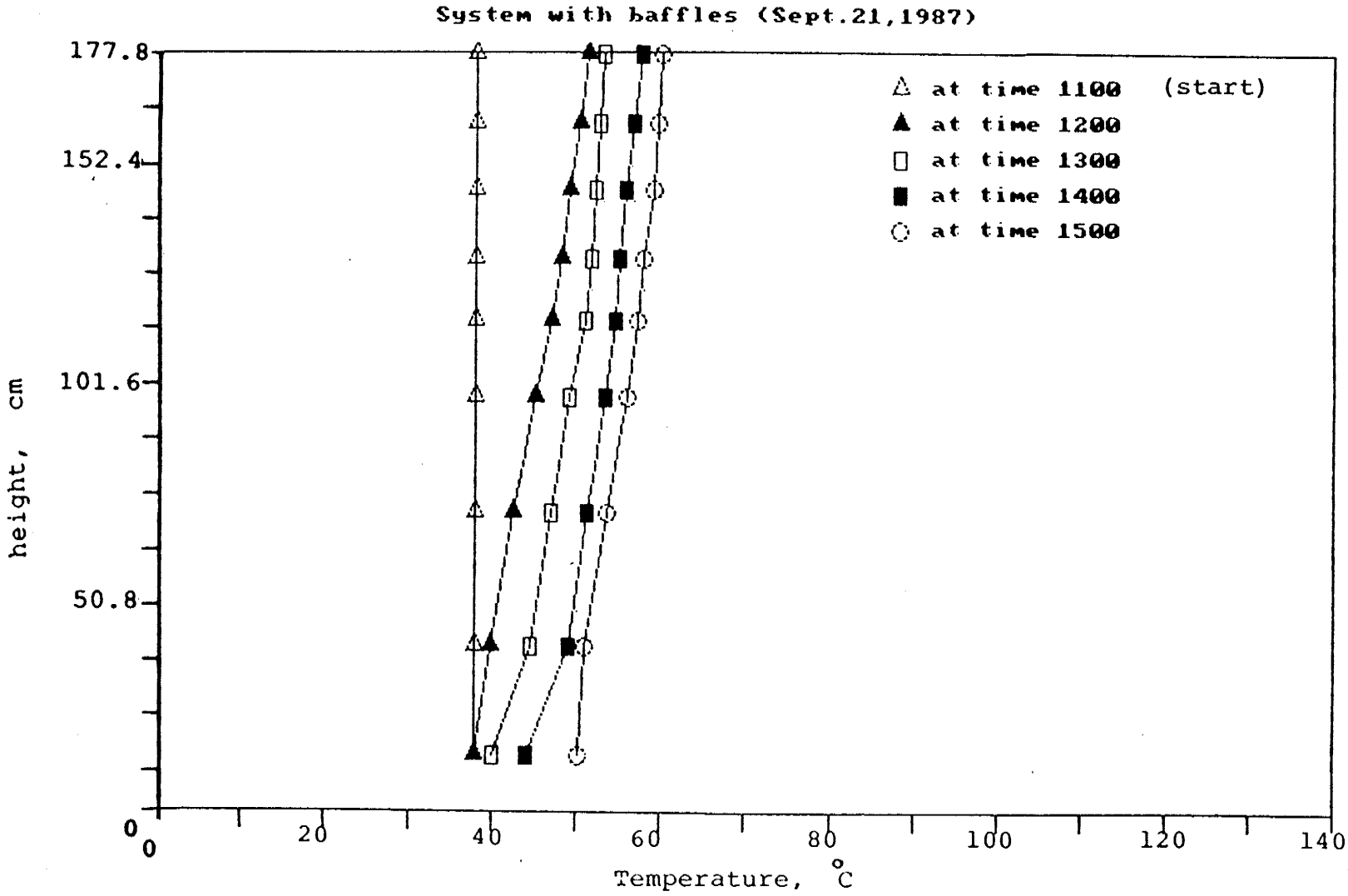

Vertical Temperature Profile Changes. From Experiment B1.

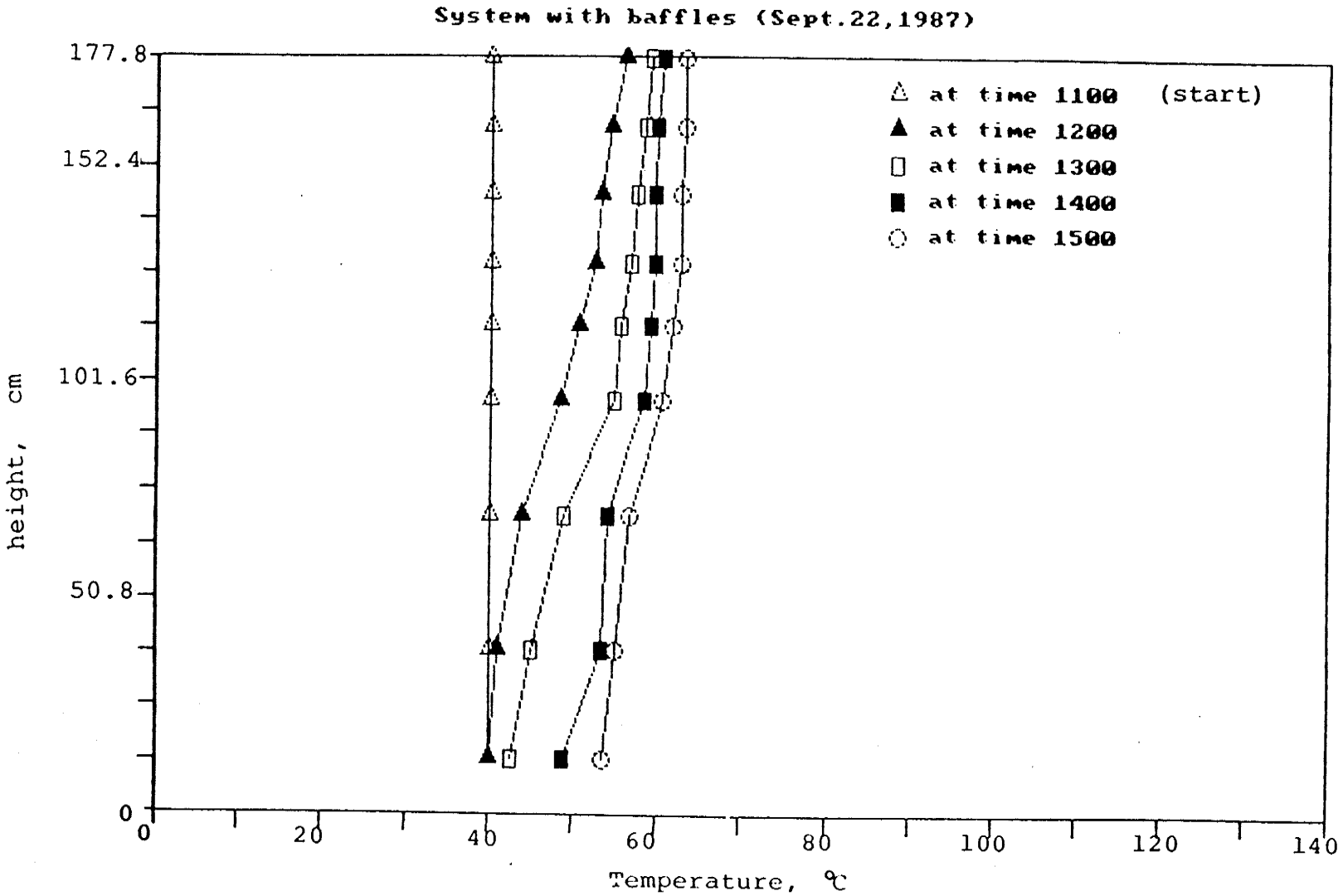

Vertical Temperature Profile Changes. From Experiment B1.

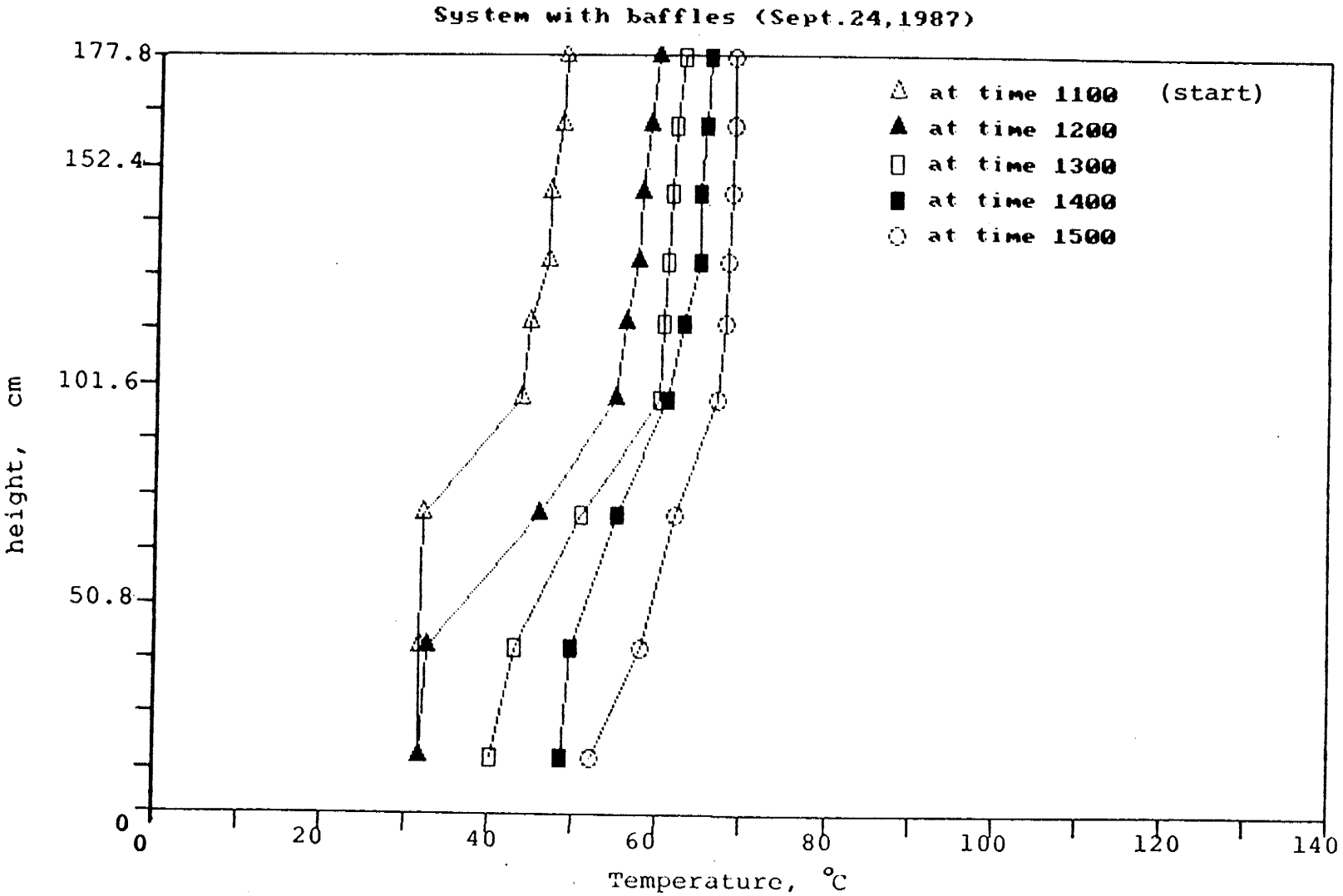

Vertical Temperature Profile Changes. From Experiment B2.

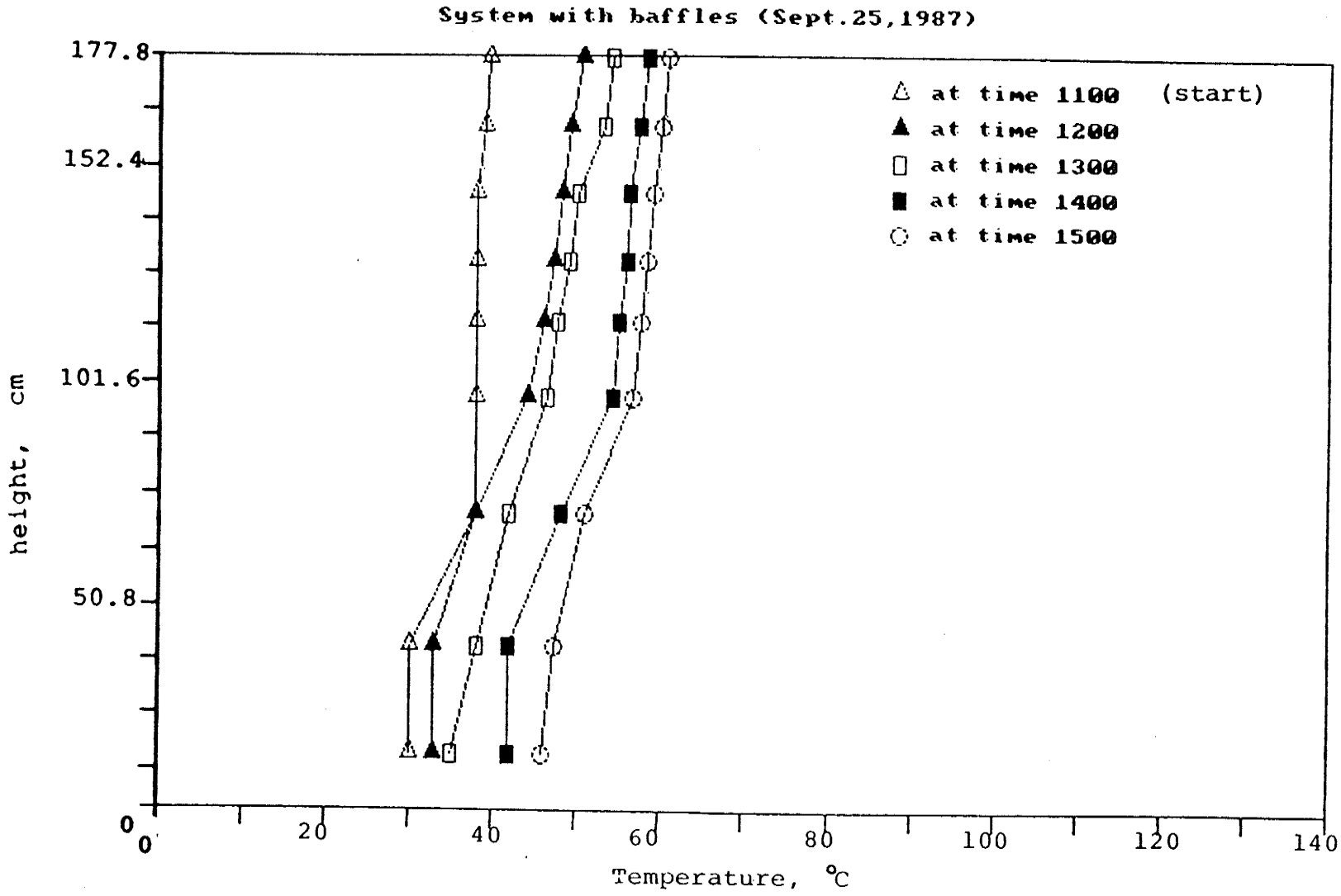

Vertical Temperature Profile Changes. From Experiment B2.

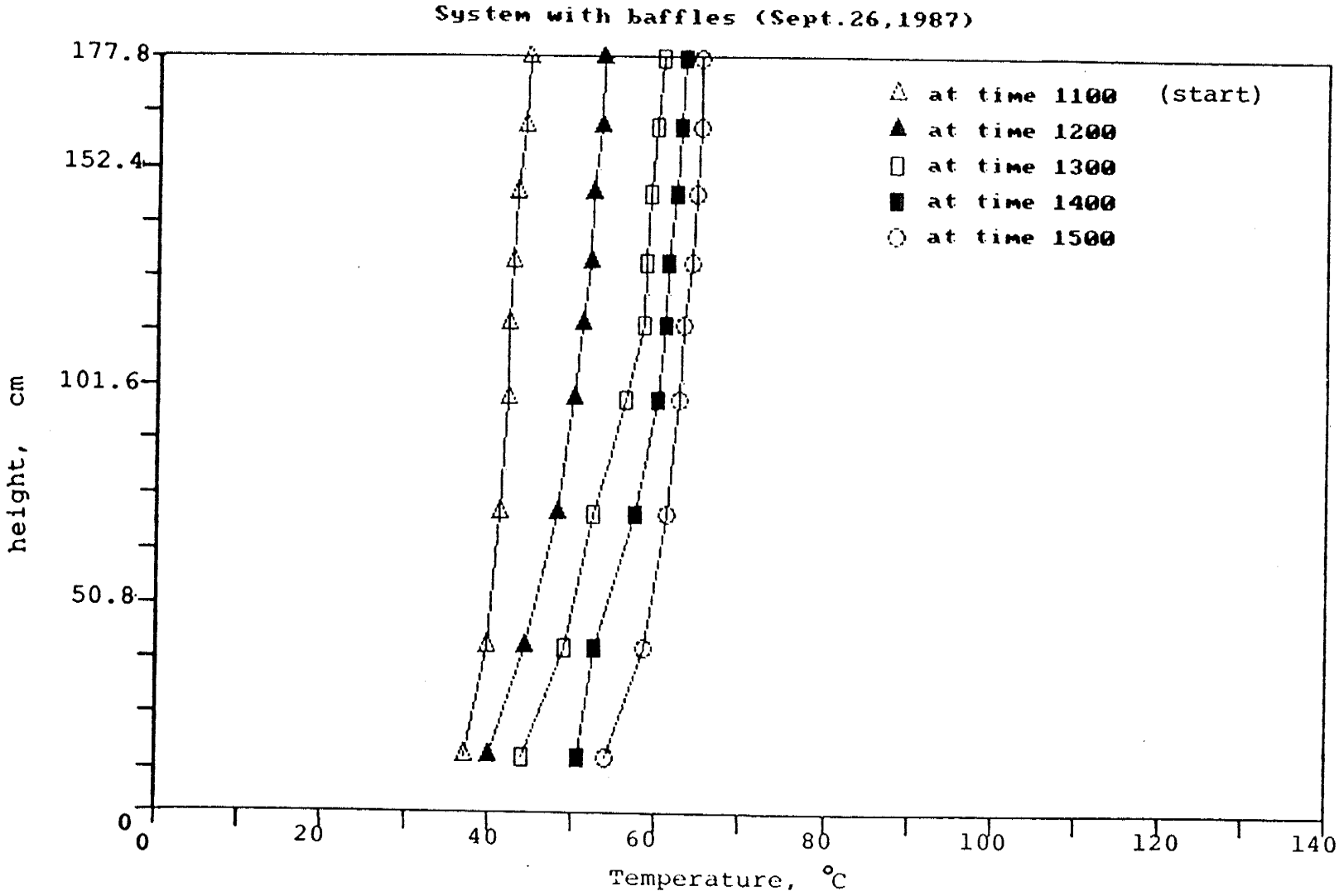

Vertical Temperature Profile Changes. From Experiment B2.

Appendix D

Free (Natural) Convection Flow

Free Convection Flow*

In forced convection flow, the fluid flow originates due to the external forcing condition. For example, fluid motion may be induced by a fan or pump, or it may result from propulsion of the solid to the fluid.

Consider situations for which there is no forced velocity, yet convection currents exist with in the fluid. Such situations are referred to as free or natural convection, and they originate when a body force acts on a fluid in which there are density gradients. The net effect is a buoyancy force, which induces the free convection currents. In the most common case, the density is due to a temperature gradient, and the body force is due to the gravitational field.

Since free convection flow velocities are generally much smaller than those associated with forced convection, the corresponding convection transfer rate are also smaller. But in many systems involving multimode heat transfer effects, free convection may provide the largest resistance to heat transfer and therefore plays an important role in the design or performance of the system.

Physical Considerations.

In free convection fluid motion is due to the buoyancy forces within the fluid, which in forced convection is externally imposed. Buoyancy is due to the combined presence of a fluid density gradient and a body force, usually gravitational. There are also several ways in which a mass density gradient may arise in a fluid, but for the most common situation it is due to the presence of a temperature, generally decreasing (due to fluid expansion) with increasing temperature ($\partial\rho / \partial T < 0$).

In this section we focus on free convection problems in which the density gradient is due to a temperature gradient and the body force is gravitational. Note, however, that the presence of a fluid density gradient in the gravitational field does not ensure the existence of free convection currents. Consider the condition in Fig. D1, a fluid is enclosed by two

large, horizontal plates of different temperatures ($T_1 \neq T_2$). In case (a) the temperature of the lower plate exceeds that of the upper plate, and the density decreases in the direction of gravitational force. This condition is unstable, and free convection currents must exist. The gravitational force on the dense fluid in the upper layer exceeds that acting on the lighter fluid in the lower layers, and the designated circulation pattern will exist. The heavier fluid will descend, being warmed in the process, while the lighter fluid will rise, cooling as it moves. However, this condition does not characterize case (b), for which $T_1 > T_2$ and the density no longer decreases in the direction of gravitational force. Conditions are now stable, and there is no bulk fluid motion. In case (a) heat transfer occurs from the bottom to the top surface by free convection; for case (b) heat transfer (from top to bottom) occurs by conduction.

Free convection flow may be classified according to whether the flow is bounded by a surface. In the absence of an adjoining surface, free boundary flows associated with fluid rising from a submerged heat object. Consider the heat wire of Fig.D2 (a) which is immersed in an extensive, quiescent fluid. Fluid that is heated by the wire rises due to a buoyancy force, entraining fluid from the quiescent region. Although the width of the plume increases with distance from the wire, the plume itself will eventually dissipate as a result of viscous effects and a reduction in the buoyancy force caused by cooling of the fluid in the plume. The distinction between a plume and a buoyancy jet is generally made on the basis of initial fluid velocity. This velocity is zero for the plume, but finite for the buoyancy jet. Fig.D2 (b) shows a heated fluid being discharged as a horizontal jet into a quiescent medium of lower temperature. The vertical motion that the jet begins to assume is due to the buoyancy force.

* Incropera, D.W., " Fundamental of Heat and Mass Transfer, " John Wiley & Sons, 2nd Ed., 1981.

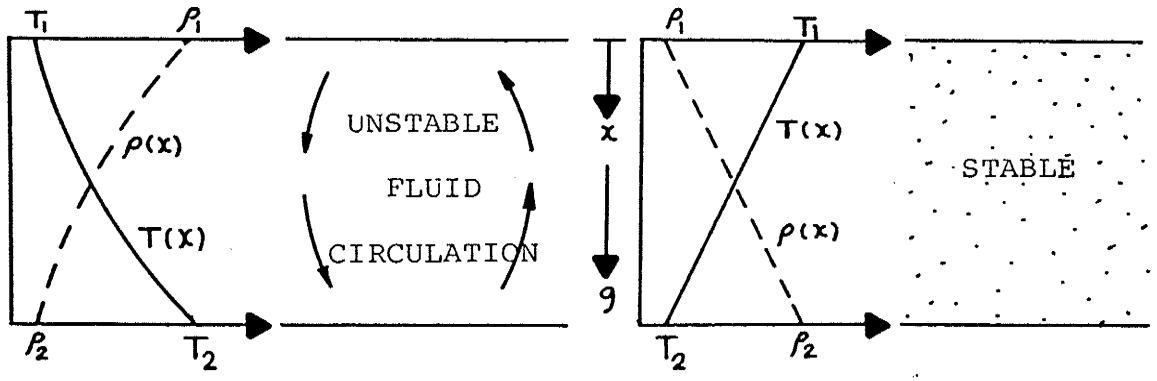

Fig.D1 Conditions in fluid between large horizontal plates at different temperatures. Case (a), unstable temperature gradient. Case (b) stable temperature gradient.

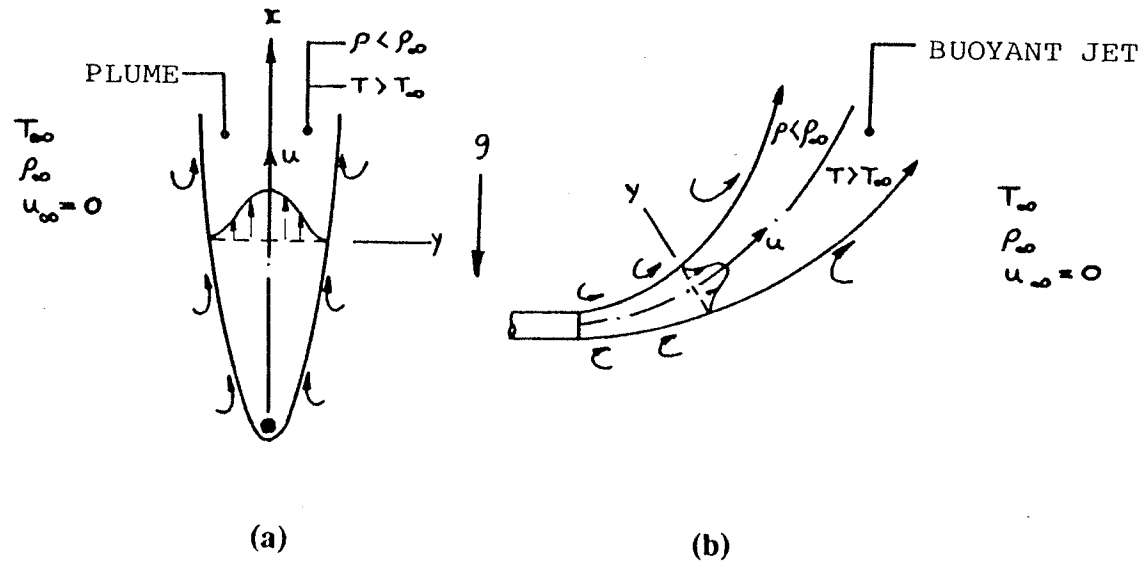

(a) (b)

Fig.D2 Buoyancy-driven free boundary layer flows in an extensive, quiescent medium. (a) Plume formation above a heated wire. (b) Buoyancy jet associated with a heated discharge.